# Understanding RanGTP dependent microtubule assembly,

## Identification of DnaJB6 as a RanGTP regulated factor involved in microtubule organization during mitosis

Miquel Rosas Salvans

Supervisor: Isabelle Vernos

Cell and Developmental Biology research programme

TESI DOCTORAL UPF / 2017

Universitat Pompeu Fabra

# Acknowledgments

I would like to acknowledge, of course, Isabelle Vernos. I would like to thank you the decision of accepting me in your lab, and give me the opportunity to do this PHD. I want to thank you to trust in me, as a person that could do the job but also as a person that could learn a new language that was essential in this institute. I want to thank you because you have known how to motorize my work but keeping my own space, what is really important for me. And of course, thank you for teaching me, for the discussions, for the support and for your kindness when it has been necessary.

I want to say thanks specially to Sylvain Meunier. Moltes gràcies per compartir amb mi el teu temps, el teu coneixement i, sobretot, la teva amistat. Gracies per haver rigut amb mi i també per haver-te enfadat algun dia i deixar-me aquest graciós record.

Vull donar les gràcies també a la Marta Martin. Tot i que no sé si ho llegiràs, tu em vas obrir les portes del laboratori, i si soc a aquí és perquè tu em vas donar la primera oportunitat. He recordat la teva frase de "Miquel, anem derrapant" en varies ocasions.

Vull donar les gràcies a tota la meva família pel seu suport incondicional. A vosaltres, Ramonet i Carmeta, mai hi han paraules suficients per agrair-vos tot el que us hauria d'agrair. A tu alba, la millor germana que es pot demanar, sé que sempre estàs a aquí i puc contar amb tu. I als meus petardos, Claudia i Eudald, no hi ha res més divertit que jugar amb vosaltres i tornar a ser un nen.

A tu, Alba, moltes gràcies pel teu suport, per aguantar-me aquests dies d'estrès i tots els altres. Gràcies per estar sempre al meu costat, per estimar-me tant amb les meves coses bones com amb les meves rareses. Ets fantàstica, i soc molt afortunat d'estar al teu costat.

I would like to thank to all the people that has passed by the lab in these 4 years. Thanks to Jacopo, Krystal, Nathalie, Tommaso, Nuria, Georgina, Claudia, Mónica,

Farners, Leonor, Alvaro. Thank you and good luck with your PHD Aitor, Alejandra, Ivan.

Special thanks to Andrea, it has been a pleasure to meet you! També a tu Linus, and to all the rest of the people I have met in CRG that mean something to me, who are many actually.

Voldria donar les gràcies a tots els meus amics de Sabadell, Barcelona, Tàrrega, arreu de Catalunya i del món en general. Gràcies per tots els moments de no-tesis, en que no s'està treballant, que són la salsa de la vida i el que realment ens empeny endavant. Espero poder gaudir de vosaltres molts anys més.

Finalment vull agrair a la Montserrat el seu suport més que incondicional. Hi ha moltes coses no segures a la vida, però a no ser que passi quelcom realment insòlit, tu sempre estaràs a allà esperant que vingui i t'arrenqui un tros. Les visites que et faig em donen força i m'ensenyen com afrontar altres reptes en tots els àmbits de la meva vida.

I'm sure I forgot some one, so if you feel like this, this word is for you:

THANKS!

## Abstract (English version)

Three microtubule (MT) assembly pathways participate in the assembly of the bipolar spindle: the centrosomal pathway, the augmin dependent amplification pathway and the RanGTP/chromosome dependent pathway. To form the spindle, all these MTs are organized by various classes of motor proteins into two interdigitating antiparallel arrays with their minus ends focused at the spindle poles. This focusing activity is provided by the minus-end directed motor proteins Dynein-Dynactin and HSET.

Spindle assembly can occur in the absence of centrosomes indicating that the RanGTP and augmin dependent pathways are sufficient. The RanGTP pathway can be studied in Xenopus laevis egg extracts. Addition of RanGTP to these extracts triggers a dynamic process of MT nucleation, stabilization and organization into asters and mini spindles. To obtain a global picture of the RanGTP pathway we used a proteomics approach and determined the interactome of the RanGTP-MTs that consists of 1263 proteins. Moreover we have analyzed the changes in this proteome to try to correlate them with the change in MT dynamic and organization observed upon different time of incubation of the egg extract with RanGTP. Although the composition of the proteome did not change, we found different patterns of recruitment for various protein groups. The proteome includes most of the known RanGTP regulated factors in mitosis and significantly overlaps with previously published spindle and taxol-MT proteomes. In addition it contains a large number of other proteins with described functions in various cellular processes as well as undescribed proteins. We used this proteome to identify novel putative RanGTP regulated spindle assembly factors (SAFs). We identified DnaJB6 as a RanGTP regulated protein involved in spindle assembly. We found that it interacts with dynactin p150 in a RanGTP dependent manner specifically in M-phase. We show that DnaJB6 favors the stabilization of the Dynactin complex specifically in mitosis, regulating the activity of Dynein-Dynactin complex in bipolar spindle assembly and MT focusing at the spindle poles.

## Abstract (català)

Tres vies de formació de microtúbuls (MT) participen en la formació del fus mitòtic: la centrosòmica, la via d'amplificació dependent d'Augmin i la via dependent de RanGTP o cromosòmica. Per formar el fus, tots aquests MTs són organitzats per diferents classes de proteïnes motores en dos feixos interconnectats de MTs antiparal·lels, amb els seus extrems negatius concentrats al pols del fus. Dynein-Dynactin i HSET s'encarreguen de concentrar els extrems negatius als pols.

El fus es pot formar també en absència de centrosomes, indicant que les vies de RanGTP i d'Augmin són suficients per formar-lo. La via de RanGTP es pot estudiar utilitzant extractes d'ous (EE) de *Xenopus Laevis*. L'addició de RanGTP activa un procés dinàmics de nucleació, estabilització i organització del MTs en asters i mini-fusos. Hem utilitzat la proteòmica com una aproximació per obtenir una visió global de la ruta de RanGTP i em descrit un interactoma dels RanGTP-MTs de 1263 proteïnes. A més, hem analitzat els canvis en aquest proteoma intentant correlacionar-los amb canvis en la dinàmica i l'organització observades al llarg de diferents temps d'incubació de l'EE amb RanGTP. Tot i que la composició del proteoma no varia, hem trobat diferents patrons de reclutament per varis grups de proteïnes. El proteoma inclou la majoria dels factors regulats per RanGTP en mitosis que es coneixen i te un elevat grau de solapament amb altres proteomes del fus i dels Taxol-MTs publicats prèviament. A més, conté un elevat nombre de proteïnes amb i sense roles descrits en varis processos cel·lulars. Hem utilitzat el proteoma dels RanGTP-MTs per identificar nous possibles factors regulats per Ran involucrats en la formació del fus. Hem identificat DnaJB6 com una proteïna regulada per Ran amb una funció en la formació del fus mitòtic. Hem descrit la interacció de DnaJB6 amb p150, dependent de RanGTP específicament en fase M. DnaJB6 afavoreix l'estabilització el complex Dynactin específicament en mitosis, regulant l'activitat de Dynein-Dynactin en l'establiment de la bipolaritat del fus mitòtic i la concentració dels extrems (-) dels MTs als pols del fus mitòtic.

# TABLE OF CONTENTS

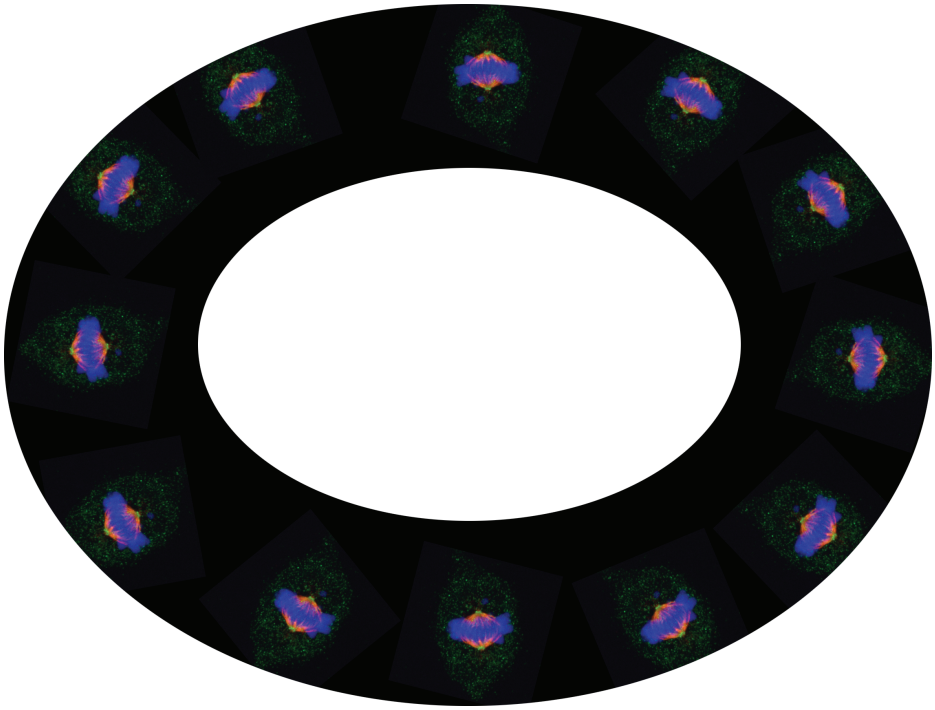

Table of contents

# Figures and Tables index

**Figures**

**Tables**

# Abbreviations list

Cdk- Cyclin Dependent Kinase
CLS- Cilia Localization Signal
CPC- Cilia Pore Complex
CSF- Cytostatic Factor
DMEM- Dulbecco's Modified Eagle's Medium
DMSO- Dimethyl sulfoxide
DNA- Deoxyribonucleic Acid
DnaJB6-L- DnaJB6 Long isoform
DnaJB6-S- DnaJB6 Short isoform
Dynein HC- Dynein heavy chain
Dynein IC- Dynein Intermediate Chain
Dynein LIC- Dynein light intermediate chain
EE- Egg Extract
FBS- Fetal Bovine Serum
Fig- Figure
GO- Gene Ontology
GST- Glutathione S-Transferase
IF- immunofluorescence
IFT-Intraflagelar Transport
K-Fiber- Kinetochore Fiber
KI- Potasium iodide
KLP- Kinase-Like protein
LGMD1D- limb girdle muscular dystrophy
MAP- microtubule Associated Protein
MBP- Maltose Binding Protein
Min- minute
MT- Microtubule
MTOC – MT Organizing Centre
NE- Nuclear Envelope
NEBD- Nuclear Envelope BreakDown
NES- Nuclear Export Signal
NLS- Nuclear Localization Signal
NPC- Nuclear Pore Complex
ON- OverNight
polyQ- polyglutamine
RanGAP – Ran GTPase Activating Protein
RanGEF – Ran Guanine nucleotide Exchanging Factor
RanMT proteome – RanGTP MTs associated proteome
Rd-Tubulin – Rhodamine tubulin
RT- room temperature
SAC- Spindle Assembly Checkpoint
SAF- Spindle Assembly Factor
SD- Standard Deviation
WB- Western Blot
x-DnaJB6- Xenopus DnaJB6
γ-TuRC – γ-Tubulin Ring Complex
γ-TuSC – γ-Tubulin Small Complex

# Preface

The cell cycle is a general and essential process for life. This process starts from a single cell that has to “decide”, either to get specialized and stop the cycle or to follow the cycle and undergo cell division, forming two new daughter cells that will follow the same process. This cycle can be divided in two big blocs, interphase (divided in G1, S and G2) and M-phase. When the cell is generated it enters G1, in this state the cell determines if it continues the cycle in order to divide or if it exits the cycle. If the cell exits the cell cycle it enters G0 and differentiates. Many cells develop a cilium in G0. If the cell continues the cell cycle, the DNA replicates and the centrosomes duplicate (in S and G2) and the cell will eventually divide. Two types of cell division can take place in eukaryotes, Mitosis (in somatic cells) and Meiosis (for gamete production). In both cases, the bipolar spindle is the structure that is responsible for DNA segregation, but some differences exist between these two kinds of division, as we will explain latter. Many proteins are involved in the assembly and regulation of the spindle. Although a general picture of how this structure is assembled is known, many open questions remain to be elucidated. The role of many proteins involved in spindle assembly and mitosis progression is known, but which factors are still missing and how are all of these proteins coordinated in order to regulate the process of cell division is a complex and extended question still far to be solved.

In this thesis, I aimed at understanding bipolar spindle formation focusing on the RanGTP dependent MT assembly pathway and its role driving MT organization. Using a proteomics approach I have studied the protein networks that underlie RanGTP dependent microtubule assembly. I identified and characterized a novel RanGTP regulated protein that promotes bipolar spindle organization and spindle pole focusing by regulating the stability and activity of the Dynein-Dynactin complex.

# INTRODUCTION

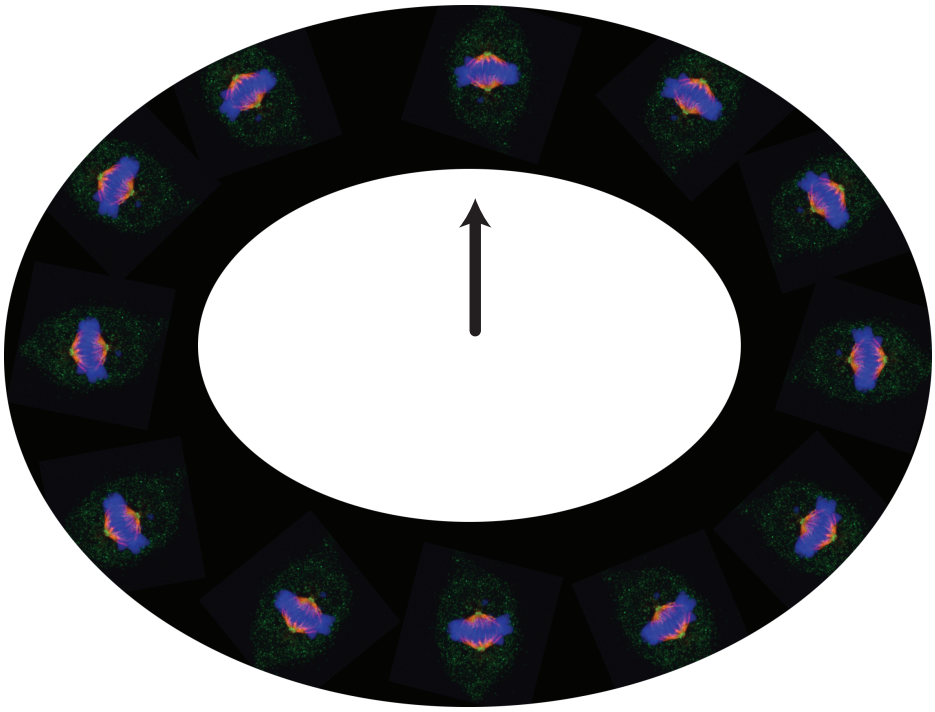

# 1. The bipolar spindle

The bipolar spindle is the molecular machine that segregates the chromosomes. Three main components constitute this structure: the chromosomes, the microtubules (MT) and the centrosomes at the spindle poles. The bipolar spindle is not a static structure but instead it presents a range of features that evolve throughout mitosis, mainly due to changes in the microtubule network properties and organization. Relevant differences exist in different eukaryotes and cell types concerning the spindle size and length as well as the nature of the spindle poles and their organization. In some organisms such as yeast, the spindle assembles within the nucleus in the presence of an intact nuclear envelope. In this thesis, I will focus on the spindle of metazoans, which assemble after nuclear envelope breakdown.

Typically, the metaphase spindle is bipolar, with chromosomes aligned at its middle region, forming the "so-called" metaphase plate, and linked to each spindle pole through microtubules. When present, the two centrosomes that nucleate microtubules are located at the spindle poles (one per pole) (Fig.I.1).

As mentioned, the spindle is not a static structure, instead, it changes and reorganizes along cell division. Mitosis is mainly divided in 5 phases: prophase, pro-metaphase, metaphase, anaphase and telophase. During prophase, the DNA starts condensing forming the chromosomes and the two centrosomes start their separation. The nuclear envelope breakdown initiates pro-metaphase and leads to the "release" of the chromosomes and all the nuclear proteins to the cytoplasm. MTs are nucleated in the vicinity of the chromosomes and at the centrosomes; they grow and capture chromosomes so to eventually form a bipolar structure where chromosomes are directed to the center of the structure to generate the metaphase plate (O'Connell & Khodjakov 2007). Once all chromosomes are aligned at the center of the spindle the cell is in metaphase. Subsequently, the sister chromatids of each chromosome will start to migrate towards the spindle poles, due to the forces exerted by the MTs, and the cell will enter anaphase. Also, in this phase a new array of MTs is formed between the two chromosome masses,

forming the central spindle. Once the chromosomes reach the spindle poles, in telophase, the NE is reassembled around the DNA mass and the chromosomes start to de-condense. In the final step of the division, the cytokinesis, the cytoplasm is also divided generating two daughter cells with a closed plasma membrane and a nucleus.

An extended set of proteins is involved in the highly regulated process of cell division. Their recruitment and functioning is very well regulated and coordinated; however, it is not sufficient to coordinate the action of all these proteins. The proteins present indeed another level of regulation of their activity, obtained by post-translational modifications of specific residues or domains of these proteins. Post-translational modifications can induce changes on a protein so to modulate its activity and its interaction with different factors. Most of the proteins can be regulated in this manner. A major post-translational modification that regulates many events during mitosis, and also during all the cell cycle, is phosphorylation (Ma & Poon 2011). Protein kinases are responsible for phosphorylating the proteins at specific residues, and on the other side protein phosphatases can then remove these phosphates, specifically regulating their activity (Kim et al. 2016; Manning 2002).

Another feature that regulates protein activity is how it is folded. The chaperon machinery regulates the process of protein folding. Chaperons are involved in many processes of the cell, from mediating early protein folding and protein complexes formation to protein degradation, including also roles in mitosis (as detailed in chapter 5).

In the following sections of this chapter, I will explain the main features and roles of microtubules, chromosomes and centrosomes in the mitotic spindle.

**Fig.I.1. Bipolar spindle schematic representation:** In yellow the cytoplasm, in red the microtubules, in grey the chromosomes and dark green the centrosomes with the centrioles in purple. Different MT populations are shown, Astral MTs (radial red lines connecting the centrosome with the plasma membrane), interpolar MTs (thin red lines located between the two centrosomes) and K-Fibers (wider red lines connecting the centrosomes and the chromosomes).

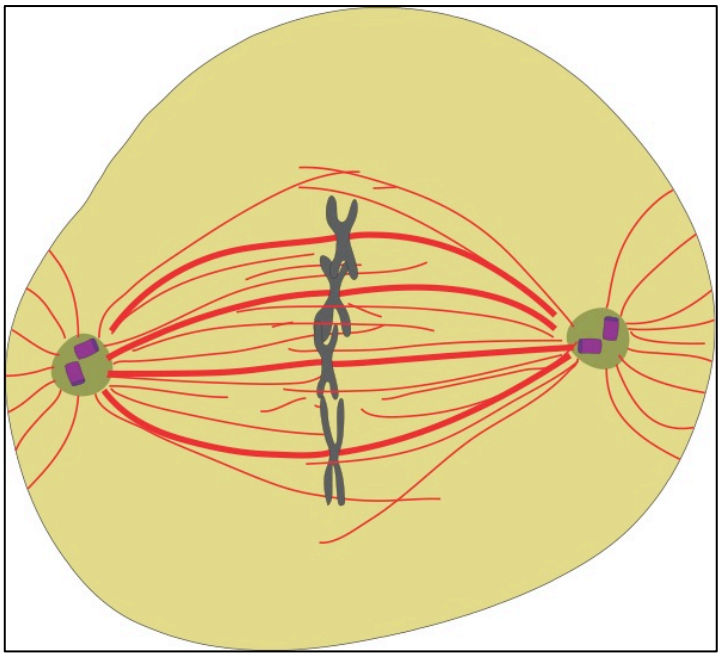

## 1.a. The microtubules in cell division

Microtubules are filamentous polymers made of α- and β-Tubulin heterodimers. The tubulin dimers associate linearly in a head to tail fashion forming a polarized protofilament. 13 protofilaments interact laterally forming a hollow tube of 25nm diameter with a plus-end where the β-Tubulin is exposed, and a minus-end where the α-Tubulin is exposed (Evans et al. 1985) (Fig.I.2.a and b). The tubulin C-terminal tails are all exposed to the external surface of the microtubule and provide sites for most of the tubulin post-translational modifications to occur as well as for protein interactions. Microtubules grow by incorporation of new tubulin dimers mainly at the plus-end in a GTP dependent way. The new tubulin dimers are indeed associated with GTP, and GTP hydrolysis takes place on the β-Tubulin subunit shortly after polymerization. This mechanism results in the formation of a GTP-cap at the plus-end of the growing microtubule with stabilizing properties, whereas the majority of the microtubule length consists of GDP-tubulin. The GTP hydrolysis induces a conformational change that leads to microtubule instability (Walker et al. 1989; Hyman et al. 1995; Tran et al. 1997; Alushin et al. 2014; Zhang et al. 2015). Microtubules undergo successive cycles of growing and shrinking, known as “dynamic instability”. The transition from a growing to a shrinking status is defined as catastrophe, while the opposite event as

rescue (Fig.I.2.c). Both ends of the microtubules can grow *in vitro*, but they have different properties. The microtubule minus-ends grow much slower and undergo catastrophe less frequently than the plus-ends (reviewed in Desai & Mitchison 1997). *In vivo*, many different microtubule associated proteins (MAPs) regulate the dynamic properties of the microtubule. Different MAPs regulate microtubule dynamic instability by either protecting the tips of the microtubules from depolymerization or by enhancing or inhibiting the incorporation of new tubulin dimers to the plus-end (as explained in chapter 3).

Within the spindle, microtubules have a specific orientation, with the minus-ends focused at the spindle poles and the plus-ends pointing to the opposite direction (oriented away from the pole) either towards the cell cortex or interdigitating in between the two spindle poles. Three different populations of microtubules are present within the spindle: the astral microtubules, the interpolar microtubules and the kinetochore fibers (K-Fibers) (Fig.I.1). The astral and interpolar microtubules are individual microtubules with similar dynamics (half-life= 30sec-1min) (Mitchison & Kirschner 1984). Astral MTs emanate from the centrosomes and reach the cell cortex playing a role in centrosome separation and spindle positioning (reviewed in Rosenblatt 2005). They are very important for asymmetric and polarized cell divisions (reviewed by Knoblich 2010). However, astral microtubules are absent in some cell types (Khodjakov et al. 2000; Mahoney et al. 2006). The interpolar microtubules are present between the two spindle poles although not necessarily associated to them. They are involved in chromosome positioning, through interactions with chromokinesins (reviewed by Vanneste et al. 2011) (detailed in chapter 5.a.i) or by lateral attachments to the kinetochores (Cai et al. 2009; Wignall & Villeneuve 2009; Magidson et al. 2011; Muscat et al. 2015). Interpolar microtubules are also involved in spindle bipolarity establishment and maintenance and spindle length regulation. Although it has no been demonstrated a direct implication of the interpolar microtubules in chromosome segregation, a kinetochore or K-fibers independent chromosome segregation has been shown in *Caenorhabditis elegans* oocytes (in meiotic acentrosomal spindles) (Dumont et al. 2010; Muscat et al. 2015). The last

population of spindle microtubules are the K-fibers, bundles of 20-40 parallel microtubules much more stable than the other spindle microtubules (half-life= 4-8min) (Rieder 1981; Zhai et al. 1995; McEwen et al. 1997; Bakhoum et al. 2009). The K-fibers link the paired sister kinetochores of each chromosome with the respective spindle pole and actively drive chromosome segregation. The K-Fiber microtubules are however not static. During metaphase, a poleward tubulin flux is generated by the incorporation of tubulin dimers at the plus-end of the microtubules and their removal at the minus-end (at the spindle poles) (Miyamoto et al. 2004; Mitchison et al. 2005; Sawin & Mitchison 1991; Mitchison et al. 2004). Various proteins regulate microtubule dynamics and the poleward flux during cell division (see chapter 4). I will explain the features and main events of mitotic MTs in chapters 2 and 3.

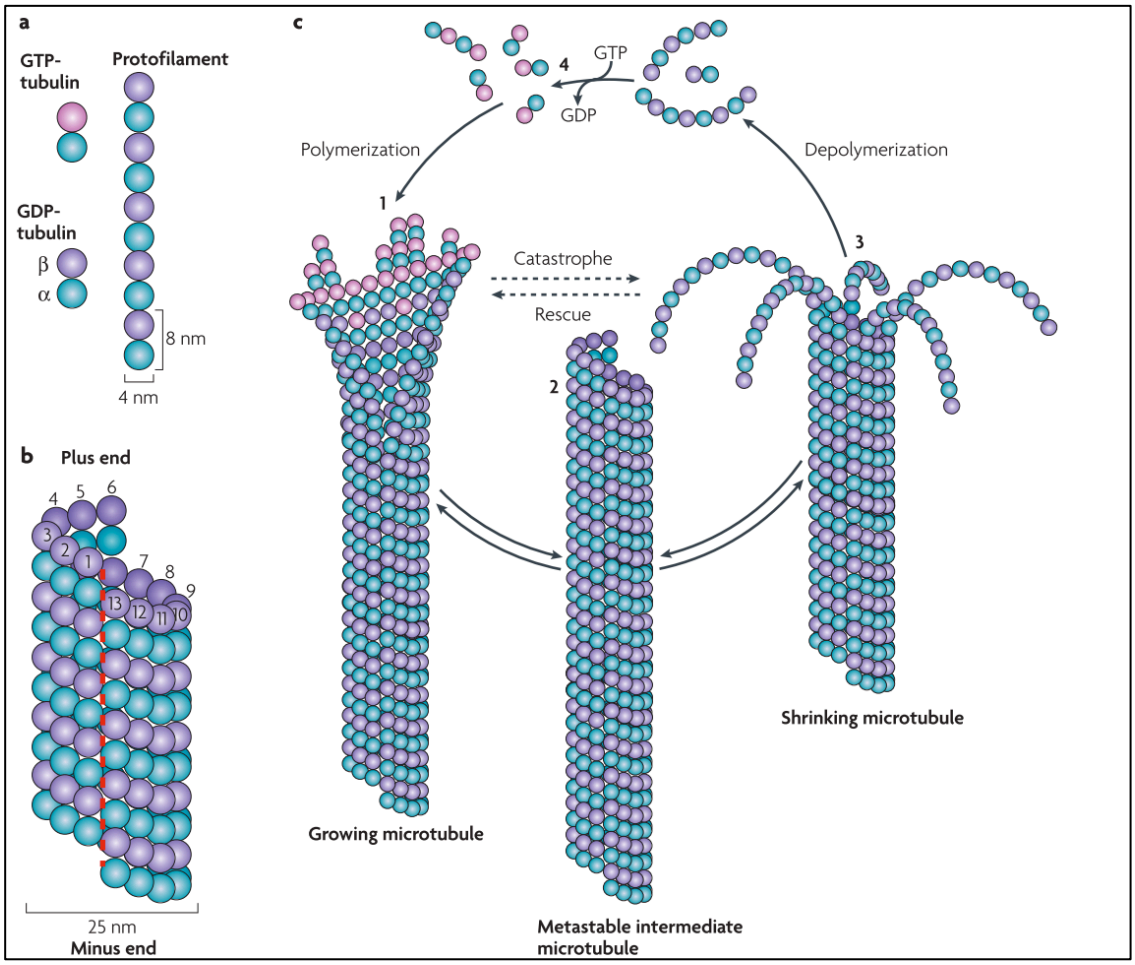

**Fig.I.2. Microtubules:** A) Microtubules are composed of stable α/β-tubulin heterodimers that are aligned in a polar head-to-tail fashion to form protofilaments. B) The cylindrical and helical microtubule wall typically comprises 13 parallel protofilaments *in vivo*. C) The 12-nm helical pitch in combination with the 8-nm longitudinal repeat between α/β-tubulin subunits along a protofilament generates the lattice seam (red dashed line). Assembly–polymerization and disassembly–depolymerization of microtubules is driven by the binding, hydrolysis and exchange of a guanine nucleotide on the β-tubulin monomer (GTP bound to α-tubulin is non-exchangeable and is never hydrolysed). GTP hydrolysis is not required for microtubule assembly per se but is necessary for switching between catastrophe and rescue. Polymerization is typically initiated from a pool of GTP-loaded tubulin subunits (part c;(1)). Growing microtubule ends fluctuate between slightly bent and straight protofilament sheets. GTP hydrolysis and release of inorganic phosphate occurs shortly after incorporation and is promoted by burial and locking of the partially exposed nucleotide as a result of the head-to-tail assembly of dimers. It has been postulated that GTP hydrolysis changes the conformation of a protofilament from a slightly curved tubulin-GTP to a more profoundly curved tubulin-GDP structure125. This nucleotide- dependent conformational model predicts that the curved tubulin-GDP is forced to remain straight when it is part of the microtubule wall. Growing microtubule sheets are thus believed to maintain a 'cap' of tubulin-GTP subunits to stabilize the straight tubulin conformation within the microtubule lattice. Closure of the terminal sheet structure generates a metastable, blunt-ended microtubule intermediate (part c; (2)), which might pause, undergo further growth or switch to the depolymerization phase. A shrinking microtubule is characterized by fountain-like arrays of ring and spiral protofilament structures (part c; (3)). This conformational change, which is presumably directed by tubulin-GDP, may destabilize lateral contacts between adjacent protofilaments. The polymerization–depolymerization cycle is completed by exchanging GDP of the disassembly products with GTP (part c; (4)). Figure and legend reproduced from (Akhmanova & Steinmetz 2008)

## 1.b The Centrosome

The centrosome was discovered in the 1880s by Theodor Boveri and Beneden, who postulated that it could have a role in generation of multipolarity and cancer (https://archive.org/details/zellenstudien02bove). Centrosomes are present in metazoans and many unicellular eukaryotes, but they are absent in the majority of land plants. The centrosome is composed of a pair of centrioles surrounded by an electron dense pericentriolar material forming a mesh made of different proteins. The pericentriolar mesh was thought to be disorganized, but recent data suggest that it may instead have a defined regulated organization (Mennella et al. 2012; Lawo et al. 2012). The human centriole is a cylinder of 250nm diameter and 500nm length approximately (Fig.I.3). Each human centriole is typically made of 9 triplets of microtubules, which are laterally associated around a cartwheel structure forming a barrel-like structure. Some organisms have single microtubules or doublets instead of triplets (Carvalho-Santos et al. 2011). The microtubules of a triplet are named A (the most internal one), B (in the middle) and C (at the external side). Whereas A is a complete microtubule with 13

protofilaments, B and C share 3 protofilaments with the juxtaposed microtubules of the triplet, having 10 protofilaments each. The daughter centriole is tethered to the basal side of the mother centriole by protein linkers, forming a 90º angle (reviewed in Bettencourt-Dias & Glover 2007 and Winey & O'Toole 2014). The centriole is present in all eukaryotic groups, although the structure of the centrosome is not conserved in all the organisms (Carvalho-Santos et al. 2011).

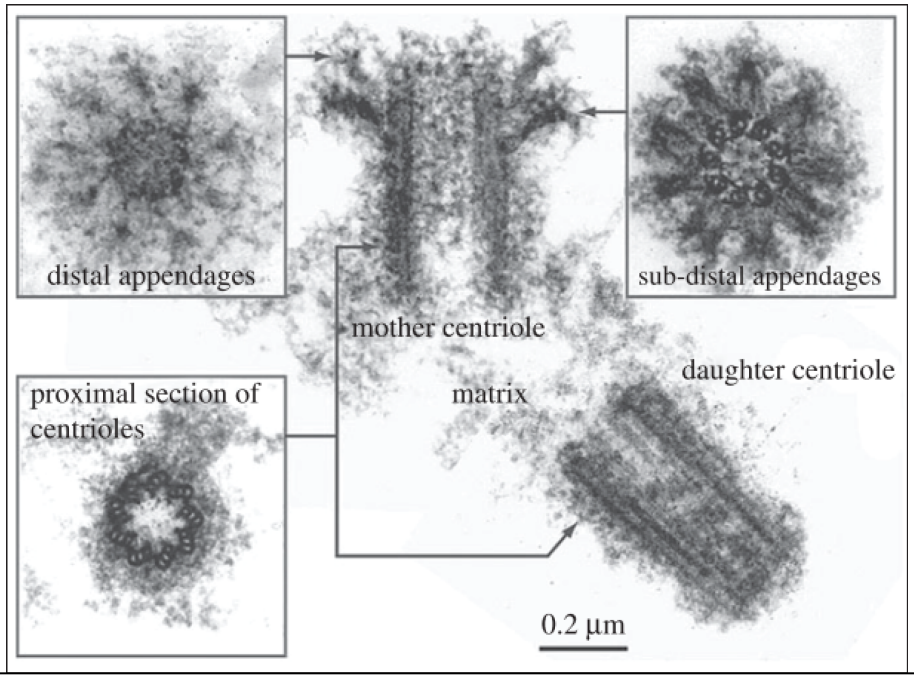


**Fig.I.3. Centriole structure:** Electron micrographs of centrioles in isolated centrosomes shown in longitudinal section and informative cross sections highlighting the distal and sub distal appendages. Figure and legend reproduced from (Winey & O'Toole 2014)

The centrosome plays different roles along the cell cycle. In G0 arrested differentiated cells, sperm cells and many unicellular organisms, a specialized centrosome forms the basal body of cilia and flagella. In cycling cells, the centrosome is the main microtubule organizing center of the cell during interphase and in mitosis it actively nucleates microtubules, defines the poles of the mitotic spindle and plays an essential role in asymmetric division and spindle positioning.

Centriole containing cells have two centrosomes in mitosis that define the two spindle poles of the mitotic spindle. After cytokinesis, one centrosome is inherited by each daughter cell. This single centrosome duplicates (during interphase) before the cell divides again. This involves the formation of two new centrioles that begins at the onset of S phase. However, the first step of the process started before.

In early G1, before the end of cytokinesis, the two centrioles start to disengage, a process that depends on the action of separase. Centriole assembly only starts at the beginning of S phase with the recruitment of centrin. A procentriole starts to form on the side of both centrioles and their elongation starts in late S phase to form the daughter centriole. The new centrioles will keep maturing along the next cycle to become a new mother centriole. Centrosome separation starts during G2, conditioning the establishment of the bipolarity of the mitotic spindle (reviewed in Tanenbaum & Medema 2010). In late G2 the active recruitment of pericentriolar material, a process of centrosome maturation, results in a an increased microtubule nucleation capacity of the centrosome (Piehl et al. 2004).

Although all mammals have centrosomes, they are not present in all of their cells. Mammalian oocytes assemble a centrosome-free meiotic spindle. During fertilization, a centrosome will be typically provided to the egg by the sperm (reviewed in Clift & Schuh 2013). However, this is not the case for all mammals. For example mice embryos carry out the first divisions without centrosomes that will only appear at the blastocyst stage (Calarco-Gillam et al. 1983). Interestingly, the removal of the centrosome does not impair cells to assemble the bipolar spindle (Basto et al. 2006; Mahoney et al. 2006; Khodjakov et al. 2000; Megraw et al. 2001). Finally, most superior plants do not have centrosomes, although they assemble a bipolar spindle in mitosis.

## 1.c. The Chromosomes: the kinetochore

The kinetochore is a complex protein structure that assembles at the centromeric region of the chromosomes. It is a dynamic structure essential for faithful chromosome segregation. In mitosis, each chromosome has two kinetochores (one per sister chromatid) and each kinetochore can be divided in three parts: the inner-, the central- and the outer-kinetochore. Spindle microtubules associate with the kinetochores, first forming transient side-on attachments that eventually will lead to the formation of end-on attachments with the formation of K-Fibers (kinetochore-microtubules) (Kalantzaki et al. 2015). Chromosome segregation only takes place once all the kinetochores are properly bi-oriented through K-Fibers and all chromosomes are aligned at the metaphase plate.

The kinetochore is constituted by at least 80 proteins in humans, and organized in several sub-complexes (Cheeseman & Desai 2008). CENP-A, a Histone 3 variant, is a key element for kinetochore assembly. It forms nucleosomes at the centromere and maintain its identity. Together with CENP-A, 16 other proteins reside at the centromeric DNA along the cell cycle; these proteins are termed the constitutive centromere-associated network (CCAN). Many other components are recruited during G2-M, and some of them will disappear from the KTs during mitosis (like most of the spindle assembly checkpoint factors) and others only at the end of cell division (reviewed in Cheeseman & Desai 2008; McAinsh & Meraldi 2011; and Cheeseman 2016). A protein complex has been identified as the responsible for the kinetochore-microtubule interaction, the KMN. The KMN is composed by three protein complexes: the Knl (Knl1 and Zwint), the Mis12 (Nnf1, Mis12, Dsn1 and Nsl1) and the Ndc80 (Ndc80 (Hec1), Nuf2, Spc24 and Spc25) complexes (Cheeseman et al. 2006). In addition, the KMN complex is also involved in the recruitment of some spindle assembly checkpoint (SAC) proteins. The SAC is the machinery which controls that chromosome segregation starts just after proper chromosome alignment has occurred at the metaphase plate with all the kinetochores correctly attached to the K-Fibers, ensuring faithful segregation of the chromosomes. The SAC senses proper kinetochore-microtubule attachments and also the tension generated within the kinetochore (Uchida et al. 2009). As consequence of the tension, the removal of SAC proteins from the kinetochore occurs (by the Dynein-Dynactin motor protein complex), silencing the checkpoint (Lampson & Cheeseman 2011). This induces changes in plus-ends dynamics of the K-fibers that will promote the segregation of the DNA and the dissociation of securin from the chromosomes, which enables sister chromatid separation (Maresca & Salmon 2010).

Not all the organisms have a defined kinetochore. Some organisms have holocentric chromosomes (for instance, *Caenorhabditis elegans*) that have diffuse kinetochores along the surface of the chromatids (Monen et al. 2005).

# 2. Microtubule assembly and dynamics

## 2.a Microtubule nucleation

Three microtubule nucleation pathways coexist during mitosis in most animal cells: the centrosomal, the chromosomal (or RanGTP) and the amplification (or augmin) pathways. The microtubule nucleation core machinery is shared between the three pathways, but specific factors and protein modifications define their activity. The core machinery consists of a preformed seed complex called the gamma tubulin ring complex (ϒ-TURC). The ϒ-TURC is a 25nm diameter ring (Moritz et al. 1995) composed by several molecules of ϒ-tubulin, gamma tubulin complex proteins (GCPs) 2, 3, 4, 5 and 6, NEDD1 (or GCP-WD) and MOZART-2 (or GCP8). The first component for microtubule nucleation to be identified was ϒ-tubulin, a member of the tubulin protein superfamily essential for microtubule nucleation and present in all the microtubule organizing centers (MTOCs) within the cell (Oakley & Oakley 1989; Teixidó-Travesa et al. 2012). Several other proteins were then found to co-purify with ϒ-tubulin (Murphy et al. 1998; Teixidó-Travesa et al. 2010). Five of these, containing characteristic GRIP domains, were named GCP's (γ-Tubulin complex proteins) (Kollman et al. 2011). The minimal subunit of the ϒ-TURC is the ϒ-TuSC complex, composed of one molecule of GCP2 and GCP3 associated with two molecules of ϒ-Tubulin. Several ϒ-TuSCs interact forming a ring-like structure that includes GPC4, 5 and 6 (reviewed in Teixidó-Travesa et al. 2012). Finally, the ϒ-TURC also include additional non conventional GCPs (without GRIPs motifs) like NEDD1 (Lüders et al. 2006) and MOZART (Teixidó-Travesa et al. 2010) .

During mitosis, microtubules are nucleated through these pathways specifically regulated both spatially and temporally. Indeed, microtubule nucleation occurs from the two centrosomes already before nuclear envelope breakdown; then after nuclear envelope breakdown, nucleation starts in the vicinity of the chromosomes (through the RanGTP dependent pathway); and finally on the lattice of preexisting microtubules (defining the Augmin or microtubule amplification pathway). It is

still not entirely clear if microtubules originated from the different pathways play differentiated roles during mitosis.

An essential factor of the ϒ-TURC, common to all the pathways, is NEDD1. NEDD1 specific phosphorylation on three different sites regulates ϒ-TURC targeting and the activity of each specific MT nucleation pathway. NEDD1 phosphorylation on S377 by Nek9 (downstream PLK1) promotes the recruitment of the ϒ-TURC to the centrosome in G2/prophase (Sdelci et al. 2012; Lüders et al. 2006), an essential event for centrosome maturation. NEDD1 phosphorylation on S411 by Cdk1 is required for the interaction of the ϒ-TURC with the Augmin complex (Uehara et al. 2009; Johmura et al. 2011; Lüders et al. 2006). Augmin is a 8 proteins complex that binds the lattice of a pre-existing microtubule inducing the nucleation of a new microtubule and branching (Uehara et al. 2009; Lawo et al. 2009; Hsia et al. 2014). Finally, phosphorylation of NEDD1 on S405 by Aurora-A promotes the MT nucleation in the vicinity of the chromosomes (Pinyol et al. 2013) in a RanGTP dependent manner (see next section).

## 2.b. The Ran pathway

The small GTPase Ran is a member of the Ras-GTPase superfamily (Drivas et al. 1990). As for other members of the family, the specific nucleotide associated state (either GDP or GTP) changes the affinity of the protein for its interactors and thereby its activity (Scheffzek et al. 1995; Vetter et al. 1999). In interphase, RanGTP accumulates in the nucleus because its Guanosine-exchange factor (GEF) RCC1 is nuclear (F. Ralf Bischoff & Ponstingl 1991; F R Bischoff & Ponstingl 1991; Ohtsubo et al. 1987; Ohtsubo et al. 1989; Renault et al. 2001). The presence in the cytoplasm of several proteins that stimulate the intrinsically low GTPase activity of Ran, such as RanGAP1 (a GTPase activating protein (GAP)) (Bischoff et al. 1994; Becker et al. 1995; Seewald et al. 2002), RanBP1 (Bischoff et al. 1995; Coutavas et al. 1993) and RanBP2 (Yokoyama et al. 1995), results in RanGDP as the predominant form present in the cytoplasm. The differential localization of the GEFs and GAPs and the existence of the nuclear envelope (NE) in interphase promotes a gradient of RanGTP to RanGDP in which the GTP form is much more concentrated within the nucleus of the cell (Kalab et al. 2006).

In interphase, Ran is the main regulator of the nucleo-cytoplasmic transport (Moore & Blobel 1993; Melchior et al. 1993), driving the transport of Nuclear Localization Sequence (NLS) containing proteins through the NPCs (Nuclear Pore Complex). The translocation of big cargos (bigger than 40KDa approximately (Pante & Kann 2002; Lang et al. 1986; Mohr et al. 2009)) is mediated by karyopherins (importins and exportins), more than 20 in mammals. The Interaction between karyopherins and cargo proteins is regulated by Ran (Görlich et al. 1996). Proteins that must be translocated to the nucleus interact with Importins (-α or -β) through a NLS, a variable sequence rich in lysines and arginines (Görlich et al. 1995). Proteins that are transported from the nucleus to the cytoplasm interact instead with Exportins through a Nuclear Export Sequence (NES) rich in Leucines (Petosa et al. 2004). These complexes are translocated trough the NPC (Fig.I.4.a).

Since the affinity of Importins for the NLS is lower than its affinity for RanGTP, once into the nucleus, the interaction of Importin with RanGTP promotes the release of the NLS-protein. The opposite happens with the Exportins and the NES-proteins. In the nucleus, RanGTP interacts with Exportins, increasing their affinity for the NES. A RanGTP-Exportin-NES-protein complex is formed and translocated to the cytoplasm across the NPC. Once in the cytoplasm, the hydrolysis of GTP by Ran promotes the dissociation of the complex and release of the NES-protein (Bischoff & Görlich 1997).

During mitosis, after the nuclear envelope breakdown, the persistence of RCC1 association with chromosomes (Moore et al. 2002) generates a gradient of RanGTP centered on chromosomes (Fig.I.4.b). RanGTP in the vicinity of the chromosomes induces the release of NLS-proteins from Importins. Some of these NLS-proteins play essential roles in microtubule nucleation (such as TPX2), in microtubule dynamics (such as MCRS1) or in microtubule organization (such as kinesin-14) being therefore essential for spindle assembly. These proteins were also generally named as SAFs (Spindle Assembly factors) and define the RanGTP dependent microtubule assembly pathway (summarized in Table 1) (reviewed in Cavazza & Vernos 2016).

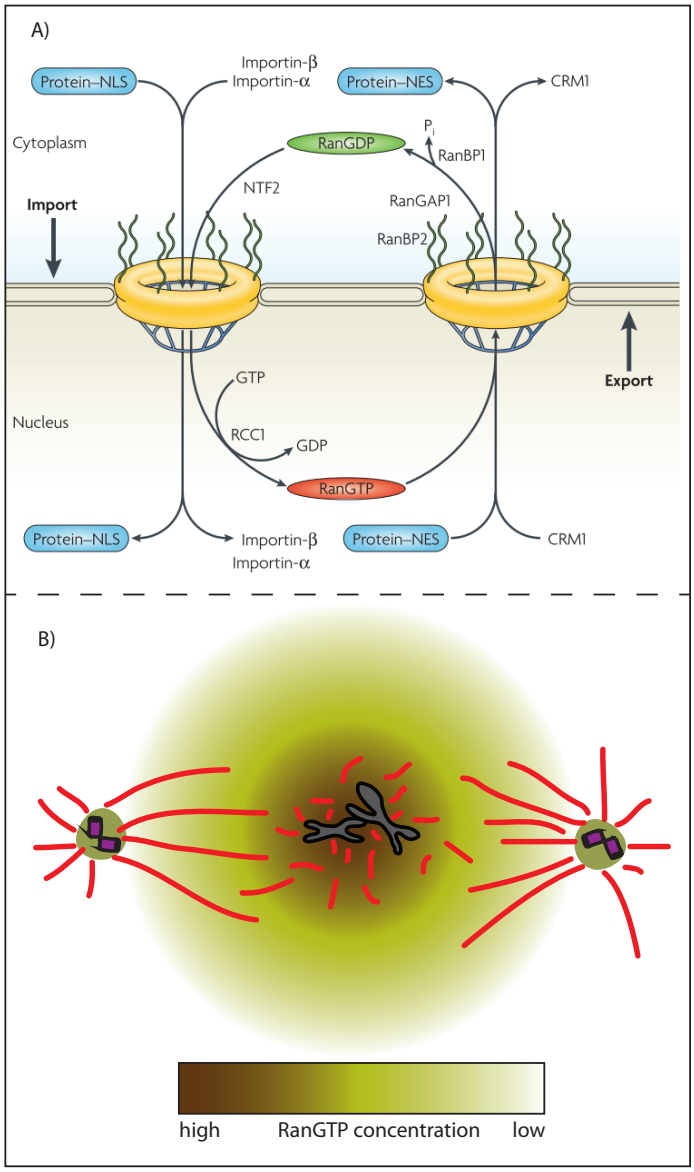


**Fig.I.4. The RanGTP system in interphase and mitosis.** A) Ran directs nucleocytoplasmic transport in interphase: Ran shuttles across the nuclear envelope through nuclear pores, but is concentrated in the nucleus because of nuclear transport factor-2 (NTF2)-mediated active import. In the nucleus, a high concentration of RanGTP is generated by nucleotide exchange. This is catalyzed by chromatin-bound RCC1 and might be promoted by the nucleotide dissociation factor MOG1 and the accessory factor RanBP3 (not shown). RanGTP causes the dissociation of imported complexes, which contain proteins that carry a nuclear localization signal (NLS), by binding to importin-β and ejecting the cargo. Conversely, binding of RanGTP to chromosome-region maintenance protein-1 (CRM1) promotes the assembly of export complexes containing proteins with a nuclear export signal (NES). In the cytoplasm, RanGTP meets RanGAP1 and RanBP1 or RanBP2, which stimulates GTP hydrolysis and the export complexes dissociate. The importins and exportins are recycled by transport back across the pore (not shown). In addition to this basic mechanism, other members of the importin family mediate the transport of specific cargoes. (Figure and legend reproduced from (Clarke & Zhang 2008)); B) The RanGTP gradient in mitosis: RanGTP is formed closed to the chromosomes by RCC1 generating a gradient centered on the chromosomes. RanGTP induces the release of the NLS-proteins in the vicinity of the chromosomes promoting microtubule nucleation and favoring MT-stabilization.

| Table. I. 1 | Protein name | Mitotic function | Mitotic localization |
|---|---|---|---|
| **Chromatin Remodeling** | CHD4 | Stabilizes MTs | MTs and DNA |
| | ISWI1 | Stabilizes MTs, mostly in anaphase | Centrosomes, Spindle poles and DNA |
| | MCRS1 | Protects MT -end, favors Chromatin MT assembly and K-fiber formation | Spindle poles, K-fibers-ends |
| **Kinesins** | Kif14-NabKin | +end directed motor, important for chromosome congression and cytokinesis | MTs |
| | Kid (Kif22) | +end directed chromokinesin, important for for chromosome arm congression | MTs and Chromatin |
| | HSET/XCTK2/KIFC1 | -end directed kinesin, important for pole focusing | MTs |
| | Kif2a | MT depolymerizing kinesin. Important for spindle length, pole coalescence, and chromosome congression | MTs |
| **Nuclear Pore Complex** | Mel28/ELYS | Ran Dependent MT nucleation, interacts with γTubulin | Spindle poles, kinetochores |
| | Nup107-160 complex | Ran Dependent MT nucleation, interacts with γTubulin, CPC localization | Spindle poles, kinetochores |
| | Nup98 | Inhibits MCAK activity | Not described |
| | Rae1 | Spindle organization; counteracts NuMA function | Spindle poles |
| | Laminin B3* | Spindle organization, supposedly through the spindle matrix | MTs |
| **Others** | TPX2 | MT nucleation, MT bundling, AurA activation | MTs |
| | NuMA | Spindle pole formation and Spindle positioning | MTs |
| | NuSAP | Important for MT stabilization and crosslinking, favors MT assembly in proximity of chromatin | MTs and chromatin |
| | HURP | Stabilizes and bundles MTs, specially k-fibers | k- fibers |
| | TACC3 | MT elongation and K-fiber formation | Spindle poles and MTs |
| | CDK11 | Centrosome maturation and MT stability) | Spindle poles/centrosomes |
| | Xnf7** | Stabilizes and bundles MTs; inhibits APC/C at anaphase on set | MTs |
| | APC | Bundles MTs | MTs and kinetochores |
| | Crb3-Clp1*** | Not charcterized function, disorganized spindles | Spindle poles |
| | Anillin | Cytokinesis, membranes elongation in anaphase | Cell cortex |

**Table.I.1. RanGTP regulated factors in mitosis** *Only amphibians have Lamin B3; ***Xenopus Laevis* name (By Blast TRIM69, 43% identity, Trim69i impairs spindle assembly); ***Crb3, no Clp1.

## 2.c. Microtubule dynamics

Microtubule dynamics change dramatically in different cell cycle stages and after differentiation. During mitosis, it is accurately regulated and coordinated with the different changes in the spindle morphology and function. Defects in the regulation of microtubule dynamics have strong detrimental consequences in spindle assembly and chromosome segregation. As we mentioned in chapter 2.A, two essential features of microtubules are the dynamic instability (growing-shrinking cycles) and the tubulin poleward flux. Several MAPs define the specific dynamic properties of the microtubules (reviewed in Akhmanova & Steinmetz 2015). Some of them bind to the microtubule along their length, while others are specific for the plus- or minus-end. Overall, MAPs can be classified into two main categories according to their role, some promote MT depolymerization or severing while others promote MT polymerization.

MT depolymerization is mainly promoted by few members of the Kinesin protein family, such as kinesin-8, kinesin-13 and kinesin-14 (only in yeast). Kinesin-13 proteins (as for example MCAK "mitotic centromere-associated kinesin") are not processive kinesins (they do not walk on microtubules). Instead, they use the energy derived from ATP hydrolysis to remove tubulin dimers from the microtubule ends. By doing so, they reduce the length of the microtubule plus-end GTP-cap promoting the destabilization of the entire microtubule (Desai et al. 1999; Moores et al. 2002; Hunter et al. 2003; Asenjo et al. 2013; Burns et al. 2014; Gardner et al. 2011). Kinesin-8 proteins have a dual activity. They can walk processively towards the MT plus-end, where they accumulate, but they also actively remove GTP-bounded tubulin dimers (using the energy of ATP hydrolysis cycles, as kinesins-13) destabilizing the MT (Gardner et al. 2011; Varga et al. 2009). Another class of proteins, the EB (End Binding) proteins, promote microtubule catastrophe *in vitro*. *In vivo,* they make microtubules more dynamic, but, surprisingly, they seem to promote microtubule elongation, maybe by competing with MT depolymerases (reviewed in Akhmanova & Steinmetz 2015). On the other hand, EBs are very important plus-end associated proteins involved in the recruitment of many other plus-end targeted proteins, playing an essential

role in the regulation of the MT plus-end dynamics (reviewed in Kumar & Wittmann 2012). Microtubule severing enzymes (katanin, fidgetin and spastin) are also actively involved in microtubule destabilization. By cutting the microtubules, MT severing enzymes increase the density of microtubules and generate unprotected MT tips (that can be easily depolymerized in absence of stabilizing proteins) (Sharp & Ross 2012). Besides the action of the microtubule depolymerizing MAPs, the contact of the microtubule growing tip with different surfaces can generate pushing forces that are able to slow down the MT growing velocity and induce the catastrophe (Janson et al. 2003).

Proteins that promote MT polymerization may do so by promoting stabilization, as many 'classical' MAPs, or by more directly facilitating the incorporation of new tubulin dimers to the microtubule tip. XMAP215 family of proteins (ch-TOG in human) is an example of this second group. XMAP215 associates with the plus-end of growing microtubules and recruits tubulin dimers, accelerating the rate of tubulin incorporation (Brouhard et al. 2008).

Microtubule stabilizing factors can prevent the activity of the MT-depolymerizing factors or promote MT rescue events. CAMSAP protein family and MCRS1 are MT minus-ends protecting factors (reviewed in Akhmanova & Hoogenraad 2015). These proteins may also function by competing with microtubule depolymerizing factors for MT end binding (already proposed for MCRS1 and MCAK for example (Meunier & Vernos 2011)). CLIPs (Cytoplasmic Linker Proteins) and CLASPs (Cytoplasmic Linker Associated Proteins) proteins promote microtubule rescue. CLIP proteins have been shown to promote MT rescue *in vivo* (Komarova et al. 2002). CLIP-170, together with EB1, recruits CLASP proteins to the microtubule plus tip (Akhmanova et al. 2001; Kumar et al. 2009). CLASP can also intrinsically interact with the microtubule lattice. CLASP proteins have been shown to promote MT rescue events and decrease the rate of catastrophes by associating stably with the microtubule lattice and incorporating new tubulin dimers to the microtubule plus-end (Al-Bassam et al. 2010). The *Saccharomyces pombe* CLASP protein cls1p binds but does not track the MT lattice of growing MTs, forming discrete regions along the microtubule. When microtubules undergo catastrophe, rescue events

occur at the regions in which cls1p is accumulated, showing that it is a MT rescue-promoting factor (Al-Bassam et al. 2010).

# 3. The organization of the mitotic spindle

As mentioned earlier, during mitosis, MTs are nucleated at different regions of the cell and need to be actively organized in order to build up a bipolar spindle. In terms of microtubule organization, two main processes cooperate to establish a bipolar spindle: spindle pole separation or establishment of the spindle bipolarity (Chapter 3.b) and MT-ends focusing at the spindle pole or spindle pole formation and maintenance (Chapter 3.c). Several microtubule dependent motor proteins belonging to the kinesin and Dynein families play essential roles in these processes (see Chapter 3.a).

## 3.a. The motor proteins

### 3.a.i. Kinesins

The first kinesin, kinesin-1 (now named KIF5B), was identified from squid giant axons in 1985 (Vale et al. 1985). From this date to the present, several kinesins have been identified and form the kinesin family of microtubule dependent motor proteins. They are characterized by a conserved ATP dependent motor domain that interacts with microtubules and, in most cases, use the energy derived from ATP hydrolysis to walk along them in a directional way.

KIF5B, as well as several other kinesins, is constituted by globular motor domain at the N-terminus linked (through a “neck” region) to a coiled-coil region (called “stalk”) important for dimerization and a C-terminal tail domain containing recognition sequences for binding regulatory proteins and cargos, that is highly divergent and specific for each kinesin (reviewed in Welburn 2013; Cross & McAinsh 2014). Some kinesins adopt a tetrameric conformation in which two dimers interact head to tail through their coiled coil stalk domains. This is the case for the mitotic kinesin Eg5. Typically, processive dimeric and tetrameric kinesins move along microtubules by a stepping cycle, coupled with an ATP hydrolysis cycle occurring in the head domains (Fig.I.5) (for extensive reviews look at Friel & Howard 2012; Cross & McAinsh 2014).

The number and function of kinesins is very wide across different species (reviewed in Vicente & Wordeman 2015). 45 kinesin family members have been identified in human and classified in 14 families according to their sequence similarities and functions (Lawrence et al. 2004), although other classifications exist.

Most of the kinesins have their motor domain at their N-terminus and walk towards the microtubule plus-end (kinesins-1 to 12), however other members of the family present a minus-end directed motility activity (kinesin-14), which is associated to a C-terminal motor domain, and others instead have a central motor domain and microtubule depolymerizing activity (kinesin-8 and kinesin-13 family proteins).

Several kinesins are required for the following processes in mitosis:

**Centrosome separation and spindle bipolarization:** During prophase, Eg5 (kif11, a kinesin-5 member) is recruited to the centrosomes and it separates them by interacting with antiparallel microtubules and sliding them apart. Another kinesin, hKLP2 (kif15, a kinesin-12 member), also contributes to spindle bipolarization after nuclear envelope breakdown during prometaphase and metaphase (see chapter 3.b for more details).

**Spindle pole focusing:** The minus-end directed Kinesin-14 family motors are required for the organization and focusing of the microtubule minus-ends at the spindle poles and for the attachment of the centrosomes to the poles. This process will be detailed in chapter 3.c.

**Chromosome capture and congression:** The interaction between the chromosome arms and the MTs is mediated by a specific group of kinesins called chromokinesins. The chromokinesins group is composed by members of the kinesin-4 (kif4), -10 (kif22 or Kid) and -12 families (kif15 or hKLP2). Due to their plus-end motor activity, chromokinesins push the chromosomes away from the spindle poles, towards the metaphase plate. Also non-chromokinesins kinesins are involved in chromosome alignment, such as members of the kinesin families 7 (Kif10 or CENP-E), 8, (Kif18-A), 13 (Kif2B, Kif2C or MCAK) and 14 (KifC1)

(reviewed in Vanneste et al. 2011b; Vicente & Wordeman 2015; Cross & McAinsh 2014).

**Microtubule dynamics regulation:** As mentioned in chapter 2.c, some kinesins (like MCAK) promote microtubule depolymerization while others promote stabilization or bundling.

**Chromosome segregation:** By regulating microtubule dynamics at the kinetochores and the spindle poles, some kinesins are involved in generating a pulling force from spindle poles to kinetochores. Some kinesins are also present at the central spindle in anaphase, where they generate pushing forces that slide antiparallel MTs apart powering anaphase B and contributing to separation of chromosomes (reviewed in Cross & McAinsh 2014).

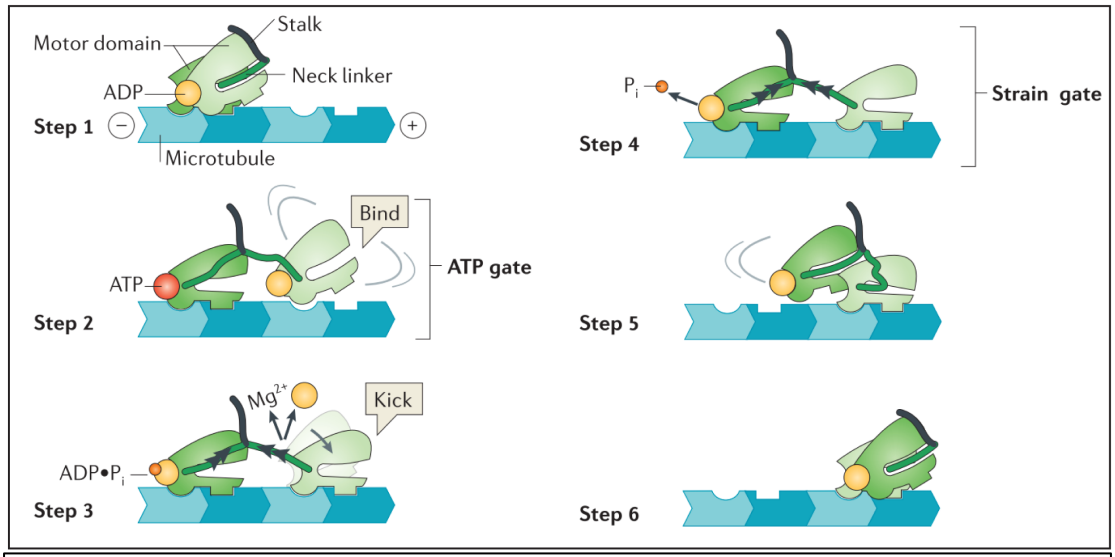


**Fig. I.5. The mechanical processivity of kinesins:** two coupled kinesin heads alternately generate force, is coordinated by two 'gates': the ATP gate and the strain gate. Kinesins pause between steps in an 'ATP waiting state', with one head bound to the microtubule and the other (tethered) head detached and parked in some way44,181 (step 1). ATP binding to the microtubule-bound head in the ATP-waiting state releases the tethered head (light green) from its parked state and effectively starts a race between the two heads, with the tethered head needing to find its next binding site and to undergo microtubule-activated ADP release before hydrolysis and organic phosphate (Pi ) release is complete on the bound head (dark green). We refer to this as the ATP gate (step 2). Once the tethered head finds its next site, it generates a kick, which is coupled to Mg2+ release (step 3). Bridging between two binding sites, which are 8 nm apart along the microtubule, requires the neck linker on the leading head to undock and places both neck linkers under strain. Backwards strain on the neck linker of the leading head inhibits ATP binding to that head until the trailing head detaches. We refer to this as the strain gate (step 4). Release of the trailing head from the microtubule (step 5) then enables the ATP waiting state to regenerate (step 6). Figure and legend reproduced from (Cross & McAinsh 2014)

### 3.a.ii Dynein

Dyneins are molecular motor complexes that move towards the minus-end of the microtubules. More than 16 Dynein heavy chain genes (the biggest subunit of the Dynein complex) have been identified in humans. 14 of these Dyneins are axonemal Dyneins, involved in the movement (beating) of cilia and flagella, but not in cargo transport (Yagi 2009). Only 2 Dyneins are involved in cargo transport along the microtubules: intraflagellar transport (IFT) Dynein (Dynein 1B or Dynein 2) and cytoplasmic Dynein or Dynein 1 (identified by (Paschal 1987; Paschal & Vallee 1987)). Cytoplasmic Dynein is involved in many essential activities during interphase, as transport of organelles (endosomes, peroxisomes, autophagosomes, mitochondria, peroxisomes, mitochondria and lipid droplets) (Allan 2011) and mRNAs (Holt & Bullock 2010), assembly and transport of stress granules and processing bodies involved in RNA homeostasis (Loschi et al. 2009). In this chapter I will focus on cytoplasmic Dynein in mitosis (the only isoform of Dynein active in the cytoplasm of eukaryotic cells), whereas I will refer to IFT Dynein in chapter 5.

During mitosis, Dynein localizes to different structures and covers a wide range of functions including spindle positioning and orientation, spindle pole focusing and organization, spindle microtubules minus-ends link to the centrosome, chromosome movement, spindle anaphase checkpoint (SAC) silencing and protein transport to the spindle poles (reviewed in Kardon & Vale 2009; Allan 2011).

**Dynein structure:** The Dynein complex is a ≈1.6 MDa complex composed of a heavy chain dimer and two each of five non-catalytic sub-units: Dynein intermediate chain (IC), light intermediate chain (LIC) and the light chains 8 (LC8), 7 (LC7) (also known as roadblock) and TCTEX1 (T-complex testis-specific protein 1) (Fig.I.6.A). Two heavy chains form a homodimer at their N-terminus, which then interact with the other subunits.

The heavy chain is the largest subunit of Dynein (≈500 KDa) and contains the microtubule binding domain and the ATPase activity (The ATP hydrolysis cycles generate the energy for the stepping of the motor protein on the microtubule). The heavy chain is a member of the AAA+ protein superfamily (Neuwald et al. 1999). It indeed contains an AAA+ domain (an AAA hexameric ring, from AAA1 to AAA6, in

which the AAA modules are not identical), that hydrolyzes ATP (reviewed in Kardon & Vale 2009; Cianfrocco et al. 2015; Bhabha et al. 2016). The microtubule-binding region is a small α-helical domain at the end of a coiled coil extension that emerges from the AAA+ (Goodenough & Heuser 1984; Gee et al. 1997; Carter et al. 2011; Kon et al. 2011). Dynein binds to the microtubule in the cleft between α- and β-tubulin (Carter et al. 2008; Redwine et al. 2012). Together, the AAA+ and the coiled coil domains define the C-terminal part of Dynein. A Dynein intermediate chain dimer and a light intermediate chain dimer bind directly to the Dynein heavy chains. Finally, dimers of LC8, LC7 and TCTEX1 are associated to the intermediated chains. In vertebrates, ICs, LICs and LCs are encoded by two different genes each. Moreover, alternative splicing variants may exist for the ICs and LICs, generating a large diversity of Dynein complexes that may confer some functional specificity, maybe by interacting with different cargos (reviewed in Allan 2011). Most of the Dynein regulators and adaptor proteins, like Dynactin and Nudel/NudE, interact with the IC (McKenney et al. 2011; Nyarko et al. 2012; Wang et al. 2013).

**Dynein processivity**: Some controversy in the field exists about the processivity of Dynein *in vitro*. Studies showed that vertebrate Dynein bound to beads is processive. In contrast, others studies using individual molecules did not detect processive movement or a very weak one (reviewed in Jha & Surrey 2015). The dimerization of two Dynein head domains is anyway needed for the processivity of the motor, which seems to move in a alternating manner (Reck-Peterson et al. 2006). Studies using yeast Dynein showed that it moves with 8nm-long steps (which correspond to the distance between spacing tubulin dimers, 8.3), with occasionally steps of 32nm and some backwards steps (Reck-Peterson et al. 2006; Mallik et al. 2004; DeWitt et al. 2012; Qiu et al. 2012). Dynein can also step laterally to the adjacent protofilament (Reck-Peterson et al. 2006).

### 3.a.iii. Dynein adaptors and regulators

**Dynactin:** Dynactin (Dynein activator) was first identified as a factor that activates the Dynein-mediated vesicle transport (Gill et al. 1991; Schroer & Sheetz 1991). Dynactin was then found to be the main regulator of Dynein. It enhances the processivity by tethering Dynein to the microtubule and increasing the time of the

interaction without affecting the velocity of movement neither the ATPase kinetics (King & Schroer 2000; Ross et al. 2006; Culver-Hanlon et al. 2006; Kardon et al. 2009; Tripathy et al. 2014). Dynein-Dynactin processivity is increased even more in the presence of a cargo and BicD2 (McKenney et al. 2014; Schlager et al. 2014). Dynactin also promotes Dynein targeting to specific locations. The average velocity of the processive runs of Dynein-Dynactin is dependent on the concentration of ATP (Ross et al. 2006). The Dynein-Dynactin complex is also able to move bi-directionally (towards the plus and the minus-end) and perpendicularly to the microtubule, changing from one protofilament to the neighbor one (Ross et al. 2006).

Dynactin is a 1MDa complex comprising 11 different subunits (Fig.I.6.b). p150 (also known as p150$^{glued}$) is the biggest subunit of Dynactin and contains the two microtubule interaction domains, a Gly-rich domain (CAP-Gly) and a basic region at the N-terminus (Culver-Hanlon et al. 2006; Tripathy et al. 2014). A dimer of p150 forms the flexible arm of Dynactin and interacts directly with Dynein ICs (Vaughan & Vallee 1995). A barbed structure is composed by a dimer of p150, a tetramer of p50 (Dynamitin) and a molecule of p24. The N-terminus of p150 is associated with a short filament of actin-related protein 1 (ARP1), that is the central scaffold of Dynactin. In turns, the ARP1 filament contains ARP11, p62, p25 and p27 at the pointed end (reviewed in Kardon & Vale 2009; Cianfrocco et al. 2015).

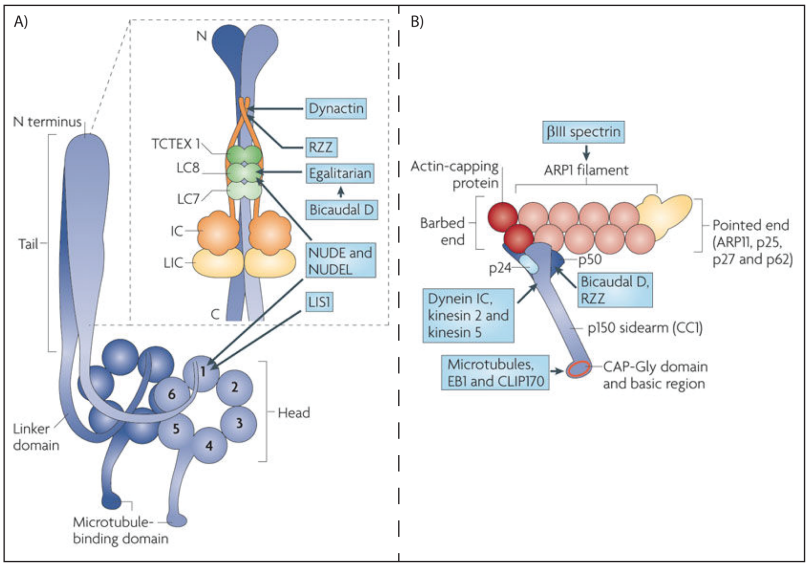

**Fig. I. 6. Dynein and Dynactin complexes: A**) Dynein complex; B) Dynactin complex. Figure reproduced from (Kardon & Vale 2009)

Together with Dynein, Dynactin has been shown to be involved in cell motility, spindle pole focusing, silencing of the SAC, centrosomes anchoring to the NE, spindle force generation (Schroer 2004). The function of the Dynein-Dynactin complex has been addressed extensively by overexpressing p50 to promote the disruption of the Dynactin complex or using the anti-Dynein 70.1 antibody, which recognizes Dynein IC and impairs its interaction with Dynactin. The overexpression of p50 promotes the release of p150 without degradation of the protein (Echeverri et al. 1996; Jacquot et al. 2010; Raaijmakers et al. 2013; Melkonian et al. 2007; Wittmann & Hyman 1999), which is still able to interact with the Dynein complex, maybe interfering with its activity. A study of the specific contribution of each of the Dynein and Dynactin subunits and the complex' adaptor proteins using specific siRNAs, was recently reported by Raaijmakers and collaborators (Raaijmakers et al. 2013). They described that the silencing of Dynactin subunits did not affect mitosis progression (until chromosome alignment at the metaphase plate), chromosome alignment, microtubule-kinetochore attachment and force generation within the spindle or spindle pole focusing (in U2OS cells). However, they observed defects in centrosome anchoring to the NE in G2/prophase and SAC silencing (cell arrested in metaphase). Considering that all the experiments have been done by silencing individual subunits of the complexes, a putative additive effect of silencing some subunits in combination cannot be excluded, as it is the case for the Dynein light intermediate chains 1 and 2. It is possible that some redundancy between the Dynactin subunits exists and that silencing only one subunit at the time may not be sufficient to impair some specific activities of the whole complex. Further work is still needed to establish the specific involvements of each of the Dynactin-Dynein complexes and their subunits in diverse cellular processes.

Several additional proteins have been described to play essential roles in the regulation of Dynein or Dynein-Dynactin activity, but a precise overview of the specific functions of each one is still under construction. Here I shortly introduce

some of them.

**LIS1 and NudE/NudEL** (gene names Nde1/NdeL1) interaction with Dynein induces a persistent-force state of the motor. In contrast, NudE interaction with Dynein alone inhibits Dynein force production (McKenney et al. 2010). NudE interacts with Dynein IC and recruits LIS1. NudE and NudEL are involved in the recruitment of Dynein and LIS1 to centrosomes and to kinetochores (McKenney et al. 2010; McKenney et al. 2011). During mitosis, LIS1 and NudE/NudEL are involved in chromosome alignment, spindle orientation, spindle pole focusing and centrosome anchoring to the spindle pole (Faulkner et al. 2000; Stehman et al. 2007; Vergnolle & Taylor 2007; Raaijmakers et al. 2013; Liang et al. 2007; Siller et al. 2005). A binding competition to Dynein IC seems to exist between NudE and p150 (McKenney et al. 2011; Nyarko et al. 2012).

**BICD2** directly interacts with Dynein and Dynactin, increasing their processivity (Schlager et al. 2014; McKenney et al. 2014; Hoogenraad et al. 2001; Urnavicius et al. 2015; Splinter et al. 2012). In late G2, Dynein is recruited to the NPCs by BICD2 (that interacts with RanBP2) and promotes centrosome attachment to the NE (Splinter et al. 2010; Raaijmakers et al. 2013).

**Spindly** recruits Dynein-Dynactin complex to the kinetochore and is transported towards the spindle poles in a Dynein dependent manner. Absence of spindly impairs the silencing of the SAC (dependent on the targeting of Dynein to the kinetochore) promoting cells arrest in metaphase (Griffis et al. 2007; Zw et al. 2008; Gassmann et al. 2010; Ying et al. 2009; Raaijmakers et al. 2013; Barisic et al. 2010). In addition, Spindly seems to also be involved in spindle orientation (Ying et al. 2009).

## 3.b. Establishment of the spindle bipolarity

The mechanism driving the assembly of a bipolar spindle starts already before NEB, with the separation of the centrosomes, and continues until metaphase. The main players in centrosome separation are Dynein and the kinesin family member Eg5 (Sawin et al. 1992; Heck et al. 1993; Slangy et al. 1995). Eg5 is a plus-end directed heterotetrameric kinesin with two motor domains in each side. Eg5 can

interact with two microtubules at the same time, with a preference for those in antiparallel orientation. By walking on both MTs towards their plus-ends, Eg5 slides the two MTs apart contributing to centrosome separation and bipolar spindle organization (Kapitein et al. 2005; Kashina et al. 1997; Slangy et al. 1995; Kashina et al. 1996; Whitehead & Rattner 1998) (Fig.I.7). Before NEB, Dynein recruits Eg5 to the centrosomes, where it plays an essential role in spindle bipolarity establishment after nuclear envelope breakdown. However, Eg5 is not essential for the maintenance of bipolarity in metaphase in the presence of another kinesin, Kif15 (Kapoor et al. 2000; Cameron et al. 2006; Tanenbaum et al. 2009; Vanneste et al. 2009; Kollu et al. 2009).

The spindle bipolarity requires equilibrium of inward and outward forces that were shown to be in large part generated by Dynein and Eg5 respectively. The inhibition of Eg5 (loss of outward forces) results in the formation of monopolar spindles (Mayer et al. 1999), due to the activity of the Dynein complex, which generates antagonistic inward forces (Saunders & Hoyt 1992; O'Connell et al. 1993; Mountain et al. 1999; Mitchison et al. 2005; Tanenbaum et al. 2008; Ferenz et al. 2009). Consistently, the double inhibition of Dynein and Eg5 rescues spindle bipolarity in mammalian cells (Mitchison et al. 2005; Tanenbaum et al. 2008; Ferenz et al. 2009; Raaijmakers et al. 2013). This result also indicates that additional factors must drive bipolar spindle assembly. Indeed, additional players have been identified, such as hKLP2/KIF15.

The growing microtubules themselves also generate pushing forces involved in the separation of the spindle poles (Mitchison, Maddox, Gaetz, Groen, Shirasu, Desai, Salmon & M. T. Kapoor 2005).

## 3.c. Spindle pole focusing

Within the spindle, the microtubules are oriented with their minus-end towards the pole. At the poles the minus-ends get focused in a variable tight fashion in large part depending on the presence or absence of centrosomes. This indicates that even in the absence of the strong MTOC activity of the centrosomes, a mechanism exists for promoting this organization and indeed several factors (motor and non-

motor proteins) were found to be involved in it. Interfering with the activity of these proteins indeed impairs the formation of the spindle poles and/or the maintenance of their integrity, both in absence and presence of the centrosome. Two main microtubule motor protein complexes are responsible for focusing microtubule minus-ends to the spindle poles and for the maintenance of their organization: Kinesin-14 (Ncd in *drosophila*, XCTK2 in *Xenopus* and HSET in humans) and Dynein. These motors alone, or in complex with their partners, can bind to two microtubules through their motor domain and a specific microtubules binding domain. By walking towards the minus-end of one of the microtubules, while keeping the attachment to the other one, they organize the microtubules and crosslink them at the minus-ends (Fig.I.7). These two motor complexes have specific and overlapping functions. Their specific role and relevance varies between organisms and between mitosis and meiosis.

In centrosome containing cells (human and Xenopus cells), the Dynein complex is the main spindle pole organizer, together with the non-motor protein NuMA (Nuclear protein that associates with the Mitotic Apparatus). The current model is that Dynein captures non-centrosomal microtubules and transport them along other microtubules towards their minus-ends. Interfering with Dynein-Dynactin impairs MT minus-ends focusing in asters formed in human cells and Xenopus egg extracts as well as spindle pole focusing in the presence or absence of centrosomes in cells and Xenopus egg extracts (Gaglio et al. 1996; Gaglio et al. 1997; Heald et al. 1996; Walczak et al. 1998; Echeverri et al. 1996; Wittmann & Hyman 1999; Mitchison, Maddox, Gaetz, Groen, Shirasu, Desai, Salmon & M. T. Kapoor 2005). Some controversy exists about the specific contribution of NuMA and Dynactin to the process of MT minus-end focusing at the spindle pole and maintenance of the spindle pole integrity. NuMA interacts with the Dynein-Dynactin complex, which transports the protein to the spindle pole, where it accumulates (Merdes et al. 1996; Merdes et al. 2000; Lydersen & Pettijohn 1980) and play a critical role in proper pole focusing (Lydersen & Pettijohn 1980; Merdes et al. 1996; Merdes et al. 2000; Gaglio et al. 1996; Silk et al. 2009; Khodjakov et al. 2003). In human cells, NuMA is necessary for the capture and transport of non-centrosome associated

microtubules minus-ends towards the spindle poles (Merdes et al. 2000; Khodjakov et al. 2003). In contrast, in mouse primary fibrolasts, NuMA is not required for microtubule minus-ends capture and transport. Instead, NuMA is required for centrosome attachment to the spindle pole and spindle pole integrity maintenance in these cells (Silk et al. 2009). As detailed in chapter 3.a.iii, although a role of Dynactin in spindle pole assembly, in association with Dynein, has been historically accepted, new data suggest that the Dynactin complex may not be required. Disruption of the Dynactin complex by addition/overexpression of p50 leads to the accumulation of free p150 (Melkonian et al. 2007; Jacquot et al. 2010) that could compete with other molecules, such as Nde1/L1 (known to be essential for pole focusing), for Dynein interaction (McKenney et al. 2011). This could induce indirect effects on other specific Dynein complexes activity. In a study made by Raaijmakers and collaborators, no defects in spindle pole focusing were observed in HeLa or U2Os cells after silencing individual Dynactin subunits (as mentioned in Chapter 3.a.iii) (Raaijmakers et al. 2013). The direct contribution of the Dynactin complex to the process of pole focusing process is therefore still unclear.

Kinesin-14 (HSET in humans or XCTK2 in Xenopus) is a minus-end directed motor involved in spindle length regulation without playing a central role in spindle pole integrity maintenance in mammals and *Xenopus* (Mountain et al. 1999; Cai, Weaver, et al. 2009; Kleylein-Sohn et al. 2012). HSET links the centrosome to the spindle pole and plays an essential role in centrosome clustering in supernumerary centrosome containing cancer cells, although this function is not evident in non-cancer cells (Kwon et al. 2008; Cai, Weaver, et al. 2009; Kleylein-Sohn et al. 2012; Chavali et al. 2016). Spindle pole fragmentation is also observed in HSET silenced cancer cells, generating acentrosomal spindle poles (Kleylein-Sohn et al. 2012).

In S2 *D. melanogaster* cells, Ncd (Drosophila Kinesin-14) is the main protein responsible for microtubule minus-end focusing at the spindle pole. In these cells, spindle poles in metaphase are dynamic structures with a continuous focusing and defocusing of the K-Fiber minus-ends (Goshima et al. 2005). Ncd plays a central

role in the focusing of the K-Fibers microtubule minus-ends at the spindle poles by crosslinking the microtubule bundles (Karabay & Walker 1999; Wendt et al. 2003; Goshima et al. 2005). Indeed, Ncd silencing results in the spreading of the spindle pole generating multipolar spindles (Goshima & Vale 2003; Goshima et al. 2005; Morales-Mulia & Scholey 2005). Ncd seems to be also involved in the capture of the K-Fibers minus-end by the plus-ends of the centrosomal-microtubules (Goshima et al. 2005). Dynein would therefore be involved in transporting these K-fibers minus-ends along the centrosomal-microtubules towards the centrosome. Dynein and Dynactin are involved in the attachment of the centrosomes to the spindle poles in these cells (Maiato et al. 2004; Morales-Mulia & Scholey 2005; Goshima et al. 2005). Although, in S2 cells, Dynein does not seems to play an essential role in maintenance of K-Fibers minus-end focused at the poles, these poles are less focused when the protein is silenced (Maiato et al. 2004; Morales-Mulia & Scholey 2005).

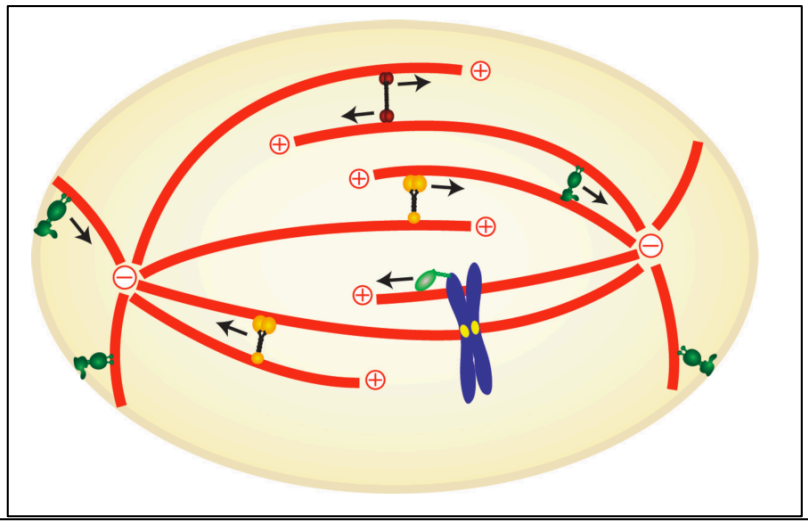

**Fig.I.7. Diverse activities of motors in the spindle:** Plus- (red) and minus-end (yellow) directed cross-linking motors that increase or decrease the overlap of antiparallel microtubules determine spindle pole separation. Cytoplasmic Dynein (dark green) in the cortex can pull on astral microtubules or focus microtubule minus-ends into poles. Chromokinesins (light green) can mediate chromosome attachment and plus end-directed movement. Figure and legend reproduced from (Gadde & Heald 2004)

## 3.d. Microtubule self-organization properties and the use of the egg extract

Microtubules in combination with their associated proteins (either motor or non-

motor proteins) have self-organizing properties (Nédélec et al. 1997). Microtubules can assemble spontaneously *in vitro* with high tubulin concentrations as well as with lower tubulin concentrations but with the addition of stabilizing drugs, such as taxol. Motor proteins alone were found to be able to provide different levels of MT organization (bundles, asters and more complex networks) depending on the protein combinations and concentration (Surrey et al. 2001; Nédélec 2002). In particular, the microtubule asters organize according to the directionality of the motor protein present: plus-end directed kinesins form MT asters with the MT plus-ends focused at the center, whereas minus-end motors (as such as kinesin-14) form MT asters with their minus-ends focused at the center (Urrutia et al. 1991; Nédélec et al. 1997; Surrey et al. 2001; Hentrich & Surrey 2010). At high concentrations, some of those kinesins can form bundles of microtubules (Nédélec et al. 1997), suggesting that the relative amount and the activation state of the motor proteins is very well regulated in the process of microtubule organization *in vivo*.

Several studies have shown that addition of microtubule stabilizer drugs (taxol or DMSO) to cell extracts or *Xenopus laevis* egg extracts (EE) leads to a massive assembly of microtubules and their organization into asters with their minus-ends focused at the center (Gaglio et al. 1996). Depletion of the activity of individual proteins induces changes in this aster organization. As an example, inhibition of Dynein, Dynactin or NuMA has been shown to abolish the minus-end focusing, impairing the formation of the aster (Gaglio et al. 1996).

The EE has been extensively used in the study of specific aspects of the spindle assembly. The basis of the system is the following: the cytoplasm of *Xenopus laevis* eggs (oocytes) is collected after crashing the eggs by centrifugation. This cytoplasm is intrinsically arrested in Metaphase 2 of meiosis, due to the presence of the cytostatic factor (CSF) from the original oocytes. One of the major power of the system that it is free of centrosomes (because they are not present in oocytes) and also of DNA (because it is removed by centrifugation). Thus, a certain volume of M2 arrested cytoplasm not surrounded by membranes is obtained, generating what we can define as “an open system”. This characteristic is a very powerful

feature, since it allows to add directly recombinant proteins, drugs or buffers, as well as deplete or inhibit specific proteins with the use of specific antibodies. This makes the EE a very useful system to perform protein depletion and rescue experiments, but also to test protein interactions using pull-down or immune-precipitation techniques. Spindle assembly can be studied in this system by adding Xenopus sperm nuclei (previously de-membranated). The sperm contains the nucleus and a centrosome, which, when incubated in CSF-EE, will induce the assembly of the spindle. At start the spindle will be monopolar and eventually becomes bipolar. The extract is a powerful tool to study mitotic spindle assembly in presence of two centrosomes because it can be cycled. To do so, sperm nuclei and calcium are added to the EE to synchronize it in interphase. After 90 minutes at 20ºC, the addition of fresh CSF-EE to the interphase EE induces the cycling and the entry into mitosis.

A third application, and one of the most important for our studies, is the possibility to independently study the centrosomal and the RanGTP mediated MT assembly pathways, by adding separately centrosomes or RanQ69L-GTP (a mutant version of Ran that cannot hydrolyze GTP (Heald et al. 1997)). Addition of RanQ69L-GTP mimics the chromosome dependent microtubule assembly pathway that dominates in meiosis but also exist in mitosis (see above). Interestingly, these microtubules with M-phase dynamic properties initially get organized forming asters (in a similar way as taxol microtubules do), but with time they evolve into more complex structures called mini-spindles (because of their similarities in organization with a bipolar spindle) (Carazo-Salas et al. 1999). Therefore this system is a good tool to identify proteins and mechanisms involved in spindle assembly as well as to address the process of spindle assembly as a self-organization process.

# 4. Chaperones, co-chaperones and their roles

## 4.a. The chaperone machinery

Chaperones are proteins that play a critical role in protein folding and thereby are key actors in the protein quality control machinery of the cell. They assist in folding nascent proteins, in protein degradation and translocation across membranes, and they also prevent protein aggregation or promote disaggregation. In addition, they also function in the assembly/disassembly, or in the stabilization/destabilization, of protein complexes. The general activity of the chaperones is to change protein conformation, in most of the cases by using energy derived from ATP hydrolysis. Many chaperones are upregulated in stress conditions and therefore named stress proteins or heat-shock proteins (HSPs). The HSPs are classified in several families, and named according to their size: sHSP (small HSPs) HSP40 (co-chaperones or DnaJ proteins), HSP60, HSP70, HSP90 and HSP100 (Bukau et al. 2006). In general, HSP60s proteins are involved in early stages of protein folding and HSP90s in integrating signaling functions, acting at late stages of protein folding and sending proteins to degradation. HSP100s cooperate with the protease ring or the HSP70s for protein unfolding and disaggregation. Finally, HSP70s coordinate several cellular functions, like protein unfolding, degradation, disaggregation and refolding. The activity of HSP70 is regulated by co-chaperone proteins belonging to the Hsp40 family (reviewed in Saibil 2013).

Several HSPs have been found to play specific roles in spindle assembly. Hsp70 and Hsp110 are involved in spindle length control (Makhnevych & Houry 2013). Additionally, Hsp70 and Hsp90 were shown to interact with PLK1 during mitosis and regulate the function of mitotic centrosomes (Fang et al. 2016; Chen et al. 2014; De Cárcer et al. 2001; Lange et al. 2000; Martins et al. 2009; Wang et al. 2009). Finally, Hsp72, an HSP70 family member, is targeted to the spindle by Nek6 and is involved in K-fiber assembly (O'Regan et al. 2015).

Although HSP70 family members are involved in a large number of specific processes in the cell, there are only 11 members in humans and they share a very

conserved structure. Despite their variety of specific functions, HSP70 proteins have a high promiscuity for interactions. This is reverted to a specific and regulated mode by the HSP40s or J-proteins and the NEFs (Nucleotide Exchange Factors), both essential for the functionality of HSP70. 13 NEFs and more than 40 HSP40s exist in humans, with a high diversity of sequences. In a typical folding cycle (Fig.I.8), HSP40 proteins interact with a specific "client" protein and delivers it to the ATP associated HSP70 that is in an "open" state (that can interact with the J-domain of HSP40). The HSP40 stimulates the ATPase activity of HSP70 (that is intrinsically very low), and induces a conformational change of HSP70 to a "closed" state (that interacts stably with the client protein) while HSP40 is released. The energy obtained from ATP hydrolysis is used to generate a conformational change of the client protein. Then, a NEF protein interacts with the HSP70 and stimulates the dissociation of the ADP. Finally, a new molecule of ATP is incorporated, inducing the dissociation of the client protein (that has low affinity for the ATP-HSP70) and the NEF (reviewed in Fan et al. 2003; Kampinga & Craig 2010).

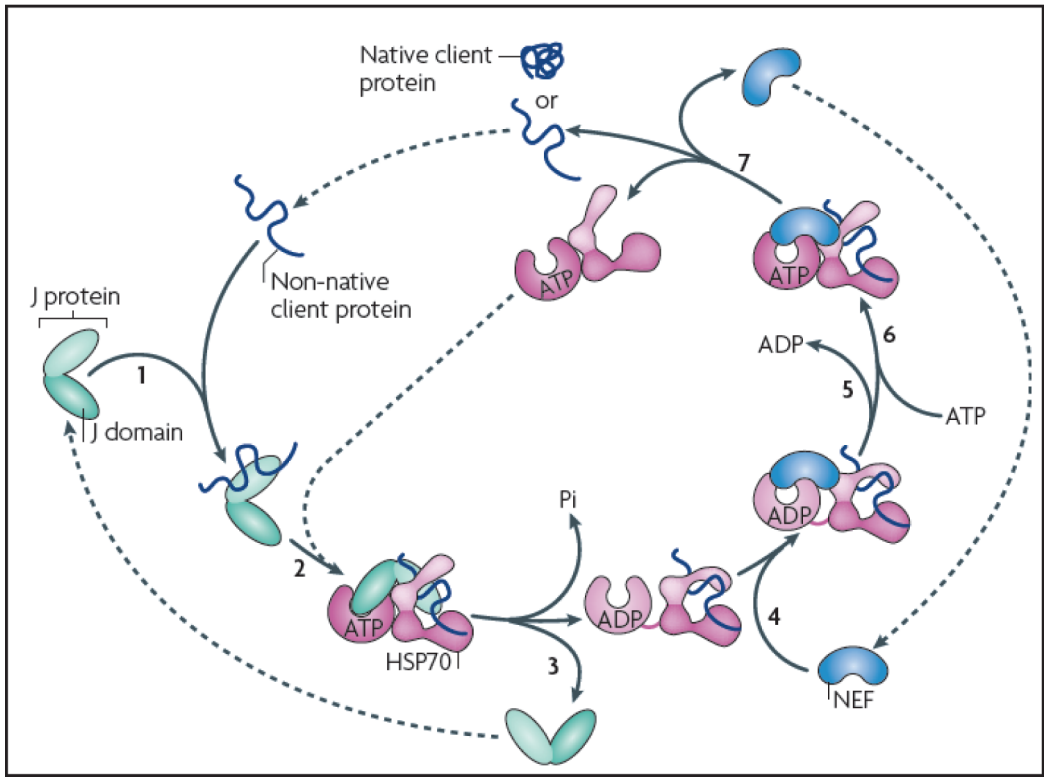

**Fig.I.8. HSP-70 and HSP-40 cycle:** The mode of action of the heat shock 70 kDa protein (HSP70) core machinery, based on *in vitro* refolding studies of denatured proteins. J proteins bind to client proteins through their peptide-binding domain (1) and interact with HSP70–ATP through their J domain (2). The client rapidly, but transiently, interacts with the 'open' peptide-binding site of HSP70. ATP hydrolysis is stimulated by both the J domain and client, causing a conformational change in HSP70 that closes the helical lid over the cleft and stabilizes the client interaction, and the J protein then leaves the complex (3). A nucleotide exchange factor (NEF), which has a higher affinity for HSP70–ADP than HSP70–ATP, binds HSP70 (4). The ADP then dissociates through distortion of the ATP-binding domain (5), after which ATP binds to HSP70 (6). The client is released because of its low affinity for HSP70–ATP (7). ATP binding to HSP70 is favored as cellular ATP concentrations are typically much higher than those of ADP. If the native state of the client is not attained on release, the J protein rebinds to its exposed hydrophobic regions and the cycle begins again. Figure and legend reproduced from (Kampinga & Craig 2010)

## 4.b. The Hsp40 family of co-chaperones

All HSP40 proteins share a conserved domain, the J-Domain, which defines the family and names its members (DnaJ-"subfamily letter"-"number"). The J-domain is a 70 amino acids region with a specific three amino acids motive, the HPD (His, Pro and Asp, located in the loop between the two main helices of the J-Domain), responsible for the interaction with the HSP70 proteins (Tsai & Douglas 1996; Greene et al. 1998; Jiang et al. 2007). The presence or absence of other protein domains defines the classification of the HSP40 proteins in three groups (1, 2 and 3, also named A, B and C): DnaJA- and DnaJB- proteins have an N-terminal J-domain followed by a Gly and Phe rich region, four repeats of a "CxxCxxGxxGxx" type zing finger motif (just presents in DnaJA-proteins) and a C-terminal extension responsible for binding the client proteins. The C-terminal region contains two domains, CTD-1 and CTD-2. The DnaJ proteins that diverge from this organization are classified as DnaJC- proteins (reviewed in Kampinga & Craig 2010).

Individual DnaJ proteins have specific roles in the cell (covering the whole range of HSP70 functions) and can be more or less promiscuous in client binding. Some HSP40 proteins can participate in different processes depending on their own localization and the one of the specific client protein they interact with. The presence of the J-domain (without the other domains of the protein) at a specific cellular location may be sufficient for some cellular functions, by targeting HSP70 proteins at this site, even though not all the functions of the protein can then be performed (Sahi & Craig 2007). In contrast, an unbalance ratio between HSP70 and

DnaJ or NEF proteins, due to an excess of DnaJs or NEFs, leads to the inhibition of HSP70 activity. *In vitro*, 10-20 times less HSP40 than HSP70 seems to be the most efficient ratio for protein folding stimulation, and the increase of DnaJ decreases this efficiency (Diamant & Goloubinoff 1998). A similar effect is observed in the excess of NEF *in vitro* (Nollen et al. 2000; Gässler et al. 2001). On the other hand, some HSP40 proteins have activities that are independent of the J-domain, and therefore also most probably independent of HSP70. Prevention of polyQ protein aggregation *in vitro* by DnaJB6 and DnaJB8 is an example of a J-domain independent function (Hageman et al. 2010), explained in the following sub-chapter.

## 4.c. DnaJB6

DnaJB6, also known as MRJ, HSJ2 and MSJ1, is a HSP40 co-chaperone from the class 2 or B, as the name indicates. Two different isoforms of DnaJB6 are present in human, a short (DnaJB6-S; accession number: NP_005485.1. ; NM_005494.2.) and a long isoform (DnaJB6-L; accession number: NP_490647.1. ; NM_058246.3), generated by alternative splicing. DnaJB6-S has a specific sequence of 10aa (from 241) at the C-terminus, whereas DnaJB6-L contains, instead, a sequence of 95 aminoacids (from 326) (Fig.I.8.a). Although some roles have been associated specifically to one or the other isoform, their specific function is not very clear and no distinction was made in many previous studies. The short isoform of DnaJB6 has been shown to stimulate the ATPase activity of Hsp70 in an *in vitro* ATPase activity assay (Chuang et al. 2002), confirming its activity as a co-chaperone. DnaJB6-S was shown to be expressed in all the human tissues analyzed (Fig.I.8.b): fetal brain, brain, heart, liver, kidney, lung, thymus, skeletal muscle, spleen, placenta, ovary and testis (Seki et al. 1999). The highest expression levels in mouse embryos are detected in trophoblast giant cells of the placenta, where its absence leads to the formation of keratin aggregates that eventually lead to the death of the embryo (Hunter et al. 1999; Watson et al. 2007). DnaJB6 interacts, indeed, with keratin8/18 filaments affecting their organization. Inhibition of DnaJB6 activity in trophoblast placental human cells impairs Keratin8/18 filaments degradation and

forms keratin inclusion bodies, whereas in HeLa cells induces Keratin8/18 filaments degradation (Izawa et al. 2000; Watson et al. 2007; Watson et al. 2011).

DnaJB6 has also been shown to play a role in preventing aggregation of proteins. DnaJB6 and DnaJB8 prevent aggregation of polyglutamine (PolyQ) peptides containing proteins. A group of progressive neurodegenerative disorders, including Huntington disease, are originated by the expansion of the PolyQ sequences within coding regions of different unrelated proteins (Gillis et al. 2013). DnaJB6 inhibits Huntingtin aggregation *in vitro* (independent of the J-Domain) and *in vivo* (dependent of the J-Domain) (Hageman et al. 2010; Chuang et al. 2002). Interestingly, mutations in DnaJB6 gene, that decrease the anti-aggregation propriety of DnaJB6 on the Huntingtin (Hageman et al. 2010), have been directly related to limb girdle muscular dystrophy (LGMD1D). All these mutations are contained in the G/F domain, which could be responsible for the client protein recognition (reviewed in Ruggieri et al. 2016). Studies in zebrafish using morpholino have shown that exclusively DnaJB6-L rescues muscle defects induced by its silencing (Sarparanta et al. 2012).

Interestingly, some studies have described an implication of DnaJB6 in cancer development, mainly in breast cancer. DnaJB6-L seems to suppress tumorigenicity and metastasis of breast cancer cells. The levels of the protein are decreased in aggressive breast cancer cells and its overexpression decrease the migration, invasion and motility of breast cancer cell lines. These DnaJB6 overexpressing cells show changes in secreted proteins: decrease of metastasis-promoting and tumor progression factors and increase of metastasis suppressor factors. Also DnaJB6-S could be involved in cancer in the context of hypoxia, but its specific contribution is still not clear (reviewed in Meng et al. 2016).

Finally, DnaJB6 has been found to interact with some members of the intraflagellar transport (IFT) B complex in ciliated cells. The IFT-complexes are two big complexes (A and B) in charge of the protein transport along the cilia (reviewed in Bhogaraju et al. 2013). DnaJB6 may stabilize the interaction of specific cargos (Guanylyl Cyclase 1) with the IFT complex, and be essential for their transport along the cilia (Bhowmick et al. 2009), although this interaction could be just

transient (Pearring et al. 2015). DnaJB6 interaction with IFTs is particularly interesting because some IFT-B members have been shown to be involved in mitosis. IF88, 52 and 20 seem to interact with the Dynein-Dynactin complex in mitosis. IFT88 and 52 are localized to the mitotic spindle poles and their depletion causes spindle orientation defects in HeLa and kidney cells, with additional defects in microtubule organization related to IFT88 (Delaval et al. 2011; Jonassen et al. 2008). In contrast, disruption of the IFT-A complex does not generate defects in spindle orientation (Jonassen et al. 2012).

Differential localization has been described for the two isoforms of DnaJB6 in interphase. The short isoform was indeed described to localize exclusively to the cytoplasm (although it can be translocate to the nucleus under stress conditions (Andrews et al. 2012)), whereas the long isoform localizes to the nucleus (Mitra et al. 2008; Cheng et al. 2008). A putative Nuclear Localization Signal (NLS) has been described within the DnaJB6-L C-terminus specific sequence (KRKKQKQREESKKKK). Mutation of the putative NLS (from "KRKKQKQREESKKKK" to "RPDRPETTEESKKKK") impairs the localization of the N-terminus EGFP tagged exogenous expressed protein to the nucleus (Mitra et al. 2008). Interestingly, in a study conducted in HeLa cells by Dey and collaborators, a cell cycle regulated differential expression was described for DnaJB6, with an increase of the protein expression in G2-M phase (Dey et al. 2009) (Fig.I.8.c and d). In addition, DnaJB6 was shown highly expressed in tissues with high cell division activity, as testis (Seki et al. 1999; Hunter et al. 1999). Altogether, these observations suggest a putative activity of DnaJB6 during cell division, although direct evidence is still lacking. Additionally, the existence of a putative NLS could indicate a possible relation between DnaJB6 and the Ran system, potentially also during cell division (Fig.I.8.a).

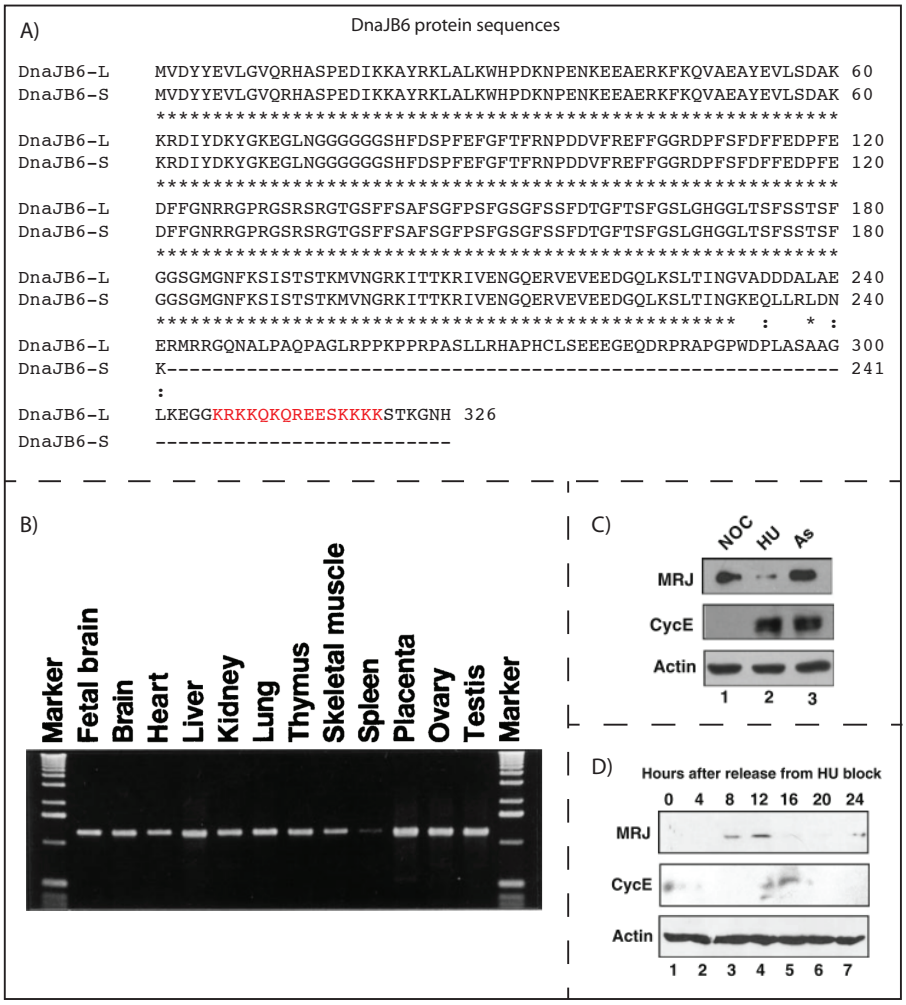


**Fig.I.9. DnaJB6 sequences and expression:** A) Human DnaJB6-S and -L sequences alignment, in red the putative NLS. B) Tissue distribution analysis of human MRJ transcript using reverse transcription-coupled polymerase chain reaction. reproduced from (Seki et al. 1999). C) Up-regulation of Mrj in M-phase. The total soluble proteins (25 lg) from nocodazole (NOC) and hydroxyurea (HU) blocked HeLa cells were analyzed with antibodies against the indicated proteins. AS, protein extract from asynchronous cells. D) Modulation of Mrj protein expression during cell cycle. HeLa cells were arrested with 10 mM hydroxyurea for 24 h and after release from the block, synchronized cells were collected at regular intervals. The soluble protein lysates (20 ug in each lane) were analyzed by western blotting with antibodies against Mrj, cyclin E, and actin proteins. Figure and legend C and D reproduced from (Dey et al. 2009)

## 5. RanGTP and cilia

As mentioned in the preface, most of the cells develop a cilium (or more) when they enter G0. The cilium is a very specialized organelle with a finger-like shape. This organelle is mainly made of microtubules and surrounded by the plasma membrane. The cilium can be either motile, and be involved in the motility of the cell or the surrounding matrix, or not motile, and work as a signaling antenna of the cell. Many ciliary proteins have to be transported from the base to the tip of the cilia, or in the opposite direction (Fig.I.9.a). The responsible of this transport are two microtubule motor proteins, kinesin-2 for the anterograde transport (towards the tip) and the Dynein complex for the retrograde transport (towards the bases). These motor proteins walk on the microtubules, which are oriented with the plus-ends towards the tip of the cilium and the minus-ends towards the base, where the centriole forms the basal body (reviewed in (Scholey 2003)). The association between the motor proteins and the cargo proteins is mediated by the IFT (intraflagelar transport) complexes A and B (for an extended review (Bhogaraju et al. 2013)). As we mentioned in the previous chapter, DnaJB6 has been shown to interact with some members of the IFT-B complex. DnaJB6 seems to be necessary for the transport of specific cargos along the cilium (Bhowmick et al. 2009).

Although there is no membrane separation between the lumen of the cilium and the rest of the cytoplasm of the cell, the proteins contained in both structures are not exactly the same. Some proteins have been shown to localize specifically inside the cilia. In addition, it has been described a size restriction protein entry to the cilium. Molecules bigger than 40-70KDa are not able to freely diffuse inside the cilium (Najafi et al. 2012; Kee et al. 2012). This selective protein transport suggests that a selective barrier exists at the base of the cilium. According to this, a putative cilia pore complex has been identified. This sequence shares some similarities with the NPC. At a first observation, the presence of nucleoporins has been described at the transition zone (an specific region at the base of the cilium), by using specific antibodies and expression of fluorescent proteins (Kee et al. 2012) (Fig.I.9.C). In addition, an electro-dense structure with a diameter similar to the NPC (≈53 nm) has been observed at the transition zone by electro-microscopy (Ounjai et al.

2013) (Fig.I.9.b). Using specific antibodies, RanGTP has been observed within the cilium (Fan et al. 2011), suggesting that a protein transport mechanism similar to the nucleo-cytoplasmatic one could exist between the cytoplasm and the cilium. In agreement with this, importin-β2 has been found within the cilia. Moreover, the transport of some specific proteins to the cilium was indicated to be dependent on the interaction with importin-β2. These proteins have a so-called Cilia Localization Signal (CLS), that when mutated prevents the localization of the protein to the cilium (Dishinger et al. 2010; Fan et al. 2007; Hurd et al. 2011). Altogether these data suggest that a RanGTP dependent protein transport could exist for intra-ciliary transport, although no RCC1 has been found in the cilium. This hypothesis however let us with two very important questions: first, if the same machinery is shared between nucleus and cilium and the signals are that similar, how can a protein be selectively transported to one location or the other? Second, considering that the cilium skeleton is made of MTs, could the RanGTP regulated MAPs be also involved in cilia assembly in a RanGTP regulated manner?

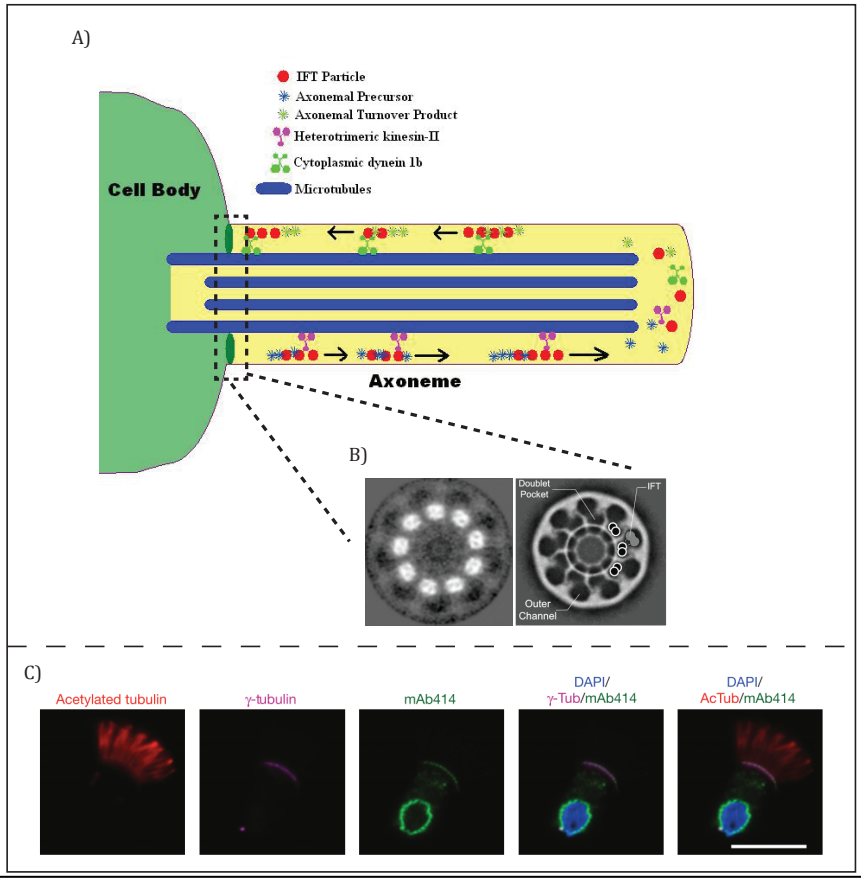


**Fig.I.10. Cilia protein transport and the putative CPC:** A) Ciliary protein transport squeme. Reproduced from wikipedia. B) The CPC in electromicroscopy: Left: Symmetrized projection of the CPC region averaged from tomograms of intact basal bodies, with contrast inverted to match that in images of the stained samples. Right: Proposed model showing how the outer channel may serve as a tunnel for intraflagellar transport system (IFT) trains (gray) moving along the microtubule doublets. Figure and legend reproduced from (Ounjai et al. 2013) C) Nucleoproteins localization to the ciliary bases: Rat trachea cells fixed and stained with antibodies to nucleoporins (mAb414, green), acetylated α-tubulin (AcTub, red) and γ-tubulin (γ-Tub, magenta). Figure and legend reproduced from (Kee et al. 2012)

# OBJECTIVES

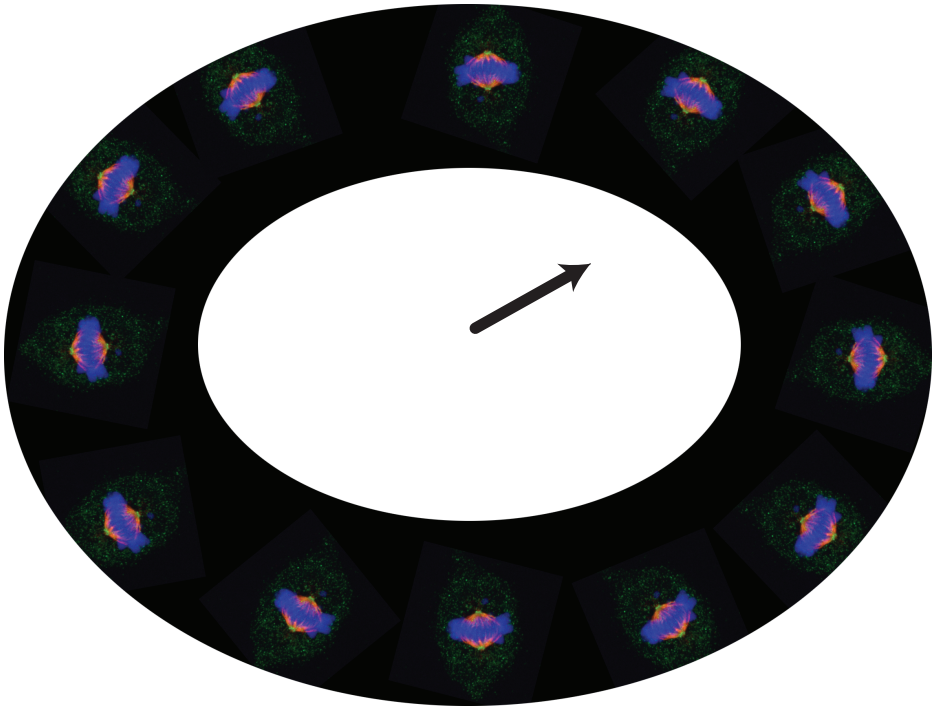

- To describe the RanGTP-MT associated proteome and correlate the dynamics of the proteome and the dynamics of MT self-organization induced by RanGTP in egg extract.

- To identify novel putative RanGTP-regulated factors involved in spindle assembly.

- To characterize functionally one of them: DnaJB6 during spindle assembly in Xenopus egg extracts and HeLa cells.

# MATERIALS AND METHODS

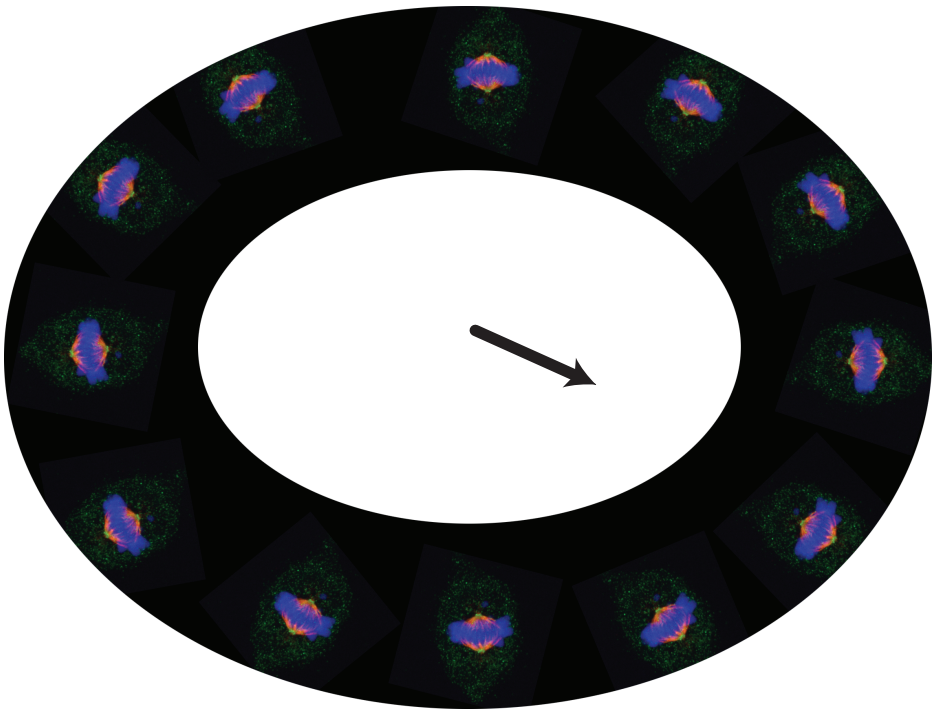

# 1. Tools and tools generation

## 1.a. Cells culture

Cells were grown at 37ºC in a 5% $CO_2$ humid atmosphere. HeLa cells were grown in DMEM 4,5g/L Glucose, with Ultraglutamine 1 (bioWhittaker, BE12-604F/U1), 10% FBS (102070-106, invitrogen) and 100units/ml penicillin and 100µg/ml streptomycin (15140-122, Invitrogen). RPE1 cells were cultured in DMEM-F12 (31330-095, gibco) supplemented with 10% FBS and 100units/ml penicillin and 100µg/ml streptomycin. Stable HeLa cells expressing H2B–eGFP/α- tubulin–mRFP were grown in the presence of 400µg/ml G418 and 20µg/ml puromycin. This cells were a gift from P. Meraldi (ETH, Zurich) (McAinsh et al. 2006).

## 1.b. Antibodies

**Primary antibodies:** Commercial antibodies: DM1A (Sigma, T6199; IF and WB-1:1000); tubulin- β (Abcam, ab6046; IF-1:200); p150 (bd transduction laboratories, 610474; IF-5µg/µl; WB-1:500); centrin (Millipore, 04-1624; IF-1:1000); TACC3 (Santa cruz, SC22773; IF-1:200); Eg5 (1:1000; 611186, BD); NUMA (Calbiochem, NA09L; IF-1:500); Importin-β/NTF97 (Abcam; ab36775-50; WB-1:500); acetylated tubulin (Sigma, T7451; IF-1:200); generic IGGs (Sigma, I5006); Ki67 (1:200; 550609 BD pharma). In-home produced antibodies hDnaJB6 (IF-5µg/µl; WB-1µg/µl); xDnaJB6 (WB-1µg/µl); HSET (1:1000); δ2-tubulin (1:100); MBP (depending on the batches); GST (depending on the batches). Gifts antibodies: Rabbit serum anti-ANT (all isoforms) was a gift from Catherine Brenner Jan (INSERM UMR-S 769-LabEx LERMIT, Universtité Paris-Sud) and was used at 1:100, rabbit anti-Arl8 was a gift from Michael Brenner (Harvard University, USA) and was used at 1:500, rabbit anti-CK2α was a gift from Claudia Götz (University of the Saarland, Germany) and was used at 1:200, rabbit anti-FOP was a gift from Erich A. Nigg (Biozentrum, University of Basel, Switzerland) and was used at 1:500, rabbit monoclonal anti-B23 was a gift from Claude Prigent (CNRS UMR 6290, Rennes and Université de Rennes 1) purchased from Abcam (ab52644) and was used at 1:500, rabbit anti-HCFC1 H12 was a gift from Winship Herr (Unversité de Lausanne, Switzerland) and was used at 1:800.

**Secondary antibodies:** all of them used at 1:1000 for IF and 1:10000 for WB. Alexa Fluor 488 Goat, anti-mouse (ref: A11017; Invitrogen). Alexa Fluor 488 goat, anti rabbit (ref: A11034; Invitrogen). Alexa fluor 568 anti-mouse (ref: A11031; Invitrogen). Alexa fluor 568 goat, anti-rabbit (A11036; life technologies S.A). Anti-mouse 800; (ref: 926-32212; Licor). Goat anti-rabbit 800 (ref: 10733944; Fisher Scientific). Alexa fluor 680 goat, anti-Rabbit (ref: A-21109; Invitrogen). Alexa fluor 680 goat, anti-mouse (ref: A21058; Life technologies).

## 1.c. Microscopy

For IF quantifications and EE confirmations: 40X and 63X objectives on an inverted DMI-6000-B Leica wide-field fluorescent microscope, equipped with a Leica DFC 360FX camera.

For confocal images: 63X objective on a Leica TCS SPE microscope equipped with the following laser lines: 405 (DAPI, Hoechst), 488 (GFP, FITC), 532 (mRFP, DsRED, Cy3, TRITC, TexasRed), 635 (Cy5, DRAQ5).

For time-laps experiments: 40X objective on a Zeiss Cell Observer HS inverted microscope equipped with a Zeiss AxioCam MrX camera and a temperature, humidity and $CO_2$ control systems.

## 1.d RACE-PCR

mRNA was obtained from *Xenopus leavis* EE. cDNA was generated by RT-PCR using an oligo-dT coupled with an adaptor sequence (5'-GGCCACGCGTCGACTAGTAC +17 "T"-3'). In order to describe the 3' end of the mRNA sequence, the cDNA was amplified by PCR using as primers the adaptor sequence and a sequence in the middle of the known xDnaJB6-S isoform (a and B in parallel) (5'-GGAGGTTTCCCTGCCTTTGGCCC-3'). After obtaining the 3' end of the xDnaJB6-L mRNA, new primers were designed for both extremes of the mRNA. The definitive sequence of the xDnaJB6-L was obtained by a PCR reaction using the new primers corresponding to each extreme of the mRNA sequence (fwd 5'-ATGGTGGAGTATTACGAAGTTTTGGGAGTCC-3'; rev 5' TTAGTAGATTGGTTTGGAAGACTTCTTTTTCTTG-3').

## 1.e. Constructs

To generate the human anti-DNAJB6 antibody, a fragment of the cDNA sequence was cloned in pMAL-C2 vector (New England BioLabs) using restriction enzymes. For the xenopus proteins and antibody production, the entire xDnaJB6-L cDNA sequence was cloned in pMAL-C2 and pGEX-4T-2 vectors by a standard Gibson protocol. The following primers and restriction sites where used:

Human DnaJB6: (fwd 5'-EcoRI-CGGGACATCTATGACAAATATGGC-3'; rev 5'-AAGTCGACCAAAGGCAATCACTAG-XbaI).

Xenopus DnaJB6 in pMAL-C2: insert (fwd 5'-GGGATCGAGGGAAGGATTTCATGGTGGAGTATTACGAAGTTTTGGGAGTCC-3'; rev: 5'-TCCGAATTCTGAAATCCTTCTTAGTAGATTGGTTTGGAAGACTTCTTTTTCTTG-3'), vector (fwd 5'-GGACTCCCAAAACTTCGTAATACTCCACCATGAAATCCTTCCCTCGATCCC-3'; rev 5'-CAAGAAAAAGAAGTCTTCCAAACCAATCTACTAAGAAGGATTTCAGAATTCGGA-3').

Xenopus DnaJB6 in pGEX-4T-2: insert (fwd 5'-GGTTCCGCGTGGATCCATGGTGGAGTATTACGAAGTTTTGGGAGTCC-3'; rev 5'-GAATTCCTGGGGATCCTTAGTAGATTGGTTTGGAAGACTTCTTTTTCTTG-3') vector (fwd 5'-GGACTCCCAAAACTTCGTAATACTCCACCATGGATCCACGCGGAACC-3'; rev 5'-CAAGAAAAAGAAGTCTTCCAAACCAATCTACTAAGGATCCCCAGGAATTC-3').

## 1.f. Antibodies production

The antibodies were generated by immunizing rabbits with the previously purified peptides. The serums were affinity-purified on MBP- or GST fusion recombinant proteins covalently bound to HiTrap columns (GE Healthcare Life Sciences) following the company's protocol. α-MBP and α-GST antibodies were obtained from the same serums and by using the same system. Antibody concentration was determined by measuring the absorbance at 280 nm and confirmed by coomassie staining.

## 1.g. Protein purification

**Mbp:** Transformation was done in bl21ril bacterial cells. Cells were grown ON at 37ºC in LB media with ampicillin and then diluted in 2L LB media to a OD ≈0,2 (nm 595). Cells were grown at 37ºC until OD ≈0,6, then IPTG was added (0,5 mM) and incubated 4 hours at 25ºC. Cells were centrifuged 15min at 3500rpm (JLA 8.1000 rotor in a J-26XP Centrifuge), $4^0$C, re-suspended in cold PBS1X and re-centrifuged 15min, 4000rpm, $4^0$C (JA 25.50 rotor in a J-26XP Centrifuge). Pellets were frozen in liquid $N_2$ and stored at -80ºC. Pellets were mechanically lysated by using a mortar and a pestle, always keeping the sample in $N_2$, and resuspended in column buffer (20 mM Tris-HCl pH7.4; 200 mM NaCl; 1 mM EDTA; 1mM DTT) with protease inhibitors (11873580001. Roche). Samples were centrifuged 30min at 20000rpm (JA 25.50 rotor, J-26XP Centrifuge) at $4^0$C. 1,5 ml mix of the amylose resin beads (E8021S, NEB) (pre-washed 3 times in 10ml column-buffer) was added to the supernatant. After 2 hours of incubation at 4ºC rotating on a weal, beads were washed 3 times in 20ml of Column-buffer with protease inhibitors (beads were pelleted by centrifugation) and loaded on a column. Protein was eluted with Column buffer plus 10mM maltose and purity and non-degradation of the protein was confirmed by coomassie staining of the gels. Finally, column buffer was exchanged by 20mM tris-HCl and 200mM NaCl, proteins were frozen in liquid $N_2$ and kept at -80ºC.

**GST:** Transformation was done in bl21lys bacterial cells. Cells were grown ON at 37ºC in LB media with ampicillin and then diluted in 2L LB media to a OD ≈0,2 (nm 595). Cells were grown at 37ºC until OD ≈0,6, then IPTG was added (1mM) and incubated ON at 20ºC. Cells were centrifuged 15min at 3500rpm (JLA 8.1000 rotor in a J-26XP Centrifuge), $4^0$C, re-suspended in cold PBS1X and re-centrifuged 15min, 4000rpm, $4^0$C (JA 25.50 rotor in a J-26XP Centrifuge). Pellets were frozen in liquid $N_2$ and stored at -80ºC. Pellets were mechanically lysated by using a mortar and a pestle, always keeping the sample in $N_2$, and re-suspended in lyses buffer (PBS1X, 0,5% TritonX-100, 200mM KCL) with protease inhibitors. Samples were centrifuged 30min at 20000rpm (JA 25.50 rotor, J-26XP Centrifuge) at $4^0$C. 1,5 ml mix of the glutathione sepharose beads (17-5132-01, GE healthcare) (pre-washed

3 times in 10ml lyses buffer) was added to the supernatant. After 2 hours of incubation at 4ºC rotating on a weal, beads were washed 3 times in 20ml of washing buffer (PBS1X, 200mM KCL, 1mM DTT) with protease inhibitors (beads were pelleted by centrifugation) and loaded on a column. Protein was eluted with elution buffer (50mM tris-HCl, 200mM KCL, 1mM DTT, 10mM reduced glutathione) and purity and degradation of the protein was confirmed by coomassie staining of the gels. Proteins were frozen in liquid $N_2$ and kept at -80ºC.

# 2. General protocols

## 2.a. Western blotting

Cells were collected in PBS1X using cell scrapers after one wash in PBS1X. Cells were centrifuged 10 minutes at 1800 RPMs and pellet was resuspended in lysis buffer (PBS1X with 1% NP40) and incubated on ice for 30 minutes. Samples were centrifuged at 13200 rpms (5415 R eppendorf centrifuge) for 15minutes at 4ºC and supernatant was kept. Loading buffer was added to the samples (in a final concentration of 1X) after measuring the protein concentration by bradford. Different percentages of SDS PAGE gels were used depending on the protein of interest. 30µg of total protein per condition was loaded to the SDS PAGE gels and running was done at 100V for 10 minutes and then at 180V until necessary. Transfer was performed by using a semidry system (Amersham biosciences; 80-6211-86; TE 77 semi-dry transfer unit) to nitrocellulose membranes (of 55$cm^2$ of area) (10600002, GE Healthcare) with transfer buffer containing 20% of MTOH for 90 minutes at 60mA per membrane. Membranes were blocked in blocking solution (PBS1X, 3%milk and 0.1% tween 20) for 30 minutes, followed by 1 hour incubation with primary antibodies in blocking solution. Three washes of 10 minutes in PBS1X 0.1%-tween-20 were conducted before and after incubation with secondary antibodies (dissolved in blocking solution) for 45 minutes. Finally, membranes were developed using an Odyssey Infrared imaging system (Li-Cor)

## 2.b. Immunostaining

**General immunostaining in cells:** Cell containing coverslips (18x18mm) were washed in PBS1X 4 times (1 second) by immersion and fixed in -20ºC MTOH for 10 minutes. MTOH was washed out by immersion in PBS1X. Samples were blocked and permeabilized for 30 minutes in PBS1X, 0.1% tritonX100, 0.5% BSA (IF buffer). If buffer was removed by aspiration and primary antibodies were added (160µl per coverslip) diluted in IF buffer at the previously optimized concentrations. After 1 hour incubation, samples were washed 3 times in IF buffer and secondary antibodies and Hoechst (Hoechst 33342; ref: H3570; Invitrogen; added at 1:1000) were added if needed and incubated for 45 minutes. A 10

minutes wash in IF buffer and two in PBS1X were done and samples were mounted with 8µl Mowiol.

**DnaJB6 immunostaining in cells:** Samples were washed 4 times by immersion in PBS1X. A pre-extraction step was performed by immersion of the coverslips for 6 seconds in BRB80-1X, 0,5% triton and 1mM DSP. Excess of buffer was removed using an absorbent paper and cells were fixed in PFA 4% for 7 minutes (previously incubated at room temperature for 2 hours). The general IF protocol was applied, starting from the blocking and permeabilization step.

**Egg extract spin-downs:** samples were not washed in PBS before fixation to avoid the de-attachment of the structures from the coverslip. Fixation was done in MTOH 10 minutes at -20ºC and general IF protocol was followed.

All the protocol was conducted at room temperature avoiding that the samples got dry and the washes were done using 1 ml of buffer approximately. Samples were protected from the light since the incubation with the secondary antibodies.

**BRB80-5X:** Pipes 80mM, MgCl2 1mM, EGTA 1mM. PH=6.8 adjusted with KOH (KOH was first added to help powder dissolving and after dissolving the PH of the solution was adjusted). The solution was filtered and stored at 4ºC.

**PFA 4%:** PFA was diluted in MiliQ water from powder by mixing it at 40-50ºC without addition of extra substances to help the dilution. Once diluted it was filtered, aliquoted and kept at -20ºC.

## 2.c. Protein abundance measurements in cells

Images were taken with a 63X objective on an inverted DMI-6000-B Leica wide-field fluorescent microscope, equipped with a Leica DFC 360FX camera. Spindles were analyzed using the FIJI program as follows. Spindles were individually rotated in order to orientate the pole-to-pole axis horizontal. A rectangle of a conserved size containing both spindle poles and centered on the metaphase plate was drawn per each image. The average pixel intensity was measured for each vertical pixels line, obtaining a list of intensities, which was exported to an Excel file. The intensities lists of all the cells for a certain condition were analyzed together using the software Prism and plotted together. A graph was generated

formed by a line (corresponding to the average intensities per vertical pixel lines) and the standard deviation of each vertical pixel line. In order to compare the protein intensities at the spindle poles, the length of the spindles was equalized by subtracting the central spindle values of the larger spindles, when necessary. Protein intensities were normalized using the intensity of the tubulin (obtained following the same protocol). The graphs obtained for DnaJB6 silenced cells and control cells for each protein of interest were compared by ANOVA tests and the significance of each "horizontal" position was obtained.

## 2.d. Protein silencing

200000 HeLa or RPE1 cells were seeded on 3cm plates with 2ml of media. 24 hours after seeding, cells were transfected with 4µg of specific siRNA complementary to DnaJB6 sequence or control siRNA. Transfection protocol was conducted as detailed in lipofectamine RNAmax manufacturer protocol (13778-150, invitrogen). Two independent tube solutions were processed in parallel: 4µg of siRNA (control or DnaJB6 specific) were diluted in 200µl optimem in one tube and 4µl of lipofectamine were diluted in 200µl of optimem in the other tube. Solutions were gently mixed, incubated 5 minutes at room temperature and mixed together. After 20 minutes of incubation at RT, 400ul of the reaction were added to a 3cm plate containing 2ml of DMEM. Media was substituted with 2ml of fresh media after 6 hours incubation at 37ºC and experiments were started 48 hours after the addition of the siRNA.

siRNA sequence for DnaJB6 was 5'- CUAUGAAGUUCUAGGCGUG-3'. Control siRNA is a scrambled sequence 5'- CGUACGCGGAAUACUUCGAUU-3'.

## 2.e. **Time-lapse imaging**

Non-synchronized HeLa cells stably expressing H2B–eGFP/α- tubulin–mRFP were used for fluorescence time-lapse imaging. Cells were imaged every 4min for a total duration of 18 hours with a 40X objective on a Zeiss Cell Observer microscope. Images were then processed and analyzed with FIJI.

## 2.f. Duolink proximity ligation assay

Previously optimized antibodies α-p150 and α-DnaJB6 were used. Samples were fixed in MTOH 10min at -20ºC and IF buffer was used until the ligation reaction. The standard protocol provided by sigma was used (DUO92101-1KT, sigma-aldrich; sigma.com/duolink).

## 2.g. Statistical analysis

Statistical analyses were conducted by using the program Prism. Fisher-exact tests were used for discontinuous quantitative data of single experiments, whereas ANOVA was used for the analysis of several replicas at once. ANOVA was also used for the analysis of continuous data (as protein intensity distribution along the spindle) adapting the comparison parameters for the specific experiments. T-test was used for comparison of continuous quantitative data from two conditions. The statistics applied in each experiment are specified within the text.

# 3. Cell treatments

## 3.a. Microtubule regrowth

HeLa cells were seeded to 3cm plates with a 18x18cm sterilized coverslip to the bottom of the plate. 48 hours after transfection, nocodazole (Sigma, M1404) was added to the media in a final concentration of 2μM. After 3 hours of incubation at 37ºC, nocodazole was washed-out with 3 washes of 2ml of pre-warmed PBS1X and one of pre-wormed media. Cells were incubated in 2ml of fresh pre-wormed media at 37ºC and fixed in -20ºC MTOH for 10 minutes after different incubation times. Immunostaining of the proteins of interest was applied after fixation and cells were analyzed under a fluorescence microscope.

## 3.b. K-fibers stability

HeLa cells were seeded to 3cm plates with a 18x18cm sterilized coverslip to the bottom of the plate. 48 hours after transfection, the medium was exchanged by cold K-fiber medium (L15 medium (Sigma) supplemented with 20mM HEPES (Sigma) at pH 7.3). Cells were incubated on ice for 10, 20 or 30 minutes before fixation (10 minutes in -20ºC MTOH). Immunostaining of tubulin and DNA was performed and cells were observed under a fluorescence microscope.

## 3.c. K-fibres length

HeLa cells were seeded in a coverslip containing 3cm plate and transfected with siRNAs. 48 hour after transfection cells were incubated with 10μM STLC (Sigma, 164739) during 3 hours at 37ºC. Media was changed by 2ml of cold K-fiber media with 10μM STLC and incubated 7 minutes on ice before fixation (10 minutes in -20ºC MTOH). Immunostaining of tubulin and DNA was done and cells were imaged using the aformentioned fluorescence microscope. The length of the individual K-fibers was measured with FIJI software in three independent experiments. T-test statistical analysis has been applied to compare the average length of the k-fibers of the control and the DnaJB6 silenced cells.

## 3.d. STLC bipolarization

HeLa cells were seeded on a coverslip containing plate and transfected with specific siRNAs. 2μM STLC (Sigma, 164739) final concentration was added to the media 48 hours after transfection. Cells were incubated 2 hours at 37ºC and fixed in MTOH. Tubulin (DM1A or tubulin-β) and DNA (Hoechst) were stained by immunostaining, and samples were analyzed with a fluorescence microscope.

## 3.e. Spindle length measurement

siRNA transfected HeLa cells were fixed and tubulin (DM1A) and DNA (Hoechst) were stained by immunostaining. Pictures of individual metaphase cells were taken with the previously indicated wide-field fluorescence inverted microscope. The length of the spindle was measured using the program FIJI and T-students test was applied to compare the spindle length distributions of control and DnaJB6 silenced cells.

## 3.f. Sucrose gradient

Cells were seeded on 15 centimeters plates (one plate for control cells and another for DnaJB6 silenced cells) and transfected 24 hours later. For interphase experiments, 48 hours after transfection cells were washed once in PBS1X and recovered on 5ml of PBS1X using scrapers. For mitosis experiments, nocodazole was added at 2μM final concentration the day before and incubated for 15 hours. Nocodazole was washed-out with 3 washes of pre-wormed PBS1X (20ml) and one with pre-wormed media. Then 20 ml of fresh media was added and cells were incubated at 37ºC during 45 minutes approximately (checking the percentage of metaphase cells with a white light inverted microscope). When the majority of the cells were in metaphase, one wash in PBS1X was done and cells were recovered by shake off in 4ml of PBS1X.

Sucrose gradients experiments were performed as described in Jones, L. A. *et al.* article (Jones et al. 2014). After recovering, cells were washed twice in 10ml of BRB80-1X (centrifuging them at 600G for 5 minutes). Cells pellets were lysated in 500μl of lysis buffer (BRB80-1X, 0.5% triton-100 with protease inhibitors)

incubating 15 minutes on ice and subsequently centrifuged at 13200rpm (5415 R eppendorf centrifuge), 10 minutes at 4ºC. Supernatant was recovered and protein concentration was measured by Bradford and equalized in both samples (diluting the most concentrated one in lysis buffer). 100µl of control or DnaJB6 silenced cell lysates were transferred to a 1,5ml eppendorf tube and potassium iodide (KI) was added at the proper concentration for each condition (0, 100 or 150 µM). Samples were incubated 1 hour on ice and 45µl of sample was added to the top of the corresponding sucrose gradient columns (previously thawed at room temperature for 1 hour, to homogenize the gradient). Columns were centrifuged at 38000rpm during 5 hours at 4ºC in a SW-55Ti rotor in a ultracentrifuge Beckman optima L-100K (the exact time from the addition of the KI to the staring of the centrifugation was 1 hour). 75µl fractions were recovered (from the top of the gradient to the bottom) and diluted in sample buffer. Samples were then loaded on SDS PAGE gels followed by a Western Blotting protocol to detect the proteins of interest.

Columns preparation: Gradients were prepared in 800 µL (0.8 mL) Ultra-Clear Centrifuge Tubes, 5 x 41 mm (Part Number 344090), specific adaptors had to be used for centrifuging (Adapter, Split, Delrin, Tube, 5mm diameter (qty. 2 halves, product number 356860). Sucrose solutions were done in BRB80-1X containing protease inhibitors (1/4000), 0,1mM ATP, 1mM DTT and sucrose and KI at the adequate concentration (samples with 100 or 150µM of KI were loaded on gradients with the same concentration of the reagent). The gradient was made manually by layers, adding each layer of a specific percentage of sucrose and freezing it (with dry ice) before the addition of the next layer, finally the gradients were kept at -20ºC. From the bottom to the top, the layers were added in the following manner: 50µL of 20%; 100µL of 18%; 100µL of 16%; 100µL of 14%; 100µL of 12%; 100µL of 10%; 50µL 8% of sucrose.

All the protocol was done on ice and using cold buffers.

## 3.g. Cilia formation

200000 RPE1 cells were seeded in 3cm diameter plates with a sterilized coverslip at the base. The day after, cells were transfected with DnaJB6 siRNA or control. 48

hours after transfection growing media was washed and substituted for starving media (DMEM-F12 supplemented with penicillin and streptomycin but without serum) to induce cells to entry in G0. 20 hours after incubation at 37ºC, cells were fixed in MTOH 10 minutes and immunostained using α-acetilated tubulin or α-δ2-tubulin antibodies in order to visualize the cilia and α-Ki67 to confirm that the cells had exit the cell cycle.

# 4. Egg extract

Experiments using *Xenopus Laevis* were performed according to the standard protocols approved by the ethical committee of the Parc de Recerca Biomèdica de Barcelona, Spain. Cytostatic factor arrested extracts (CSF extracts) were prepared as previously described (Murray 1991). Rhodamine-labeled tubulin was added to the extract to a final concentration of ≈0.2mg/ml in order to detect the microtubules. The quality of the EE was tested by adding sperm nuclei (≈500nuclei/µl) and incubating for 60min at 20ºC. Mitotic spindle structures were analyzed with a fluorescence microscope after squashing 1.5µl of EE in 3µl of fixative solution with a 18x18mm coverslip.

CSF (10 mM K-Hepes, pH 7.7, 50 mM sucrose, 100 mM KCl, 2 mM MgCl2, 0.1 mM CaCl2, and 5 mM EGTA)

## 4.a. DnaJB6 quantification in EE

Control EEs were diluted in a ratio of 1µl of EE in 9µl of sample buffer. 10, 20 or 30µl of the solution were loaded to an SDS PAGE gel, in parallel to known abundances of purified MBP-xDnaJB6-L. Western blot analysis with α-xDnaJB6 antibody was performed in order to measure the concentration of xDnaJB6 to the EE.

## 4.b. DnaJB6 immunodepletion, add back and excess experiments

Protein A-conjugated Dynabeads 280 (10002D, invitrogen) were coated with homemade antibodies α-xDnaJB6 or Rabbit generic IgGs (9µg of antibody/30µl of beads), by incubating them in 500µl PBS-NP40 (PBS 1X, 0,1% Np40) 1 hour at room temperature. Beads were washed twice in PBS-NP40 before and after coating with the antibody. Beads were then washed twice in CSF-XB and incubated in fresh EE 30min on ice. Beads were then recovered and recombinant proteins were added to the samples when necessary. For add back experiments, MBP-xDnaJB6-L or MBP was added to the extract to a 0,017µM final concentration. For the experiments with an excess of MBP-xDnaJB6-L, the recombinant protein or MBP

was added to a 1μM final concentration without the previous depletion of the endogenous xDnaJB6. Protein abundance was confirmed by western blot analysis.

## 4.c. Cycling experiments

DnaJB6 depletion was conducted if necessary. CSF extracts were supplemented with Rhodamine-labeled tubulin and sperm nuclei and released into interphase by adding 0,4mM $Ca^{2+}$. After 90 minutes incubation at 20ºC, the interphase state of the extracts were checked by squashes observation with a fluorescence microscope. Interphase extracts were cycled back to mitosis by adding one volume of CSF extract (also depleted for DnaJB6 if necessary). MBP-xDnaJB6-L or MBP was added to the EEs for add back and protein excess experiments. After 60 minutes of incubation, several squashes were performed to confirm proper cycling of the EE and also for specific analysis. When necessary, spin-downs were conducted to process the samples for immunofluorescence analysis. For spin-downs, a centrifuge tube was previously prepared with a coverslip (12mm diameter) at the bottom covered by 4ml of cushion buffer (BRB80; 40%glicerol). 20μl of extract was mixed with 500μl of dilution buffer (BRB80; 30%glicerol; 1% triton) and added to the top of the cushion buffer. Samples were centrifuged 20 RT 4000G (D-37520 centrifuge from Thermo electron corporation), the coverslips were recovered and samples were processed for immunofluorescence analysis.

## 4.d. Pull down experiments

Protein A-conjugated Dynabeads 280 were coated with homemade antibodies rabbit α-GST or α-MBP (9μg of antibody/30μl of beads), by incubating them in 500μl PBS-NP40 (PBS 1X, 0,1% Np40) 1 hour at room temperature. Beads were washed twice in PBS-NP40 before and after coating with the antibody. Proteins (GST; GST-xDNAJB6-L; MBP or MBP-xDnaJB6-L) were coated to the beads (2μg/1μg of antibody) in 500μl PBS-NP40 during 1 hour at 4ªC. Beads were washed twice with PBS-NP40 and twice with CSF-XB. Protein coated beads were incubated in 75μl of CSF extract for 15 minutes at 20ªC followed by 30 minutes on ice. Together with the beads, recombinant RanQ69L-GTP was added when necessary. Beads were recovered and washed three times in CSF-XB (for importin

interaction detection) or three times in CSF-XB and one in PBS-NP40 (for p150 interaction detection). Proteins were eluted from the beads by incubation in sample buffer for 10 minutes at room temperature. Samples were then analyzed by Western blotting.

## 4.e. RanGTP asters

Rhodamine-labeled tubulin was added to the extract to a final concentration of ≈0.2mg/ml in order to detect the microtubules. Ran asters were obtained by adding RanQ69L·GTP to CSF extracts at 15µM final concentration.

## 4.f. Asters pelleting

To improve the quality of the MT structures, cytochalasin D (C8273-10MG, sigma) was added to the CSF extracts at a final concentration of 13,3µg/ml, instead of the usual 20µg/ml. After CSF extract preparation, we clarified the egg extracts by centrifugation of 1,5-2ml of CSF extract for 15 min at 15000g in a 2ml eppendorf. After centrifugation, clarified extract was carefully retrieved using a 2ml syringe and a 1,2x40mm needle. The black pellet and the lipid top layer were not retrieved. Clarified extracts were tested for their ability to assemble spindles (by addition of Xenopus sperm nuclei as described in (Desai et al. 1998) and to form MT structures upon addition of RanQ69L·GTP. RanQ69L·GTP was added to the clarified extract at the saturating concentration of 15µM (Caudron 2005). The reactions were incubated in a water bath at 20ºC and were followed by squashing 1µl of clarified extract and 3µl of fix solution (11% Formaldehyde, 48% glycerol, 1µg/ml Hoechst in CSF-XB buffer (10mM Hepes, 100mM KCl, 0,1mM CaCl2, 2mM MgCl2, 50mM sucrose, 5mM EGTA)) below a coverslip. For RanGTP MT purification, 200µl of clarified extract were supplemented with RanQ69L·GTP and incubated in the water bath 20ºC for 15, 20, 25, 30, or 50 min. Meanwhile 5ml of aster cushion (25% glycerol, 1x BRB80, in water) were added to a thin wall, ultra-clear centrifuge tube 16x102mm (Beckman Coulter, ref 344061). After the indicated time, 1ml of aster dilution (10% glycerol, 1x BRB80, 0,1% TritonX-100, 1mM GTP) was vigorously added to the reaction and the tube was agitated by inversing it for 5 times. The reaction was then laid on top of the 5ml aster cushion

and centrifuged for 20 min, at 3200g at room temperature. Cushion was aspired, pellet was re-suspended in 50 µl of aster dilution supplemented with 20µM Taxol (T7402, Sigma) and carefully laid on top of 800 µl of aster cushion supplemented with 1mM GTP and 20µM Taxol in a 2ml tube. Samples were centrifuged for 20 min, at 4800g at room temperature. Cushion was aspired, pellet was re-suspended in 35µl of Laemmli buffer, transferred to a clean tube and boiled for 10 min at 95ºC. Five sixth of the samples obtained after the RanGTP aster purification were run on a precasted gradient gel (4- 15% Criterion TGX, 12+2 wells, 45µl, BioRad ref 567-1083) for 45 min at 60mA. Gels were stained over night using colloidal blue (Invitrogen Life Technologies, LC6025). Gels were cut in 6 bands. The two top and the two bottom bands were processed for Mass Spectrometry, the central bands that contain tubulin and actin were processed a part.

# 5. Proteomics analysis

## 5.a. Sample preparation

Gel bands were destained with 40%ACN/100mM ABC, reduced with dithiothreitol (2 µM, 30min, 56°C), alkylated in the dark with iodoacetamide (10 $\mu$M mM, 30 min, 25 ºC), dehydrate with ACN and digested with 0.7 mg of trypsin (Promega, cat # V5113) overnight at 37˚C. After digestion, peptide were extracted and cleaned up on a homemade Empore C18 column (3M, St. Paul, MN, USA) (Rappsilber et al. 2007).

Samples were analyzed using a LTQ-Orbitrap Velos Pro mass spectrometer (Thermo Fisher Scientific, San Jose, CA, USA) coupled to an EasyLC (Thermo Fisher Scientific (Proxeon), Odense, Denmark). Peptides were loaded directly onto the analytical column at 1.5-2 µl / min using a wash-volume of 4 to 5 times injection volume and were separated by reversed-phase chromatography using a 12-cm column with an inner diameter of 75 µm, packed with 5 µm C18 particles (Nikkyo Technos Co., Ltd. Japan). Chromatographic gradients started at 97% buffer A and 3% buffer B with a flow rate of 300 nl/min, and gradually increased to 93% buffer A and 7% buffer B in 1 min, and to 65% buffer A / 35% buffer B in 90 min. After each analysis, the column was washed for 10 min with 10% buffer A / 90% buffer B. Buffer A: 0.1% formic acid in water. Buffer B: 0.1% formic acid in acetonitrile.

The mass spectrometer was operated in positive ionization mode with nanospray voltage set at 2.2 kV and source temperature at 250 °C. Ultramark 1621 for the FT mass analyzer was used for external calibration prior the analyses. Moreover, an internal calibration was also performed using the background polysiloxane ion signal at m/z 445.1200. The instrument was operated in DDA mode and full MS scans with 1 micro scans at resolution of 60.000 were used over a mass range of m/z 350-2000 with detection in the Orbitrap. Auto gain control (AGC) was set to $1E^6$, dynamic exclusion (60 seconds) and charge state filtering disqualifying singly charged peptides was activated. In each cycle of DDA analysis, following each survey scan the top ten most intense ions with multiple charged ions above a threshold ion count of 5000 were selected for fragmentation at normalized

collision energy of 35%. Fragment ion spectra produced via collision-induced dissociation (CID) were acquired in the Ion Trap, AGC was set to $5e^4$, isolation window of 2.0 m/z, activation time of 0.1ms and maximum injection time of 100 ms was used. All data were acquired with Xcalibur software v2.2.

## 5.b. Data Analysis

The MaxQuant software suite (v1.5.5.1) was used for peptide identification and label-free protein quantitation (Cox & Mann 2008). The data was searched against an in-house generated database containing all proteins corresponding to phrog database (Wühr et al. 2014) and the corresponding decoy entries (release January 2016, 79214 entries). A precursor ion mass tolerance of 4.5 ppm at the MS1 level was used, and up to three missed cleavages for trypsin were allowed. The fragment ion mass tolerance was set to 0.5 Da. Oxidation of methionine, protein acetylation at the N-terminal defined as variable modification; whereas carbamidomethylation on cysteines was set as a fix modification. Identified proteins have been filtered respectively using a 1%FDR.

Protein top3 areas have been calculated with unique peptides per protein group.

## 5.c. Venn diagrams

Venn diagrams have been produced by using Venny 2.1 (http://bioinfogp.cnb.csic.es/tools/venny/)

## 5.d. Gene ontology

AmiGO 2 software was used (http://amigo.geneontology.org/).

## 5.e. Protein functional groups and interactors

Members of each functional group have been determined by literature search. One step interactions of these proteins were determined considering the following databases of reference: Reactome (Croft et al. 2014; Fabregat et al. 2016), BioGRID (Chatr-aryamontri et al. 2015; Stark et al. 2006), KEGG_pathways (Kanehisa et al. 2014), KEGG_compounds (Kanehisa et al. 2014), I2D (Brown & Jurisica 2005; Brown & Jurisica 2007), HPRD (Keshava Prasad et al. 2009), INTACT (Kerrien et al.

2012; Orchard et al. 2014), MINT (Licata et al. 2012), MATRIXDB (Launay et al. 2015) and MIPS (Pagel et al. 2005). Network graphs were obtained using the Cytoscape software.

# RESULTS

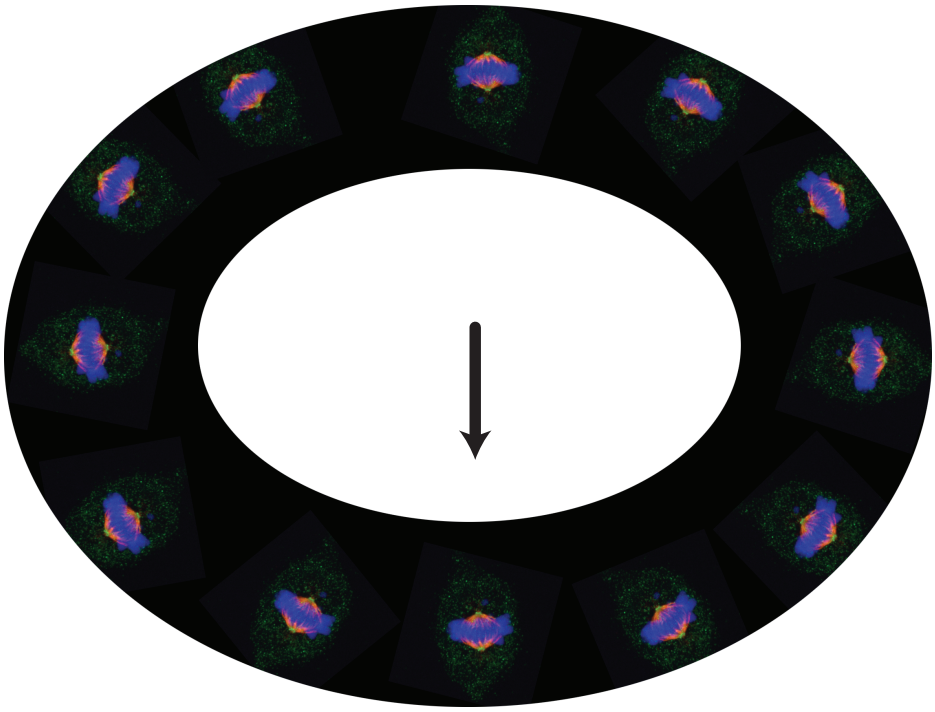

# Chapter 1- Identifying the of RanGTP-mediated microtubule self assemblies proteome in Xenopus egg extract

## 1.a. RanGTP triggers the nucleation and self-organization of microtubules in Xenopus M-phase egg extracts

Addition of RanQ69L-GTP to *Xenopus* egg extracts (EE) induces the nucleation and stabilization of MTs. Microtubules organize first into asters and later into more organized structures named mini-spindles (given their morphological similarities with the spindle but with no chromatin and with a shorter size) following a reproducible dynamic self-organization process. To characterize this dynamic process, I collaborated with Dr. Tommaso Cavazza. We quantified the type and the number of MT structures present in samples collected at different time points after RanGTP addition (Fig.1.a & b). The first structures appeared after 15 min of incubation and consisted of asters of relatively long MTs. Five minutes later, after 20 minutes of incubation, the number of this type of asters decreased, while a high number of asters with short MTs appeared. After 30 minutes of incubation, some of the asters established interactions forming mini-spindles, and so at this time point three types of MT structures were present: asters of short MTs, mini-spindles, and big aggregates including a mixture of asters and mini-spindles. At 50 minutes the system appeared to have reached a steady state, with individual asters and mini-spindles, but few or no aggregates (Fig.1.a & b). This self-assembly process therefore transits through intermediate steps that may culminate with the formation of bipolar mini-spindles.

**Fig.R.1. RanGTP asters formation and processing:** A) Representative fluorescent images of the MT structures assembled in clarified egg extracts supplemented with RanGTP and Rd-Tubulin. Different incubation times are reported. Tubulin is in grey. Scale bar = 10µm. B) Quantification of the number of each MT structure at different time-points in 1µl of EE. C) Schematic representation of the sample processing for the Mass spectrometry analysis of the RanGTP MT structures D) Representative SDS-PAGE gel in which the purified samples were analyse to separate tubulin and actin from the rest of the proteins. The gel was cut in six slices and processed for mass spec, the two corresponding to tubulin and actin were processed separately. Courtesy of Dr. Tommaso Cavazza.

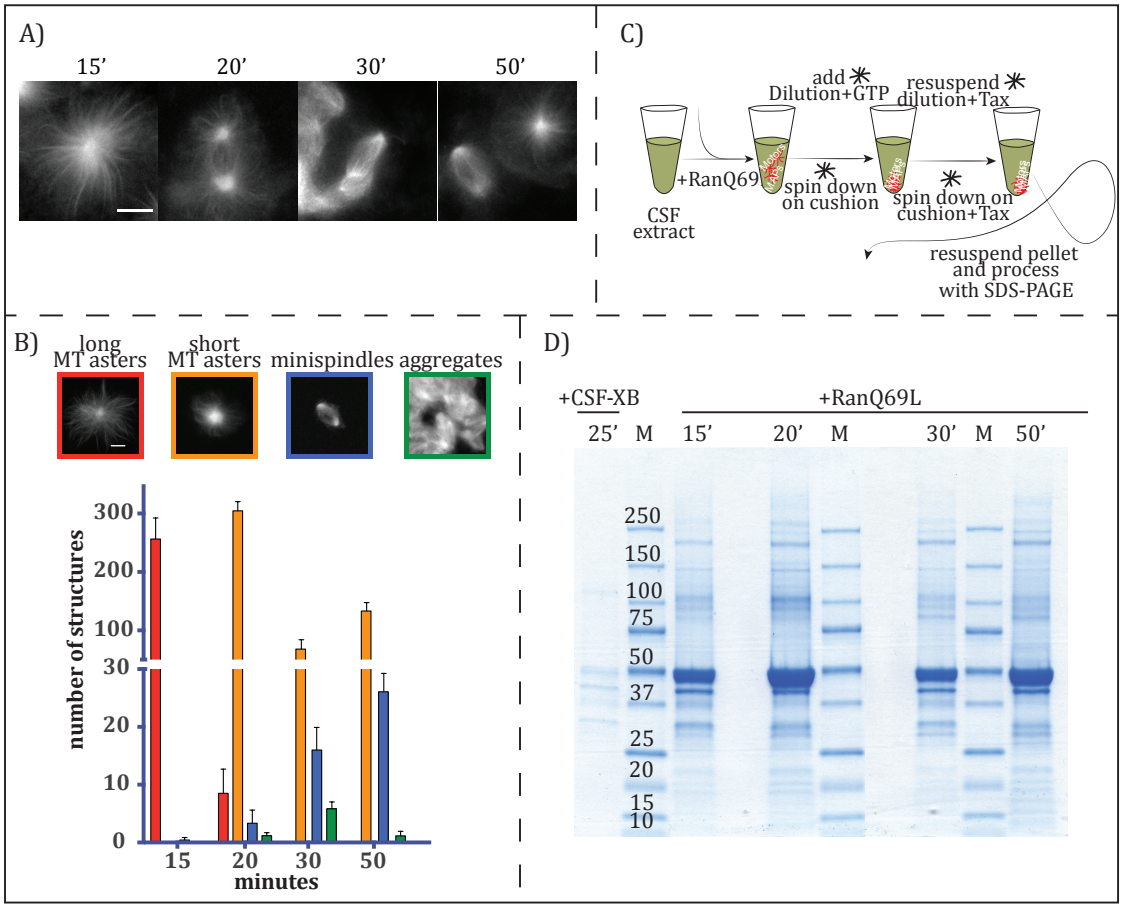


## 1.b. Identification of the proteins associated with RanGTP-induced microtubules

We aimed to gain a molecular understanding of the RanGTP MT self-organization process by identifying the full set of proteins that interact with these microtubules using a proteomics approach. First, we optimized a protocol to obtain clean preparations of RanGTP-induced MTs from *Xenopus* EEs (Fig.R.1.c). Xenopus EEs are very rich cytoplasmic extracts (more than 60mg/ml) containing a lot of material (proteins, lipids and membranes) that tend to pellet easily. To reduce the unspecific pelleting of these components we used clarified extracts, obtained by two successive centrifugations at 10K (instead of only one as in the standard protocol). MT assembly was induced by addition of RanGTP and samples were collected after 15, 20, 30 and 50 min of incubation for microtubule pelleting and for fluorescence microscopy analysis by centrifugation through a cushion (see methods section). Fluorescence microscopy analysis of the samples obtained at the

different time points of incubation showed that the morphology of the MT structures followed the general trend described above (Fig.R.1.a). Samples from egg extract supplemented with buffer without RanGTP were processed in parallel and used as negative controls. The experiment was performed in triplicate and the samples processed in parallel.

The RanGTP microtubules were recovered by two successive centrifugations steps. The first microtubule pellet was resuspended in the presence of a low dose of Taxol and centrifuged again in the same conditions through a cushion (see methods section) (Fig.R.1.c). The pellets were then analysed by SDS-PAGE and the proteins visualized by colloidal blue staining (Fig.R.1.d). Proteins with a wide range of sizes were recovered at each time point together with the tubulins visualized as a major band running at 55kDa. All the lanes were cut and processed for mass spectrometry analysis and protein identification.

Mass spectrometry analysis (nLC-MSMS) of all the different samples lead to the identification of a total number of 2307 (FDR 1%) *Xenopus laevis* proteins (Table S1) (protein contigs from the reference database (Wühr et al. 2014)). Since *Xenopus laevis* are pseudo-tetraploid organisms, most genes are duplicated and multiples isoforms of any protein are usually expressed, complicating the analysis, since there is little or no information about any functional relevance of the expression and activity of specific isoforms. To simplify our analysis as well as to access to the large pool of available information on human genes and proteins, we "translated" the Xenopus proteins into the homologous human proteins (annotated in the reference database (Wühr et al. 2014)). We used the annotated human homologue gene for each Xenopus entry in our proteome and we then merged the Xenopus entries that corresponded to the same human gene. We obtained a human proteome consisting of 1831 proteins (representing the 2307 Xenopus proteins). To reduce the number of putative false positives, we then eliminated at each time point the proteins not identified in at least 2 of the 3 replicas. We also considered that any of the true members of the proteome should be present in successive time points after their first appearance (considering sufficient a first identification in only one replica at the first time-point) (Fig.R.2). Applying these filtering criteria,

we obtained a RanGTP-dependent MT proteome of 1263 human proteins distributed along the time course of the experiment in the following way: 1102 proteins were present from 15 minutes, 150 were recruited at 20 minutes and 11 at 30 minutes (Table S2).

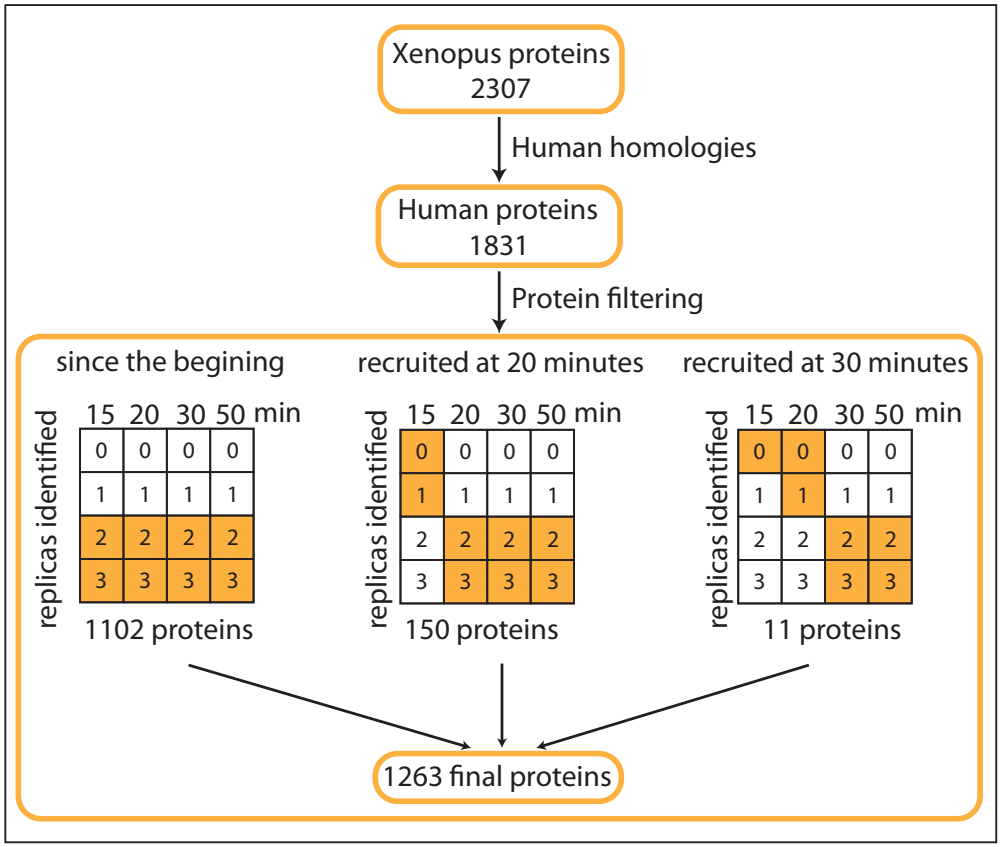


**Fig.R.2. RanGTP-MTs proteomics process:** Schematic representation of the process followed to obtain the RanGTP-MTs proteome. At the matrixs, in orange the options used to select proteins.

## 1.c. Composition of the RanGTP microtubule proteome

The proteome of the RanGTP-induced MTs should include the RanGTP targets that have been described to associate with MTs in M-phase. Indeed, we initially identified 17 out of the 20 currently known RanGTP targets. These proteins are NuMa, NuSAP, HURP, TPX2, Kif2a, Kif22, KifC1, Kif14-nabkin, Nup96, Nup107, Anillin, Rae1, ISWI CHD4, Mel28, TACC3 and MCRS1. However, we did not find the remaining three: cdk11, Xnf7 and APC. Cdk11 has not been reported to associate with the RanGTP asters and may therefore genuinely be absent from the RanGTP induced MT pellets (Yokoyama et al. 2008). On the other hand, Xnf7 was not

included in the database of reference. Our filtering criteria reduced the number of these proteins to 13, because 4 of them (CHD4, Mel28, TACC3 and MCRS1) were not present in few samples. However, we decided to maintain the strong filtering process to reduce as much as possible the number of putative false positives.

To obtain an unbiased snapshot of the composition of the proteome we performed a gene ontology (GO) enrichment analysis of the human entries using the AmiGO 2 software (fig.R.3). The proteome is highly enriched in microtubule-, centrosome- and spindle-associated proteins (21%). This category consists of 255 proteins (after manual annotation and/or correction). Another 29% corresponds to proteins with GOs related to the nucleus, including transcription and replication processes (Table S3). Finally, other proteins have variety of GOs, including translation, proteasome, mitochondria, actin, membranes and other organelles.

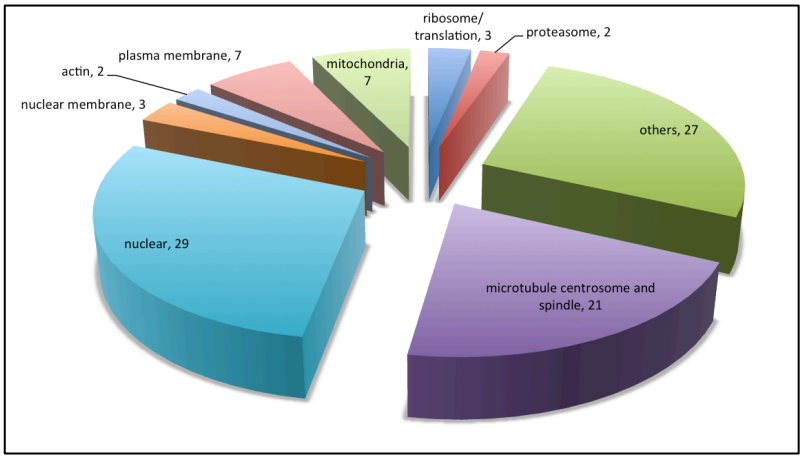


**Fig.R.3. Gene ontology:** Gene ontology unbiased analysis of the RanGTP-MTs proteome obtained using the AmiGO 2 software. Percentage from the total proteome showed per each GO.

## 1.d. Several MT related functional protein networks are enriched in the RanGTP MT proteome

To get a full picture of protein networks present in our proteome, we then used a systems biology approach. We first defined 4 main functional groups assigning a number of key proteins to each of them: microtubule nucleation (20 proteins), microtubule stabilization/elongation (23 proteins), microtubule destabilization (15 proteins) and microtubule organization (36 proteins). The interactome of the proteins defined in each group was established using available literature data and

various databases (detailed in material and methods section), taking only in consideration “one step” interactions. We then selected the proteins present in our proteome to build the functional interactome maps present in our proteome for each category. The analysis of these maps shows that our proteome includes 17 proteins from the microtubule nucleation group, 6 from the microtubule destabilization, 8 proteins from the microtubule stabilization/elongation and 23 proteins from the microtubule organization group, amongst manually selected functional lists (Table.R.1). The analysis of the different protein interactomes showed that we did identify a large number of proteins in each functional group: 136 proteins in the MT nucleation interactome (fig.R.4.a), 48 in the MT destabilization interactome (fig.R.4.b), 85 in the MT stabilization/elongation interactome (fig.R.5.a) and 133 in the MT organization interactome (fig.R.5.b) (Table S4).

| Nucleation | Stabilization | Destabilization | Organization |
|---|---|---|---|
| HAUS1 | CAMSAP1 | KATNA1 | ASPM |
| HAUS2 | CKAP2 | KATNB1 | CENPE |
| HAUS3 | CKAP5 | KIF18A | DCTN3 |
| HAUS4 | CLASP1 | KIF18B | DCTN4 |
| HAUS5 | KIF4A | KIF2A | DCTN5 |
| HAUS6 | MAPRE1 | KIF2C | DLGAP5 |
| HAUS7 | SKA1 | | DYNC1H1 |
| HMMR | SKA3 | | DYNC1I2 |
| MZT2B | | | DYNLL1 |
| NEDD1 | | | DYNLL2 |
| TPX2 | | | HOOK3 |
| TUBG1 | | | KIF11 |
| TUBGCP2 | | | KIF14 |
| TUBGCP3 | | | KIF20A |
| TUBGCP4 | | | KIF22 |
| TUBGCP5 | | | KIF23 |
| TUBGCP6 | | | KIF27 |
| | | | KIF2A |
| | | | KIF4A |
| | | | KIF7 |
| | | | KIFC1 |
| | | | NuMA1 |
| | | | PRC1 |

**Table.R.1. Protein functional groups, defining components presents in the proteome**

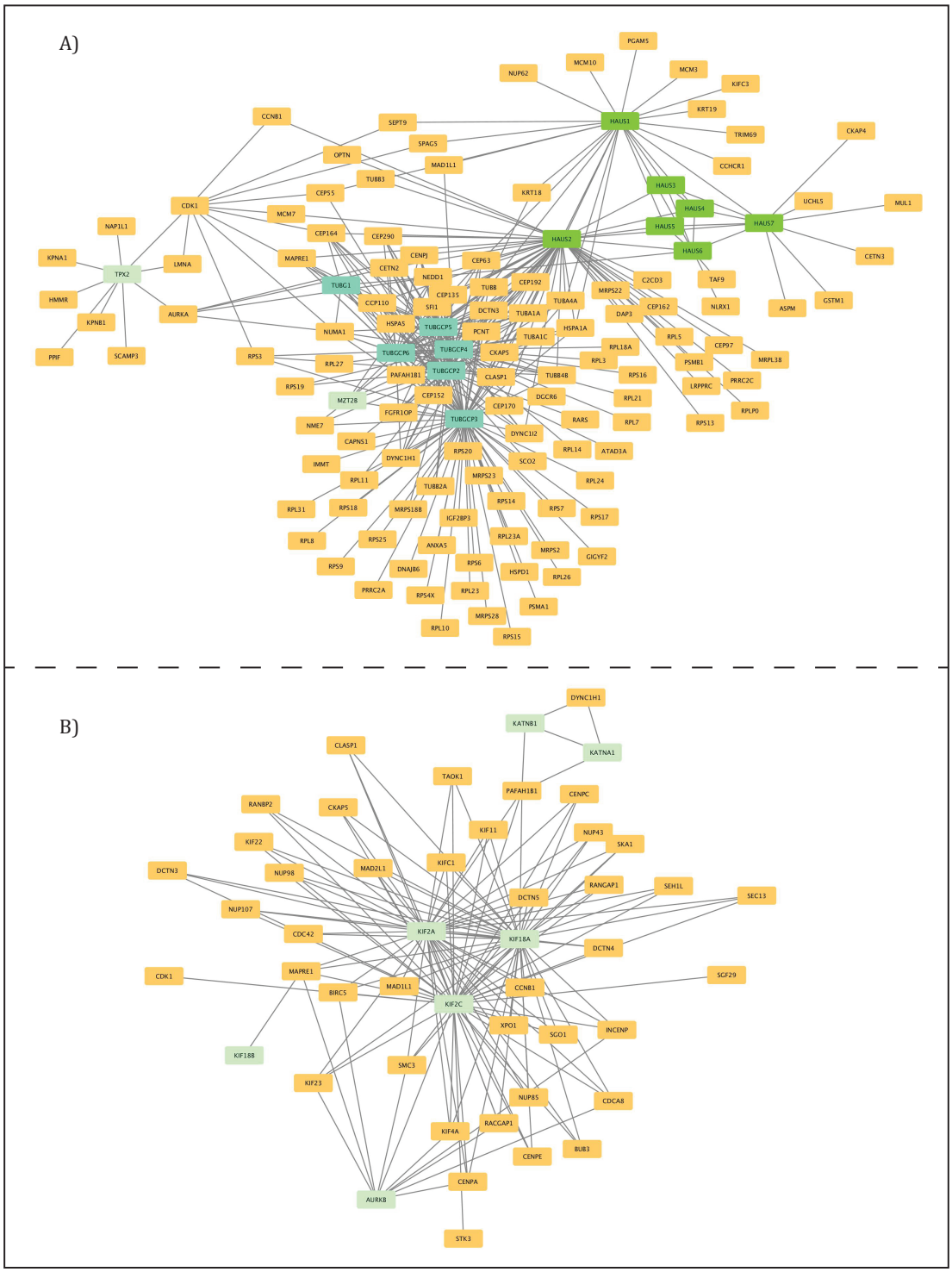


**Fig.R.4. Protein functional groups networks from the RanGTP-MTs proteome:** In yellow the protein interactors of the selected nodes identified in the RanGTP-MTs proteome. A) MT-nucleation functional group. Selected nodes in green: HAUSs, GCPs and other nodes (from darker to lighter). B) MT-destabilization functional group. Selected nodes in green.

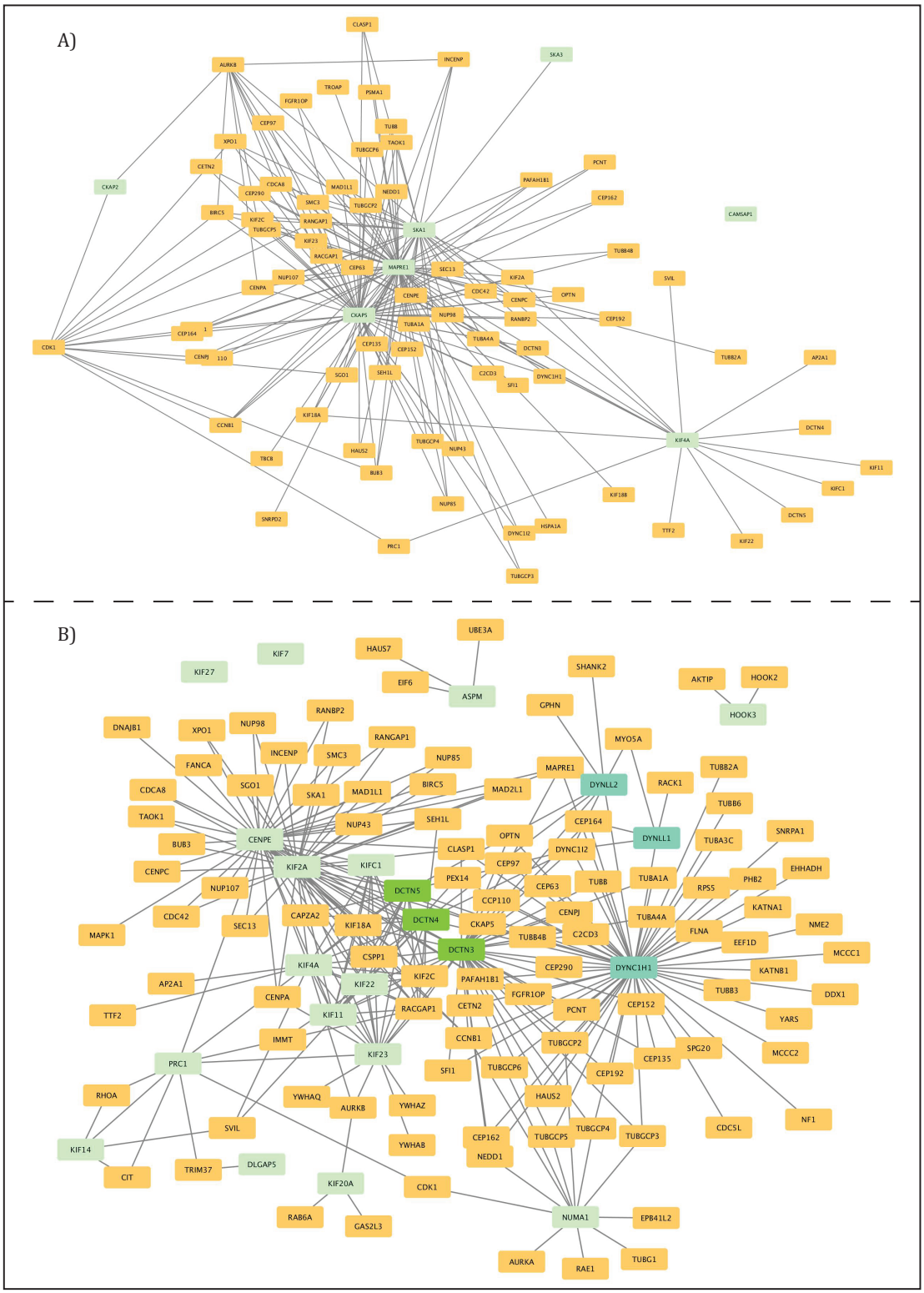


**Fig.R.5. Protein functional groups networks from the RanGTP-MTs proteome:** In yellow the protein interactors of the selected nodes identified in the RanGTP-MTs proteome. A) MT-stabilization/polimerization functional group. Selected nodes in green. B) MT-organization functional group. Selected nodes in green: Dynactin subunits, Dynein subunits and other nodes (from darker to lighter).

We then analysed our data in the light of published proteomic data on spindles and other microtubule assemblies in M-phase. An study, also performed in Xenopus egg extracts, with Taxol stabilized microtubules (Gache et al. 2010) described 296 proteins. Two other studies instead described spindle proteomes, one of them performed in HeLa cells and containing 781 proteins (Sauer et al. 2005) and the other performed in CHO cells and containing 1127 proteins (Bonner et al. 2011). We found that a large number of the proteins we identified was shared among these proteomes (Fig.R.6).

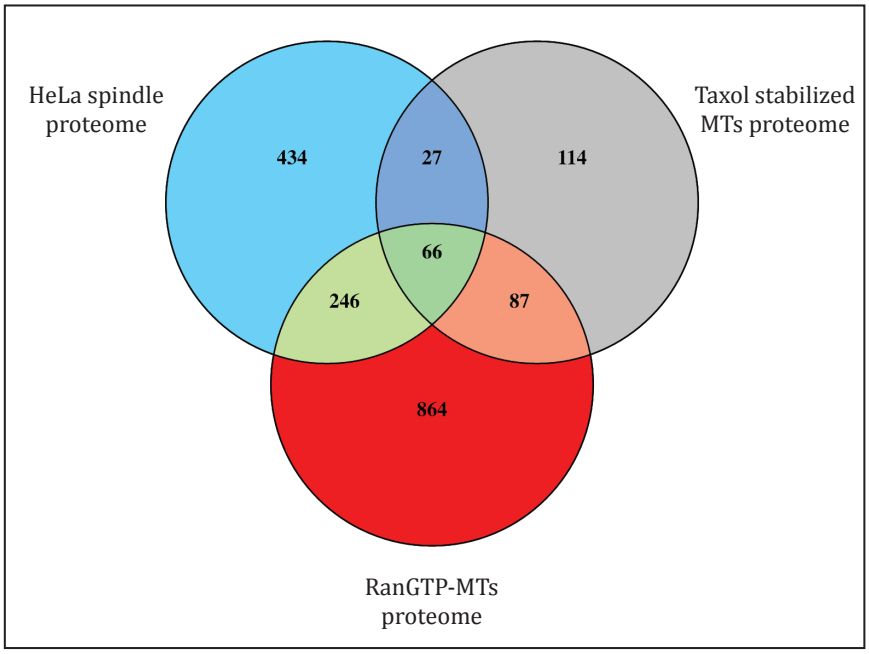


**Fig.R.6. Proteomes comparison:** Venn diagram comparing the HeLa spindle proteome, the Taxol-stabilized MTs proteome and the RanGTP-MT asters proteome. Number of proteins showed for each combination.

## 1.e. RanGTP induces a richer microtubule-associated proteome than Taxol microtubules

We identified 52% of the proteins present in the Taxol-MT proteome (Table S5), that corresponds to 153 proteins. However, this only corresponds to 12% of the proteins present in our RanMT proteome. This may not be unexpected because the addition of RanGTP to the extract triggers a whole pathway that drives microtubule nucleation, stabilization and organization by regulating directly the activity of several proteins. Instead, only proteins having intrinsic microtubule

binding activity (as well as their partners) in an M-phase cytoplasm will co-pellet with Taxol stabilized microtubules. Thus this suggests that our data are enriched in proteins that participate in the more physiological process of microtubule assembly and organization during M-phase. A more detailed analysis supported this idea. Indeed, the number of proteins from the microtubule nucleation interactome is much larger in our RanGTP-MT proteome than in the Taxol-MT proteome, which contains only 26 out of the 136 we identified (Table S5). Interestingly, the Taxol MTs proteome does not include the augmin (or HAUS) complex, that has previously been proposed to drive the amplification of RanGTP dependent MTs (Petry et al. 2013). In contrast, we found all the members of the HAUS complex in our proteome. Moreover, most of the GCPs were not found in the Taxol-MT proteome (except by GCP2) consistent with the experimental approach that did not involve microtubule nucleation.

Similarly, we identified also a larger number of proteins with a known function in MT stabilization/elongation and destabilization than those present in the Taxol-MT proteome (Table S5), including AURKB, CKAP2, SKA1, SKA3 (in the first group) and AURKB, KATNA1, KATNAL2, KIF18A, KIF18B and KIF2A (in the second group).

Finally, the network of MT organization consists of 133 proteins in our proteome (including the known factors) but only 33 in the Taxol-MT proteome (Table S5). Some of the proteins only identified in our analysis include 3 Dynactin subunits (DCTN3, DCTN4, DCTN5), two Dynein subunits (DYNLL1, DYNLL2), the adaptor protein HOOK3 and NuMA1 (which in turn is a RanGTP regulated protein) and several kinesins (KIF14, KIF23, KIF27, KIF2A, KIF7, KIFC3).

In summary, the RanGTP-MT proteome has more proteins than the Taxol-MT proteome previously described, correlating with the higher level of complexity of the microtubule structures and the regulation of the protein activity triggered by RanGTP in EE. This suggests that our proteome provides a good source of putative novel proteins regulated by RanGTP with a function in spindle assembly.

## 1.f The RanGTP-MT proteome is highly enriched in spindle associated proteins

The Ran-MT proteome contains 40% (312 proteins) of the HeLa cells spindle proteome which is a high proportion considering that the RanGTP asters and mini-spindles do not include neither centrosomes nor chromosomes (Sauer et al. 2005). Interestingly, this only corresponds to 25% of all the proteins we identified, suggesting again that our approach has provided an enriched M-phase MT associated proteome (Table S5). Interestingly, the 13 RanGTP regulated factors that we identified are also present in the HeLa cell spindle proteome that in addition includes AHCTF1 (mel28), which in our analysis was filtered out because it was absent at the 30 minutes' time point (in all the three replicas). In fact, approximately 50% of the proteins identified for each of the functional groups we defined were also present at the HeLa cell spindle proteome (Table S5). However, some highly relevant components were missing from this proteome such as for example most of the members of the Augmin complex (only HAUS 5 and 7 were identified), or NEDD1 and MZT2B, whereas all the GCPs, TPX2 and RHAMM were detected. Similarly, some important players in MT stabilization and destabilization such as MAPRE1, KATNA1 and KATNAL2 were also absent. Finally, we identified several members of the Dynein-Dynactin complex that are absent in the HeLa cell spindle proteome such as DCTN3, DCTN5, DYNC1H1, DYNC1I2, DYNLL2 and HOOK3, as well as two kinesins KIF27, KIF7 that are also involved in microtubule organization. However, the HeLa cell spindle proteome contains several proteins not present in our proteome such as the kinesins Kif15, Kif1B, Kif21B, Kif20B, Kif5A and Kif5B and the dynein subunit DYNC1LI2.

## 1.g. The RanGTP-MTs proteome is enriched in enzymes catalysing post-translational modification

In addition to the process of recruitment of proteins to the MTs, another layer of regulation occurs through several types of posttranslational modifications. We specifically focused on kinases and phosphatases, which are key regulators of mitosis. We found that our proteome includes 49 kinases (9% of the whole

kinectome in human consisting of 518 kinases (Manning 2002)) and 12 phosphatases (4% of the 251 human phosphatases (data extracted from http://hupho.uniroma2.it)). Interestingly, our proteome includes many interactors of some of these kinases like Aurora-A and CDK1 (fig.R.7).

Seven kinases had also been identified at the Taxol-MT and HeLa spindle proteomes: AURKA, CDK1, CIT, CLASP1, CSNK1A1, PKM and PRKDC. 3 kinases were also identified only in the HeLa spindle proteome (AURKB, SLTM and TRRAP) and another 6 were also identified only in the Taxol-MT proteome (ATR, CAMK2D, CAMK2G, CDC7, CDK8 and MAP4K4). The other 33 kinases we identified were not reported in the other two proteomes (Taxol-MT and spindle).

Only some of the 33 kinases present in our proteome have a known function in mitosis. The identification of protein kinases with unreported functions in mitosis in the RanGTP-MT proteome suggest they may play some as yet unknown roles in spindle assembly. Further work is required to explore this possibility.

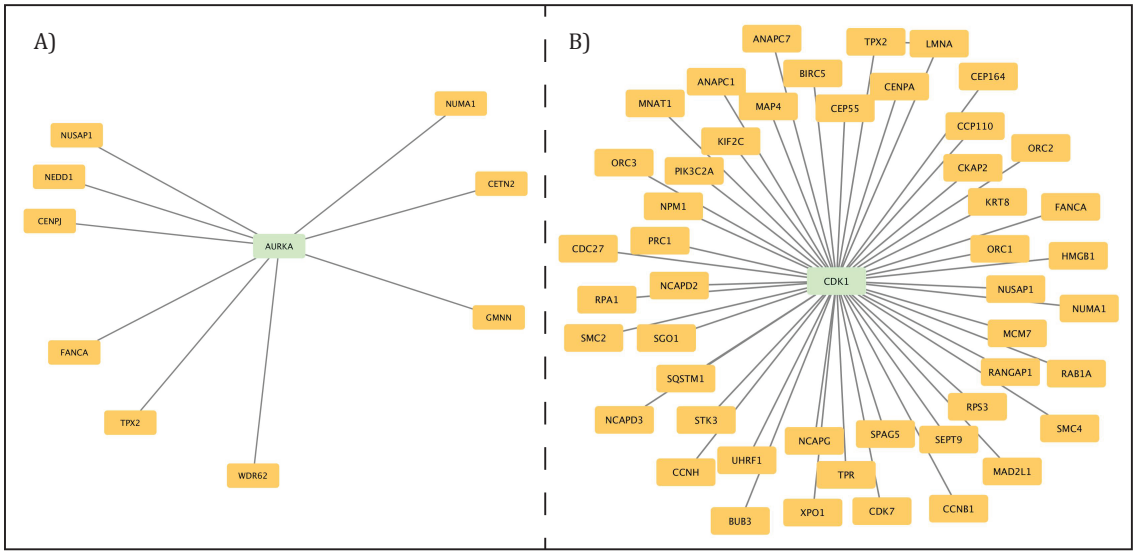


**Fig.R.7. Kinases interactors from the RanGTP-MTs proteome:** In yellow the protein interactors of the kinase identified in the RanGTP-MTs proteome, in green the kinase. A) Aurora-A interactors representation. B) CDK1 interactors representation.

# 2. Chapter 2- Identification of novel putative RanGTP regulated spindle assembly factors

## 2.a. Identification of novel spindle proteins

One of the main motivations for performing the RanGTP-microtubules associated proteome analysis was the idea that many RanGTP regulated proteins in mitosis still needed to be identified. Indeed, our data suggested that the proteome could contain novel RanGTP targets involved in the MT assembly and organization pathways. We believe that, by comparing the RanGTP-MT proteome with the previously published proteomes and GOs, this proteome could be a potent tool in order to provide a list of protein candidates to be involved in spindle assembly through a regulation by Ran. When comparing our list of proteins with the HeLa mitotic spindle proteome (Sauer et al. 2005), together with the meiotic CHO spindle proteome (Bonner et al. 2011), and the nuclear GOs, we obtained a list of 110 proteins (Table S6). This list of 110 proteins includes 40 proteins that were already included in the microtubules, spindle and centrosomes GOs. Within those 110 proteins we could observe a strong enrichment of known RanGTP regulated factors in mitosis (from a 1% of RanGTP factors in the total proteome to 7,3% after this selection), suggesting that other unknown factors could have been selected. Our list of selected proteins contained the following known RanGTP regulated factors: ANLN, KIF22, NuMA1, NUP107, NUP98, RAE1, SMARCA5 and TPX2. 4 kinesins (KIF20A, KIF22, KIF23 and KIF2C) and other described proteins with spindle assembly related activities were present (as NuMA, AURKA, INCENP, TUBG1, etc). Interestingly, 70 proteins were not included in those microtubules related GOs, generating an extensive list of putative new candidates. Within this list of 70 proteins we could identify some hits interesting to be studied. Based also on literature searches, few other candidates were selected for further analysis. The GO and protein functional groups (defined for us, considering the first level of interactions), the Mitocheck screen (Neumann et al. 2010) and in-house generated interactomes of TPX2, MCRS1, AurA, and hKLP2 were also considered. 11 proteins were selected (Table S7) including nuclear proteins (CBX3, HCFC1, NPM1,

DnaJB6), kinases (CK2, NME2), cytosolic proteins with different functions (ANT-2, ARL8B, FOP), and uncharacterized proteins (MAP7D1 and Wdr8).

First, we looked at their localization in mitotic HeLa cells by immuno-fluorescence analysis or by expressing the fluorescently tagged protein. Four candidates (B23, MAP7D1, ARL8B, and Nm23-H2) did not show any specific localization in mitotic cells (data not shown). Instead, the other 7 candidates did show an interesting localization in mitosis (fig.R.8 for all except for DnaJB6, fig.R.9.c). Two candidates, FOP and GFP-WDR8, were localized to the centrioles and the centrosomes respectively. The other 5 candidates, CK2α, ANT2, HCFC1, CBX3 and DnaJB6, associated with the spindle poles or the spindle MTs and CBX3 also localized to the chromosomes. In this thesis, we will focus specifically on the study of one of these candidates, DnaJB6.

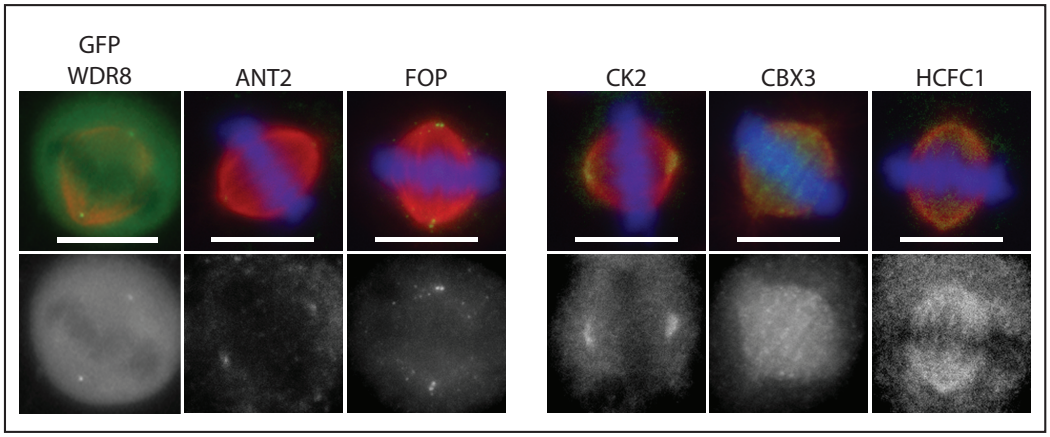


**Fig.R.8. Candidates localization to the mitotic spindle:** HeLa cells have been fixed in MTOH and processed for IF using specific antibodies for each candidate, except for WDR8 (expression of the GFP-tagged protein). In blue the DNA (Hoechst), in red tubulin (DM1A antibody) and in green the candidates. Images of the proteins detected to the centrioles and centrosomes are at the left side of the figure, on the right side the proteins detected to the spindle microtubules. scale-bar 10 μm

## 2.b. The long isoform of DnaJB6 localizes to the nucleus in interphase and to the spindle microtubules in mitosis

As detailed at the introduction (chapter 4.c), DnaJB6 is a HSP40 co-chaperon protein with two isoforms generated by alternative splicing in humans. The short isoform (DnaJB6-S) is a 241aa protein that generally localizes to the cytoplasm in interphase. On the other side, the long isoform (DnaJB6-L) is made of 326aa and

localizes to the nucleus. A putative NLS (KRKKQKQREESKKKK) is found in DnaJB6-L sequence. Although no interaction of DnaJB6-L with importins has been described yet, mutations of the NLS are shown to impair nuclear localization of the exogenous EGFP-DnaJB6-L protein in HeLA cells (Mitra et al. 2008).

We decided to test first whether we could detect the protein inside the nucleus by immunostaining using a specific homemade antibody (fig.R.9.b). The fact that our antibody was raised against a central sequence of the protein shared between both isoforms (see material and methods), does not allow us to distinguish between the two isoforms. The specificity of the antibody was tested by Western-Blot and by immunofluorescence, comparing the signal intensity in control cells and DnaJB6 silenced cells with specific siRNA (fig.R.9.a).

By using our specific antibody we could visualize a signal of DnaJB6 decorating the nucleus on interphase cells. In order to test the possible role of DnaJB6 in mitosis, we checked first its localization in the different mitotic phases by imaging fixed HeLa cells, using the same antibody. DnaJB6 localizes to the spindle microtubules in all the different phases of mitosis (from pro-metaphase to anaphase), with stronger signal at the spindle poles (fig.R.9.c). In anaphase, the protein was detected also to the central spindle microtubules.

**Fig.R.9. DnaJB6 localization in HeLa cells:** A) Western blot showing the specificity of the antibody and the efficiency of the protein silencing. HeLa cells were transfected with control siRNA or DnaJB6 siRNA and cell lysates recovered 48 hours after transfection. 30µg of total protein was loaded per sample. Membrane was blotted with a α-DnaJB6 at 1µg/µl and DM1A at 1:1000. B) and C) Interphase and mitotic fixed HeLa cells processed by IF using α-DnaJB6 at 5µg/µl and DM1A at 1:1000. In blue the DNA (Hoechst). scale-bar 10 µm

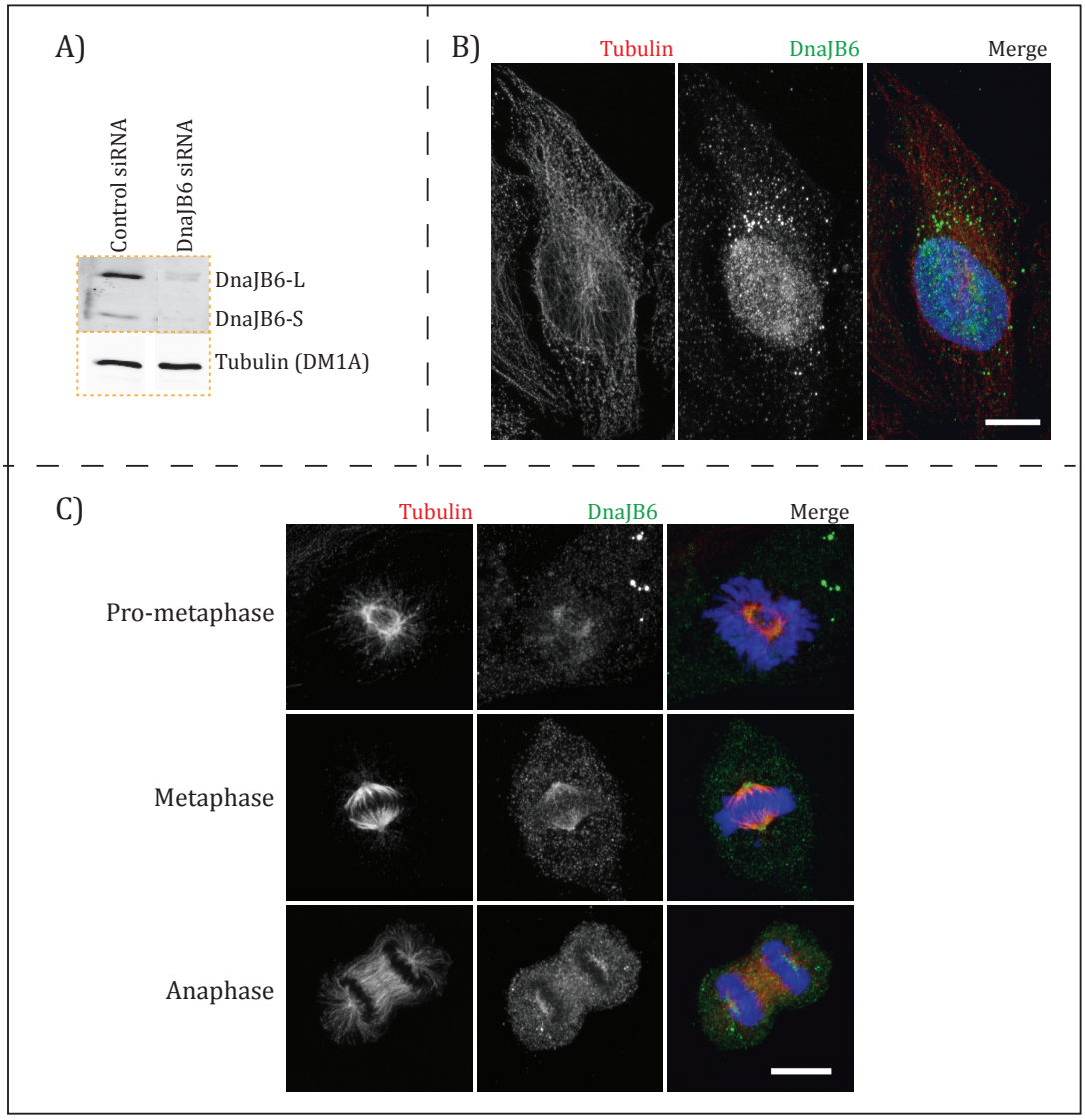


## 2.c. DnaJB6 plays a role in chromosome-dependent microtubule asters formation

In order to look specifically at the RanGTP dependent microtubule assembly pathway, we performed a microtubule regrowth assay in mitotic cells. In this assay, cells are treated with 2µM of nocodazole to induce microtubule depolymerization. Nocodazole sequesters the free tubulin dimers of the cell, and this induces the depolymerization of the microtubules (Lee et al. 1980). After 3 hours of incubation in nocodazole (when all the microtubules have been depolymerized), the drug is washed out (releasing the tubulin dimers) to allow the re-polymerization of the microtubules. In mitotic cells, many small microtubule

asters are formed after nocodazole washout. Two bigger asters (corresponding to the centrosomal microtubules) are observed from the beginning, together with a variable number of microtubule asters that are formed close to the chromosomes, due to the presence of the RanGTP gradient. The microtubule asters grow and contact each other getting organized in a bipolar spindle. This experimental approach allows us to examine RanGTP regulated microtubule assembly, as well as microtubule organization, by fixing the cells after selected times of incubation (in normal growing media at 37ºC) and staining for tubulin to perform IF analysis. Silencing of many RanGTP regulated factors, such as TPX2 or MCRS1 (Tulu et al. 2006; Meunier & Vernos 2011), affect the dynamics of these asters, affecting the number of asters per cell observed at the different time-points.

Control and DnaJB6 silenced cells were fixed after 1, 2, 3, 5, 7 and 10 minutes of nocodazole washout and processed for IF. The number of asters per cell was measured in approximately 150 mitotic cells per sample. In both conditions, the highest number of asters was observed 1 minute after nocodazole release, with a progressive decrease of this number over time. In control cells, an average of 8.731 (SD=2.461) small asters per cell was found at 1 minute. A decrease in the number of asters per cell was observed in control cells along the time-points, in parallel to the increase in size of the microtubule asters, resulting in few big asters at 10 minutes (3.304 asters per cell; SD=1.177). By direct observation under the microscope, the MT-asters seem to be smaller and more abundant in DnaJB6 silenced cells across all the time-points (fig.R.10.a). When quantified (fig.R.10.b and c), indeed, the number of asters per cell was higher in DnaJB6 silenced cells than in control cells in all the time-points except at 5 minutes (Mann-Whitney tests, p-values<0.0001 at 1, 2, 3, 7 and 10 minutes; p-value>0.05 at 5 minutes). On average, an increase between 1.2 and 1.7 asters was found in DnaJB6 silenced cells across all the time-points (exception made for the 5 minutes time point). The increase in number of asters did not seem to be correlated with a difference in the intensity of the total polymerized tubulin, although we did not quantify this intensity. In conclusion, DnaJB6 silenced cells have more microtubule asters in early time-points, suggesting an implication of DnaJB6 in the assembly of the Ran-

mediated chromosomal microtubules asters. This effect could be due to a higher nucleation activity around the chromosomes, an increase of the stability of the microtubules or a defective clustering of the asters in order to become organized in less but bigger asters overtime. It's important to notice that the asters in DnaJB6 silenced cells seem to be smaller, but we could not quantify this difference. The presence of smaller but more abundant microtubule asters in DnaJB6 silenced cells with no effect in tubulin intensity suggest a possible link between the protein activity and the organization capability of those asters, although we did not quantify neither the size nor the intensity.

## 2.d. xDnaJB6 long isoform interacts with importins α and β in a RanGTP regulated manner

In order to confirm the functionality of the NLS we decided to test the interactions of DnaJB6-L with the importin machinery. Due to its easy manipulation as an open system, we used the *Xenopus laevis* EE to conduct pull down experiments. We generated a recombinant *Xenopus laevis* DnaJB6 long isoform (xDnaJB6-L) with a tag sequence in order to do the pull downs. By looking at the literature, no described sequence was found for this long isoform. In contrast, two different mRNA isoform sequences were described for the short form (xDnaJB6-S) (accessions: xDnaJB6-SA Q5FWN8; NM_001095775; xDnaJB6-SB Q5XGU5; NM_001094833 (Klein et al. 2002)). To obtain the mRNA sequence of the xDnaJB6-L and confirm its existence in Xenopus, we followed a RACE-PCR approach. We obtained cDNA from *Xenopus laevis* EEs (using an oligo-dT with an adaptor sequence to increase the amplification efficiency) and tried to amplify the xDnaJB6-L cDNA sequence using a primer corresponding to the first 5' nucleotides of the annotated xDnaJB6-SA and xDnaJB6-SB sequences. Using the primers from the 5' sequence of xDnaJB6-SA isoform, we obtained a 1020 nucleotides mRNA sequence corresponding to xDnaJB6-L (Fig.R.11), corresponding to 339 aminoacids (Fig.R.12). The firsts 720 nucleotides were almost identical to the first 720 nucleotides of the previously described xDnaJB6-SA sequence, whereas the last 300 were different (only 33 in the case of the short isoform A). Two point mutations were found within those 720 nucleotides, but no changes were found at

the level of the aminoacids (Fig.R.13). Similarly, to the human proteins, the first N-terminal 240 aminoacids are shared between both isoforms, the short one contains a specific sequence of 10 aminoacids at the C-terminus and 39 for the long one.

In order to check the putative regulation of the protein by RanGTP in mitosis, we tested whether xDnaJB6-L was able to interact with importins in a RanGTP dependent manner.

We produced a recombinant x-DnaJB6-L tagged with a GST or MBP sequence at the N-terminus (GST-xDnaJB6-L or MBP-xDnaJB6-L). The recombinant protein was expressed in bacteria and purified as described in the material and methods section. The purity of the proteins was checked in coommassie stained SDS PAGE gels (data not shown). In order to test the interaction of the protein with importins, we performed pull downs in M-phase *Xenopus laevis* EEs using the recombinant GST-xDnaJB6-L protein (fig.R.10.d). GST-xDnaJB6-L was coated to magnetic Dynabeads using homemade anti-GST antibodies and then incubated in the EE in presence or absence of RanQ69L-GTP (a mutated version of Ran without GTPase activity). We loaded the pulled-down proteins on a gel. By using specific antibodies we detected an interaction with importin-β when RanGTP was not added to the extract (fig.R.10.e). This interaction was not observed when RanGTP was added to the extract, and neither with the control GST-coated beads (used as negative control). This observation suggested that importin is able to interact with xDnaJB6-L (with the predicted NLS). This interaction would regulate the translocation of the protein to the nucleus in interphase, as proposed for the human protein (Mitra et al. 2008; Cheng et al. 2008), and the activity of the protein during mitosis, if exists.

Interestingly, when aligning the predicted NLS sequence of the human DnaJB6 long isoform (KRKKQKQREESKKKK) with our sequenced xDnaJB6-L (fig.R.10.f), a highly conserved sequence is found with only a single aminoacid substitution (“S” to “Y”). The presence of the conserved predicted NLS sequence suggests that a similar regulation through RanGTP could exist in both species.

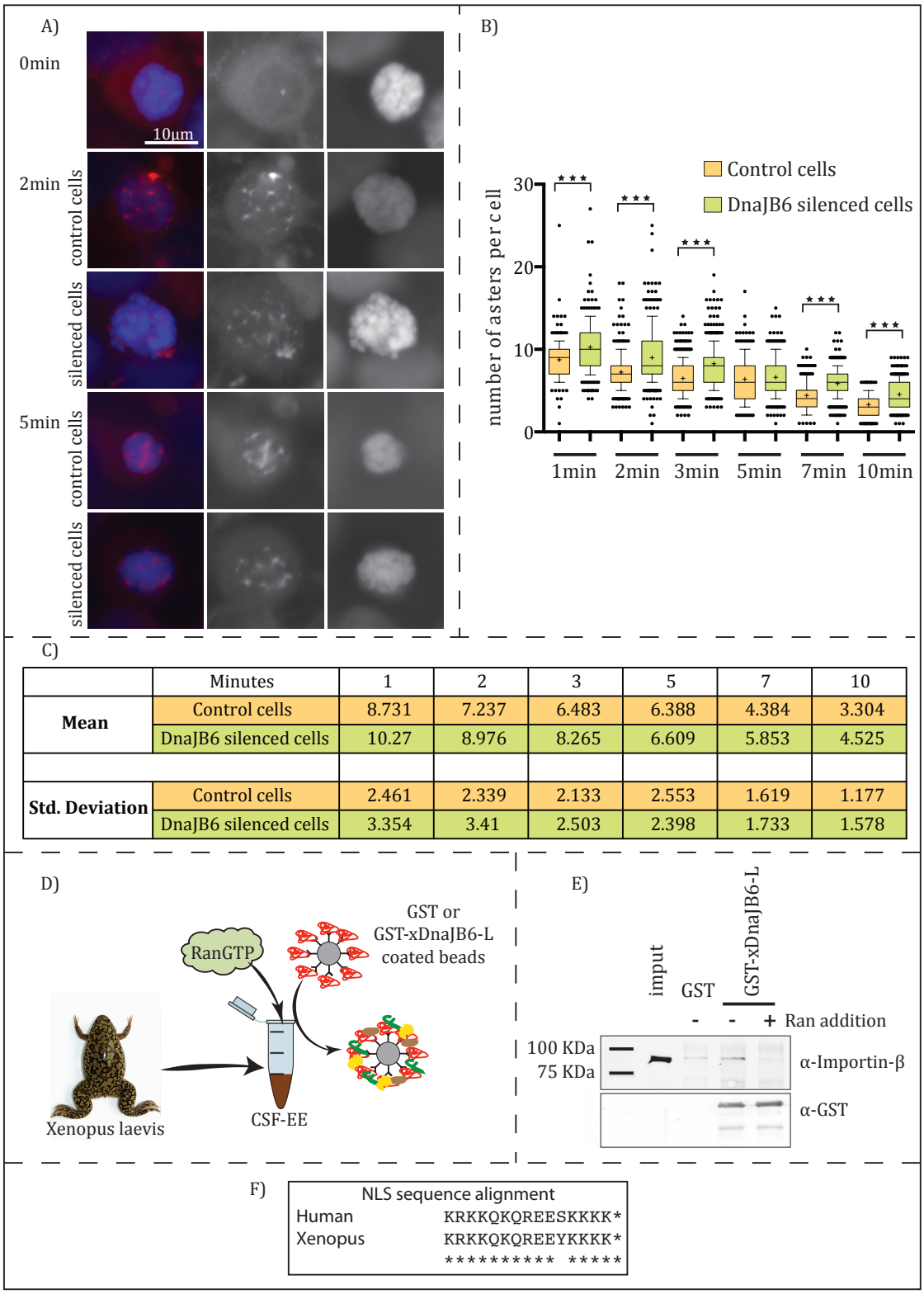


C)

| | Minutes | 1 | 2 | 3 | 5 | 7 | 10 |
|---|---|---|---|---|---|---|---|
| **Mean** | Control cells | 8.731 | 7.237 | 6.483 | 6.388 | 4.384 | 3.304 |
| | DnaJB6 silenced cells | 10.27 | 8.976 | 8.265 | 6.609 | 5.853 | 4.525 |
| | | | | | | | |
| **Std. Deviation** | Control cells | 2.461 | 2.339 | 2.133 | 2.553 | 1.619 | 1.177 |
| | DnaJB6 silenced cells | 3.354 | 3.41 | 2.503 | 2.398 | 1.733 | 1.578 |







F)

NLS sequence alignment

```
Human     KRKKQKQREESKKKK*
Xenopus   KRKKQKQREEYKKKK*
          ********** *****
```

**Fig.R.10. DnaJB6 affects chromosomal MT-asters assembly and interacts with importin-β in a RanGTP regulated manner:** A, B and C) MT-regrowth experiments in HeLa cells: MTs were depolymerized by incubating the cells with nocodazole and MT asters formation was analyzed after washing out the nocodazole and fixing the samples at consecutives time-points. Samples were processed by IF using DM1A antibody and Hoechst. A) Representative pictures of 0, 2 and 5 minutes. B) Quartiles graph representing the quantifications of the number of MT-asters per cell. 3 experiments with ≈ 150 cells quantified per condition and experiment. Average shown with a "+". (★★★) Indicates p-value<0.001. C) Table with the values of the quantifications from the graph shown in B. D and E) Pull down experiments in EE using GST-xDnaJB6-L. D) schematic representation of the experimental procedure. E) Western blot membrane showing the co-precipitation of importin-β in absence of RanGTP, whereas the protein is not detected when RanGTP was added to the EE, neither in the control (GST). F) Sequence alignment between the predicted NLSs of h-DnaJB6-L and xDnaJB6-L.

**xDnaJB6 long isoform mRNA**

```
  1 ATG GTG GAG TAT TAC GAA GTT TTG GGA GTC CAG AGG AAT GCC TCT GCA GAT GAT ATT AAG
  1  M   V   E   Y   Y   E   V   L   G   V   Q   R   N   A   S   A   D   D   I   K

 61 AAA GCA TAC CGC AGG CTA GCC TTA AAG TGG CAT cCC GAT AAG AAC CCT GAC AAT AAA GAT
 21  K   A   Y   R   R   L   A   L   K   W   H   P   D   K   N   P   D   N   K   D

121 GAA GCC GAG AGG AGG TTC AAA GAA GTT GCT GAA GCT TAT GAG GTC CTG TCA GAT TCT AAA
 41  E   A   E   R   R   F   K   E   V   A   E   A   Y   E   V   L   S   D   S   K

181 AAG AGA GAT ATT TAT GAT AAA TAT GGA AAA GAA GGA CTG ACA AAT CGT GGT GGT GGC AGT
 61  K   R   D   I   Y   D   K   Y   G   K   E   G   L   T   N   R   G   G   G   S

241 CAC TTT GAT GAA GCG CCA TTT CAA TTT GGA TTT ACA TTC CGA AGC CCA GAT GAT GTT TTC
 81  H   F   D   E   A   P   F   Q   F   G   F   T   F   R   S   P   D   D   V   F

301 AGG GAC TTC TTT GGG GGA AGA GAT CCA TTt TCA TTT GAT TTA TTC GCC GAC GAT CCA TTT
101  R   D   F   F   G   G   R   D   P   F   S   F   D   L   F   A   D   D   P   F

361 GAT GAT TTC TTC GGC AGA AGT CGT CAC AGA GCA AAC AGA AGT AGG CCA GCA GGA GGC GGA
121  D   D   F   F   G   R   S   R   H   R   A   N   R   S   R   P   A   G   G   G

421 GGA GGT CCC TTT CTC TCT ACC TTT GGA GGT TTC CCT GCC TTT GGC CCT AGC TTC TCT CCA
141  G   G   P   F   L   S   T   F   G   G   F   P   A   F   G   P   S   F   S   P

481 TTT GAC TCT GGT TTT AGT TCT TCA TTC GGG TCA TTT GGT GGC CAT GGG GGT CAC GGT GGT
161  F   D   S   G   F   S   S   S   F   G   S   F   G   G   H   G   G   H   G   G

541 TTT ACT TCA TTT TCC TCT TCG TCG TTT GGC GGT TCA GAA ATG GGT AAC TTC AGA TCC GTA
181  F   T   S   F   S   S   S   S   F   G   G   S   E   M   G   N   F   R   S   V

601 TCG ACC TCA ACT AAA GTA GTT AAT GGA AGA AGA GTT ACA ACA AAG AGA ATT GTT GAA AAT
201  S   T   S   T   K   V   V   N   G   R   R   V   T   T   K   R   I   V   E   N

661 GGA CAA GAG CGC GTT GAA GTA GAA GAA GAC GGG CAG TTA AAG TCC TTA ACA GTA AAT GGT
221  G   Q   E   R   V   E   V   E   E   D   G   Q   L   K   S   L   T   V   N   G

721 GTT GCA GAC GAA GCA GCG TTG GTG GAA GAG TGC CGG CGC CGG GGA CAG AAC GCT CTA CCT
241  V   A   D   E   A   A   L   V   E   E   C   R   R   R   G   Q   N   A   L   P

781 TTT CAA CCC TCC AGT AGC AGC AGC AGC GGC GGT GGC GGC GCA AGA ACC TCC AAA CCT CAC
261  F   Q   P   S   S   S   S   S   S   G   G   G   G   A   R   T   S   K   P   H

841 CGG CCT GCT GGT CTT CCT AGA cac GGC CAT AAC TAC AAA AGC GAC GAC GAG GAG GAA CCG
281  R   P   A   G   L   P   R   H   G   H   N   Y   K   S   D   D   E   E   E   P

901 GAA AGG ATG AGG GGT ACA AGC AaC TGG GAA TCT GCA GGA CAC AAA GAA GGG AGC AAG AGA
301  E   R   M   R   G   T   S   N   W   E   S   A   G   H   K   E   G   S   K   R

961 AAG AAG CAG AAG CAA AGA GAA GAG TAc aAG AAA AAG AAG TCT TCC AAA CCA ATC TAC TAA
321  K   K   Q   K   Q   R   E   E   Y   K   K   K   K   S   S   K   P   I   Y   *
```

**Fig.R.11. xDnaJB6-L protein and mRNA sequence**

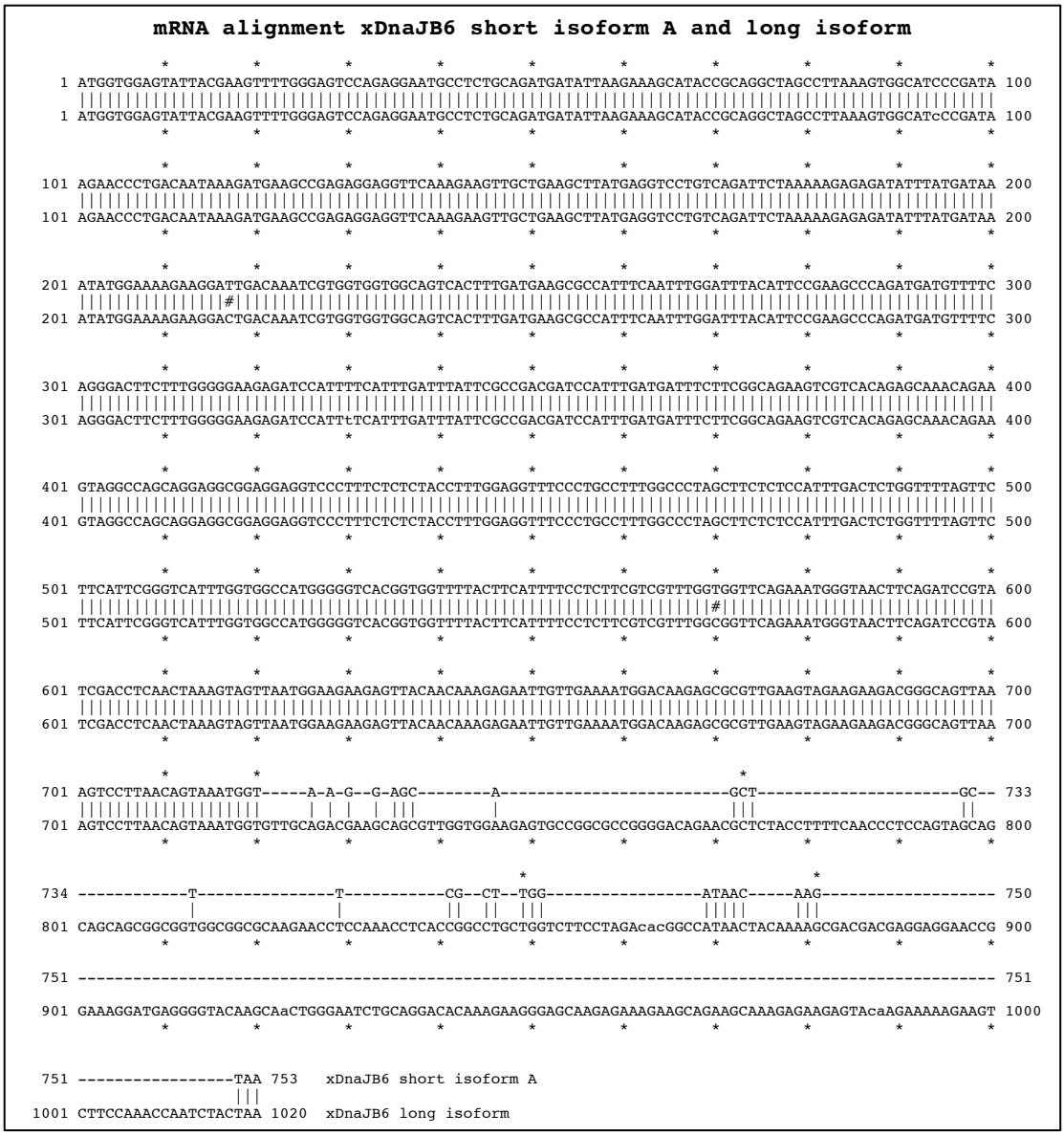


**Fig.R.12. Nucleotide sequence alignment between xDnaJB6-L and xDnaJB6-SA**

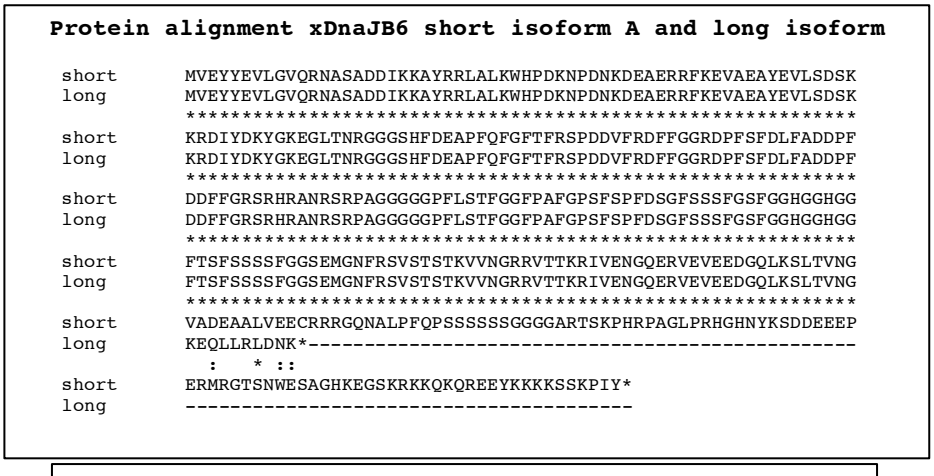


**Fig.R.13. Protein alignment between xDnaJB6-L and xDnaJB6-SA**

# 3. Chapter 3- DnaJB6 plays a role in microtubule organization in mitosis.

## 3.a. DnaJB6 silencing induces a mitotic delay

After confirming that DnaJB6 is a RanGTP regulated protein that localizes to the spindle during mitosis, we tested whether it has a role in spindle formation during mitosis. We first tested the effect of silencing the protein (both isoforms at once) in the progression of non-synchronized cells through mitosis. We used HeLa cells stably expressing H2B–eGFP/ α-tubulin–mRFP and filmed them during 18 hours (taking images every 4 minutes with a Zeiss Cell Observer microscope) starting the recordings 48 hours after transfection with the siRNA (either control or DnaJB6 specific). We measured the time that cells needed to progress through mitosis considering separately from nuclear envelope breakdown to anaphase onset (fig.R.14.b), and from anaphase onset to the end of mitosis. 281 control and 250 silenced cells were analyzed in three independent experiments. On average, DnaJB6 silenced cells spent 55.73 minutes (± 29.18 SD) to progress from the nuclear envelope breakdown to anaphase onset, significantly more than control cells (Mann whitney test, P-Value <0.0001), which needed 41.1 minutes (± 17.51 SD). No differences were detected in anaphase duration in DnaJB6 silenced cells. Interestingly, other defects in spindle orientation and chromosome congression were observed in DnaJB6 silenced cells, but the low resolution of the images did not allow us to analyze them in detail.

## 3.b. Mitotic phenotypes in DnaJB6 silenced cells

### 3.b.1 Silencing of DnaJB6 promotes a decrease of cells in metaphase and the presence of multipolar spindles

We have shown that silencing of DnaJB6 promotes a delay in the progression of cells through mitosis. In order to understand the reason for the delay, we checked whether cells accumulate at some specific phases of mitosis and if spindle defects could be detected. We silenced DnaJB6 in HeLa cells, fixed them after 48 hours and stained for tubulin and DNA. We then quantified the percentage of cells in each

phase of mitosis in control and silenced cells dividing them in six categories: prophase, pro-metaphase, metaphase, anaphase, monopolar spindles and multipolar spindles (Fig.R.14.a). We observed a change in the distribution of the cells in the different mitotic phases (fig.R.14.c). The percentage of cells in metaphase was reduced to 34.7% (± 7.0 SD) in DnaJB6 silenced cells compared with the 55.3% (± 7.2 SD) in controls (Sidak's multiple comparisons test; p-value<0.0001). A small increase in the percentage of cells in the steps before metaphase was observed, but this difference was not statistically significant. Interestingly, a statistically significant increase of the proportion of multipolar spindles was observed in DnaJB6 silenced cells (Sidak's multiple comparisons test; p-value<0.01). Indeed only 3% (± 1.5 SD) of the mitotic control cells did have a multipolar spindle, whereas this percentage increased to 14% (± 3.1 SD) in the DnaJB6 silenced cells. This multipolarity phenotype was not detected in the live cells analysis, probably due to the low resolution of the images. Not differences were detected for the other categories (anaphase and monopolar spindles).

**Fig.R.14. DnaJB6 silencing impairs mitosis progression:** A) Representative pictures of the mitotic phases and spindle defects (HeLa cells). Scale-bar 10 μm B) Mitosis progression assay: Quartiles graph comparing the time needed from NEBD to anaphase onset of control and DnaJB6 silenced cells. Average shown with a "+". HeLa cells were transfected and imaged by tame-laps during 18 hours, imaging them every 4 minutes. C) Mitotic phases quantification: Columns representing the average percentage of cells in each phase of mitosis. Standard deviation between replicas represented with a line on top of each column. Cells were transfected, fixed after 48 hours and processed for IF and stained with DM1A and Hoechst. Three replicas with ≈ 150 cells quantified per condition and experiment. (★★) Indicates p-value<0.01 and (★★★) Indicates p-value<0.001.

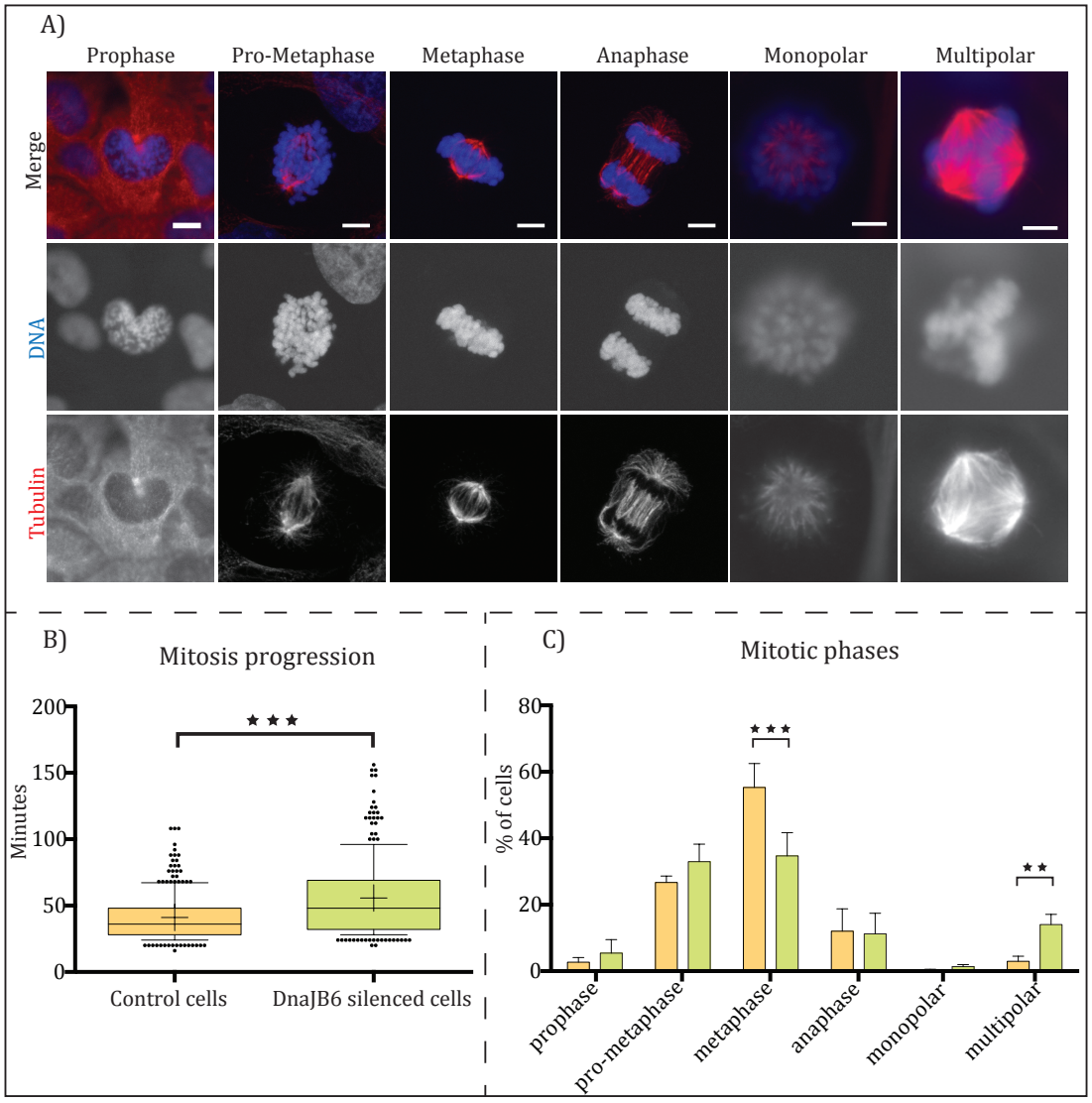


### 3.b.2. Silencing of DnaJB6 affects the length of the mitotic spindle

In order to characterize better the consequences of the silencing of DnaJB6, we looked at fixed HeLa cells in metaphase. We measured the length of the metaphase spindles in control and DnaJB6 silenced cells (with a LEICA inverted wide-field fluorescent microscope) analyzing the images with the FIJI software. The spindle length was measured by drawing a line from pole to pole in each spindle. The average length of the control spindles was 9.937µm (± 0.92 SD), while the DnaJB6 silenced spindles had an average length of 10.4µm (± 1.2 SD). Although the effect is not major (fig.R.15.A), statistical analysis indicated that DnaJB6 silenced cells have significantly longer spindles than control cells in metaphase (Mann Whitney test P-Value<0.0001; 267 control and 294 silenced cells analyzed).

### 3.b.3 DnaJB6 localizes to K-fibers and affects their resistance to cold but not their length

We wondered if the observed differences in spindle length in DnaJB6 silenced cells could be related to an effect on the Kinetochore-fibers (K-Fibers). Two different features were tested, the length of the K-Fibers and their resistance to cold induced depolymerization.

As a first approach, we tested whether DnaJB6 specifically localizes to K-fibers. We incubated HeLa cells on ice for 10 minutes (to depolymerize the non-bundled microtubules) and immunostained DnaJB6 with our homemade antibody. A clear signal of DnaJB6 was detected along the k-Fibers (fig.R.15.b).

We then measured the length of K-Fibers in control or DnaJB6 silenced cells. We first treated the cells with STLC (2 hours) in order to get monopolar spindles with straight microtubules and incubated them on ice for 7 minutes (to keep the K-Fibers). The length of the K-Fibers in control cells was 1.54µm on average (± 1 SD) and 1.624µm (± 0.94 SD) in DnaJB6 silenced cells (fig.R.15.d and e). Unexpectedly, the difference was no statistically significant.

In order to test the K-Fibers stability after cold treatment in absence of DnaJB6, we transfected the cells with specific siRNAs and 48 hours later we incubated them on ice for 10, 20 or 30 minutes. Then, we fixed the cells and looked at K-Fibers by immunostaining for tubulin (with α-DM1A) and DNA. We classified the mitotic cells as containing or not K-Fibers (fig.R.15.c). In control cells, the percentage of cells without K-fibers increased as the time of incubation increased. In control cells, 1.1% (± 1 SD) of the cells did not contain detectable K-Fibers at 10 minutes, 19.7% (± 11.5 SD) at 20 minutes and 36.9% (± 8.4 SD) at 30 minutes of incubation on ice. No significant differences were observed at 10 and 20 minutes when DnaJB6 was silenced (2.3% ± 3 SD cells without K-Fibers at 10 minutes and 18% ± 15.6 SD at 20 minutes). Interestingly, a significantly higher percentage of cells without K-Fibers was detected at 30 minutes (Sidak's multiple comparisons test with P-Value<0.0001), reaching 60.7% ± 8.5 SD (24% more than what was observed in control cells).

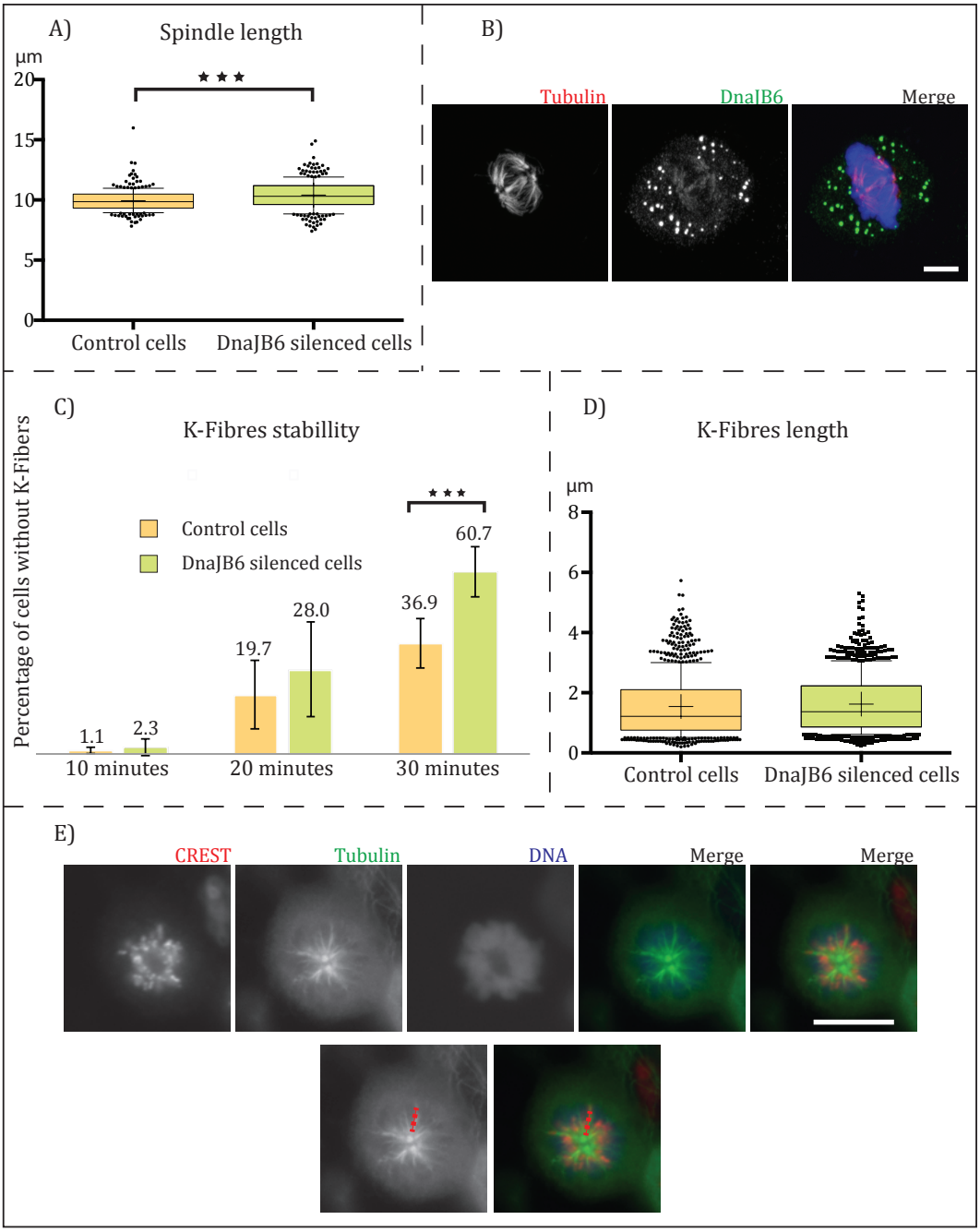


**Fig.R.15. DnaJB6 affects the length of the bipolar spindle and localizes to the K-Fibers affecting their stability but not the length:** A) Spindle length measurements in HeLa cells: Transfected HeLa cells were fixed and processed for IF staining with DM1A and Hoechst. Quartiles graph representing the length of 267 control and 294 silenced cells. Statistical analysis by Mann Whitney test (★★★) Indicates p-value<0.001. B) DnaJB6 localization to the K-Fibers: IF done on HeLa cells incubated 10 minutes on ice. α-DnaJB6 at 5µg/µl and DM1A at 1:1000 were used. C) K-Fibers stability test: HeLa cells were transfected and incubated on ice before fixation. K-Fibers presence was analyzed processing the samples for IF (with DM1A) and observed with a fluorescence microscope. Graph showing three replicas quantification average (≈ 200 cells per condition and replica). (★★★) Indicates p-value<0.001 using ANOVA test. D) K-Fibers length measurement from STLC treated Hela cells incubated 7 min on ice and processed for IF. DM1A staining. More than 1000 fibers measured, from 3 experiments. E) IF example of the K-Fibers length measurement. Red line indicates the measurement protocol.

### 3.b.4. Silencing of DnaJB6 promotes spindle multipolarity

As shown in chapter 3.b.1 of the results section, an increase of cells with multipolar spindles is observed when silencing DnaJB6 in non-synchronized HeLa cells. To precisely describe this multipolarity phenotype, we specifically analyzed it in an independent experiment. We fixed non-synchronized HeLa cells (silenced for DnaJB6 and controls) and look specifically at the organization patterns of the microtubules by staining tubulin. We classified the structures in two groups: bipolar spindles and multipolar spindles. A strong increase in the percentage of cells with multipolar spindle was found when DnaJB6 was silenced (fisher's exact test p-value<0.0001 for each individual experiment), although the percentage differs between experiments (probably due to differences in the efficiency of the silencing). In control cells, a 5% of the structures were classified as multipolar, whereas in DnaJB6 silenced cells the percentage was 22% and 48% for each experiment (fig.R.16.a).

Interestingly, by looking closely at bipolar spindles, we noticed another phenotype related to the organization of the microtubules. In some metaphase cells, we could distinguish the presence of a small microtubule aster not incorporated into the bipolar spindle (fig.R.16.c and d). These ectopic microtubule asters were present in 1.1% of control metaphase cells, whereas the percentage increased to 11.5% in DnaJB6 silenced cells (Fisher's exact test, P-Value<0.0001).

Altogether, these phenotypes suggest that DnaJB6 could be involved in the organization of the microtubules to form the bipolar spindle.

## 3.c. Multipolar spindles formation in DnaJB6 silenced cells is independent of the presence of extra centrioles

Previous studies pointed to different causes for the formation of an extra-pole during mitosis. One of the most common is the presence of extra centrosomes, upon defects in centrosome duplication (as described in many cancers), or cytokinesis failure. However, multipolarity can also occur in absence of extra centrosomes, by centriole disengagement or pericentriolar material fragmentation (Reviewed by Maiato & Logarinho 2014).

To determine the origin of the extra-poles generated in the absence of DnaJB6, we examined whether centrioles were present at the extra poles of the multipolar spindles. We transfected HeLa cells with siRNAs against DnaJB6 or control and 48 hours later we fixed the cells. We used antibodies against centrin and tubulin and we analyzed the samples under an optical fluorescence microscope. In multipolar spindles from control cells, most poles were positive for centrin (77.8% ± 6.7 SD of the multipolar spindles in which all the poles were centrin positives), suggesting that the origin of the multipolarity was due to the presence of an excessive number of centrosomes that did not cluster together in order to generate two poles. In contrast, this was not the case for the DnaJB6 silenced cells (fig.R.16.b and c). Only 11.7% (± 5,6 SD) of the multipolar spindles had all the poles positives for the centrin. In other words, in DnaJB6 silenced cells, 88.3% (± 5,6 SD) of the multipolar spindles did contain some centrin negative pole (ANOVA test, P-value<0.001). This result suggests that the multipolarity present in cells silenced for DnaJB6 is not due to the existence of an aberrant number of centrosomes. Instead, this suggest that the extra poles reflect defects in the organization of the microtubules.

We confirmed that the bipolar spindles did contain a normal number and positioning of the centrosomes (4 centrioles per spindle and 2 centrin dots per pole) in both samples (data not shown).

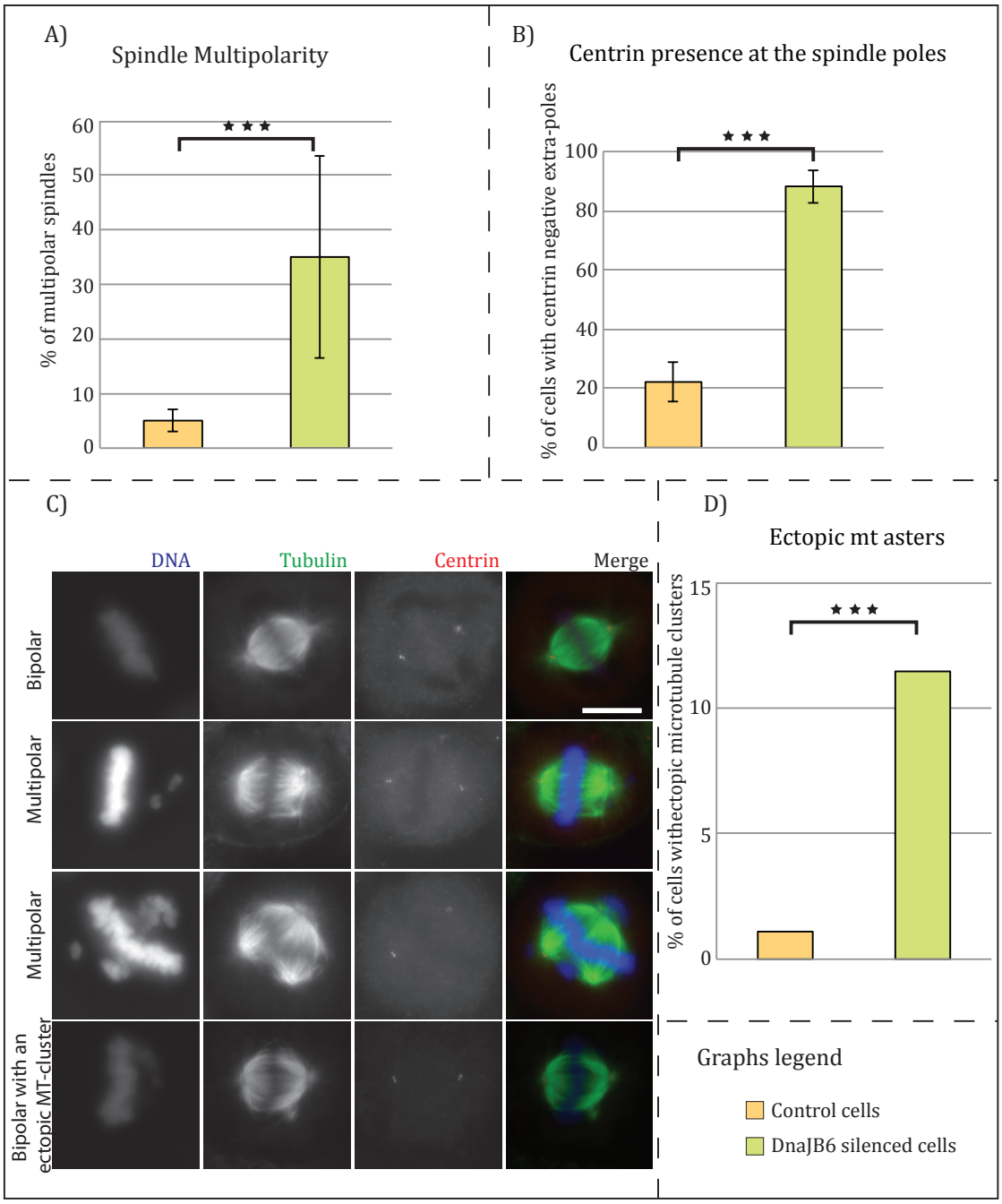


**Fig.R.16. DnaJB6 silencing induces spindle multipolarity:** Cells were transfected, fixed after 48 hours and stained with α-centrin, α-tubulin-β and Hoechst in all the cases. A) Spindle multipolarity quantification: Spindle structures were quantified and classified as bipolar or multipolar. Average of the three replicas is represented with the standard deviations (top line). B) Centriole presence at the spindle poles analysis: graph shows the percentage of multipolar spindles with centriole negative poles (from the total multipolar spindles). C) Bipolar spindle and spindle organization phenotypes examples of HeLa DnaJB6 silenced cells D) Ectopic microtubule clusters presence in bipolar spindles quantification. Percentage from the total of bipolar spindles. ANOVA tests in all the experiments except in D (fisher's exact test). (★★★) Indicates p-value<0.001

## 3.d. DnaJB6 silencing impairs the organization of the microtubule asters to form the bipolar spindle after nocodazole washout

The acentrosomal extra poles could be originated through two types of mechanisms: the disruption of the spindle poles by the tension and forces transmitted by the microtubules or "*de novo*" formation of the extra poles, due to the self-organization of the microtubules by minus end directed motors.

We decided to analyze the organization of the mitotic microtubules by looking at long times of incubation after nocodazole washout in HeLa. We transfected the cells and after 48 hours we added nocodazole at 2μM final concentration (incubating for 3 hours). After nocodazole washout, cells were fixed at different time points and processed for IF. Microtubule asters organization in bigger asters and finally in bipolar spindles was analyzed. We observed that the organization of the microtubules into bipolar spindles was severally impaired in DnaJB6 silenced cells.

We quantified the number of asters per cell at 10, 20, 30, 40, 50, 60 minutes after nocodazole washout. The number of asters observed in DnaJB6 silenced cells was significantly higher than in control cells in all the different time points (ANOVA test comparing the two conditions per each time point, P-value<0.0001). The average number of asters per cell in each sample are summarized in fig.R.17.b These results indicate that the silencing of DnaJB6 impairs the organization of microtubules to form the spindle (fig.R.17.a).

We already reported that DnaJB6 silenced cells have higher number of asters per cell, however how this affects the organization of microtubules in two big asters and subsequently in the construction of a normally shaped bipolar spindle is still unclear. To address these questions we first looked at how many cells had been able to organize the microtubules in just two asters in different time-points (fig.R.17.c). We took samples at 5, 10, 20, 30, and 60 minutes. The proportion of cells with only 2 microtubule asters (or one) was reduced in DnaJB6 silenced cells since the 20 minutes' time-point (20 minutes included; P-values <0.0001 in fisher's tests) (5 minutes was also lower in DnaJB6 silenced cells, P-Value=0.0036). Two

different patterns were observed in cells with two asters after 60 minutes. Approximately half of the control cells had a standard bipolar spindle (57% ± 0.7 SD of the control mitotic cells), whereas two separated asters were observed in the other cells (no bipolar spindle like structure). Instead, only 24.8% (± 13.5 SD) of the mitotic DnaJB6 silenced cells had a bipolar spindle (fisher's test, P-Value<0.0001 in each experiment replica) (fig.R.17.d).

Altogether, these results suggest that DnaJB6 could be involved in the MT organization in a bipolar spindle. This spindle organization in cells after their release from a nocodazole arrest would be impaired in absence of DnaJB6.

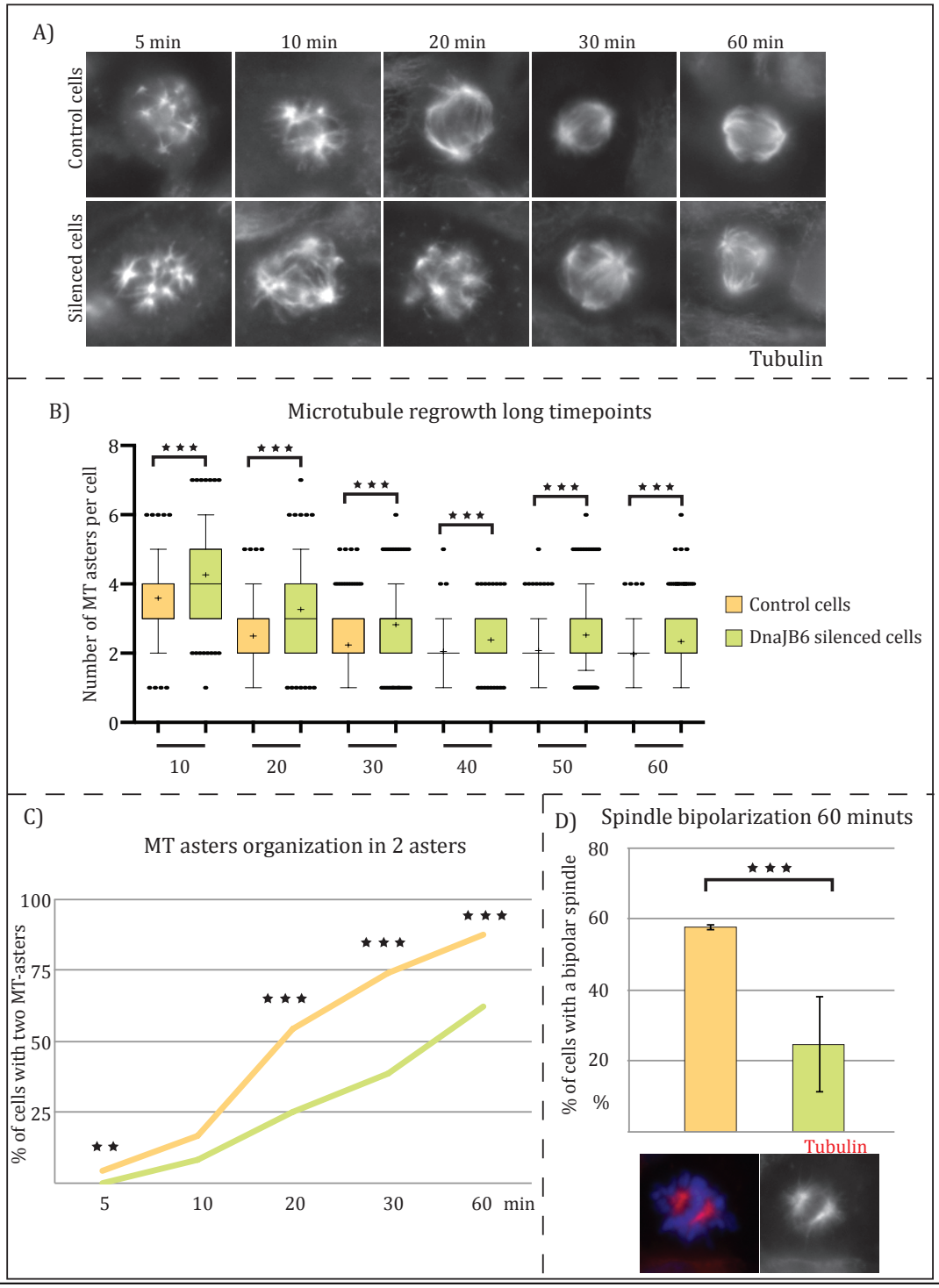


**Fig.R.17. DnaJB6 is involved in the organization of the MTs:** MT- regrowth experiments with long incubations after nocodazole release are shown for all the sections. Cells were fixed and processed by IF staining with DM1A antibody and Hoechst. A) Representative images of several time-points, taken with a Leica wide-field microscope. B) Quantifications of the number of MT asters per cell at different time-points after nocodazole release. C) Quantification of the percentage of cells with just two MT-asters (organized or not as a bipolar spindle) at different time points. D) Percentage of cells with two asters in which those are organized as a bipolar spindle. Image representing a cell with 2 asters not forming a bipolar spindle. ANOVA tests for B and fisher's test for C and D. (★★) Indicates p-value<0.01 and (★★★) Indicates p-value<0.001.

# 4. Chapter 4- DnaJB6 interacts with p150 and promotes the Dynein-Dynactin complex activity in mitosis

## 4.a. xDnaJB6-L interacts with the Dynactin subunit P150 in a RanGTP dependent manner

The defects in spindle organization observed in DnaJB6 silenced cells suggest that DnaJB6 could play a role in the organization of the microtubules during mitosis, more specifically in spindle pole formation or maintenance, characterized by the focusing of the microtubule minus-ends. Spindle pole organization and maintenance depends on the activity of minus-end directed motor proteins and associated proteins. The two main minus-end microtubule motor proteins in human are the Dynein-Dynactin complex and HSET (detailed in introduction, Chapter 3.c). We therefore hypothesized that DnaJB6 may interact with any of these motors and play a role in regulating their activity.

We tested this idea performing pull down experiments using the recombinant DnaJB6-L. Due to its easy manipulation as an open system, we decided to use the again *Xenopus laevis* EE. MBP or MBP-xDnaJB6-L was coated to magnetic Dynabeads using homemade anti-MBP antibodies. The beads were incubated in meiotic *Xenopus laevis* EE in presence or absence of RanGTP. The EE was incubated at 20ºC for 15 minutes (to allow RanGTP dependent protein-protein interactions to take place) and then on ice in order to depolymerize the microtubules. The proteins associated with the beads were recovered, run in SDS-PAGE and processed for western blot analysis. By blotting the membrane with anti-p150 antibodies, a clear band was detected at the input line approximately at 150KDa, corresponding to the size of p150. The same band was also detected at the line of the MBP-xDnaJB6-L pull down corresponding to the condition in which the beads had been incubated in EE in presence of RanGTP (fig.R.18.a). Interestingly, this band was not detected in the condition in which the beads were incubated in an EE without RanGTP. No band was observed in the control line, in which MBP-coated beads were incubated in EE. The detection of these bands indicates that p150 co-pellets with MBP-xDnaJB6-L coated beads incubated in EE specifically in presence

of RanGTP. The results suggest a putative RanGTP regulated interaction between DnaJB6-L and the Dynactin complex, although we do not know if this interaction is direct or not.

In order to confirm the putative interaction between DnaJB6-L and p150 and test whether we could also detect it in human cells, we decided to do co-immunoprecipitation assays using HEK293 stable cell lines expressing flag-DnaJB6-L or flag-DnaJB6-S. We could not detect any interaction between DnaJB6 and p150 through co-immunoprecipitation, neither in mitosis nor in interphase cells (data not shown). This negative result could be due to many different experimental problems, so we decided to follow an alternative approach using a Duolink proximity ligation assay (sigma-aldrich). The principle of the technique is the following: in fixed cells, two specific antibodies recognize two proteins, then a pair of oligonucleotide linked secondary antibodies are added and, after addition of a ligase, a ligation reaction occurs between the two different oligonucleotides (if they are closer than 40nm), finally, a DNA amplification with fluorescently labeled oligonucleotide occurs and the signal is detected with a fluorescence microscope after mounting the sample. We performed the duolink assay on non-synchronized HeLa cells with the previously optimized specific antibodies against DnaJB6 and p150. As shown in fig.R.18.b, a positive signal is observed to the spindle microtubules of mitotic cells. As expected, no signal was detected in DnaJB6 silenced cells, confirming the reliability of this result. This result indicates that both proteins, DnaJB6 and p150, localize to the same region of the mitotic spindle and that the distance between them is lower than 40nm, suggesting that DnaJB6 and p150 could interact in mitotic HeLa cells. Interestingly, no signal was detected on microtubules in interphase cells. This result is particularly interesting because DnaJB6-S and p150 are both present at the cytoplasm of HeLa cells in interphase, in the case of p150 interacting with the microtubules. The results suggest that this interaction would occur specifically in mitosis and maybe would also be exclusive for the long isoform of DnaJB6.

Altogether, our results suggest that the long isoform of DnaJB6 interacts with p150. Although we do not know if this interaction is direct, the results from the

duolink assay indicate that the distance between both proteins is lower than 40nm in mitosis. In addition, our results suggest that the interaction occurs specifically in mitosis and that it is RanGTP dependent.

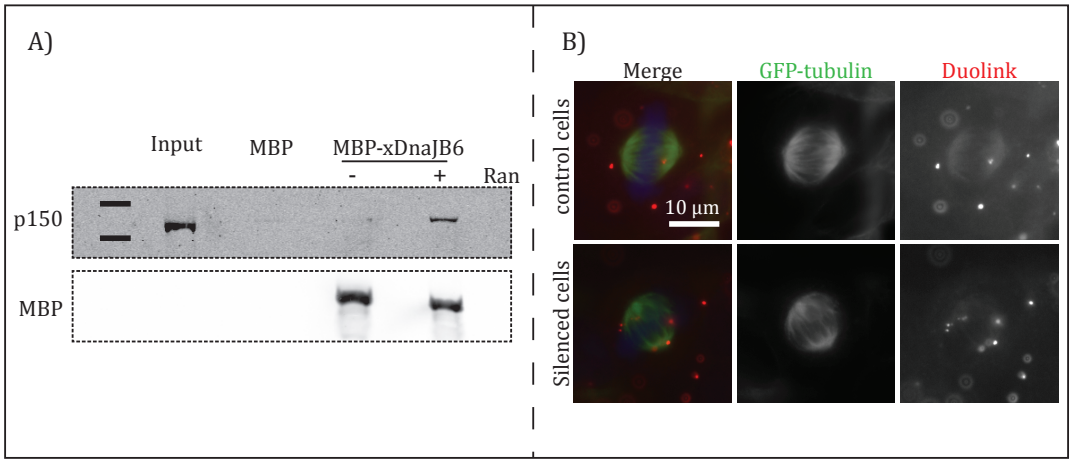


**Fig.R.18. DnaJB6 interacts with p150 in a RanGTP-regulated manner:** A) Pull down experiment in EE using recombinant purified MBP-xDnaJB6-L. Western blot membrane showing the co-precipitation of p150 with xDnaJB6-L in presence of RanGTP, whereas the protein is not detected when RanGTP is not present, neither in the control (MBP). B) Duolink proximity ligation assay: Duolink test using α-DnaJB6 and α-p150 in HeLa cells, showing a positive signal in control cells that is substantially reduced in DnaJB6 silenced cells.

## 4.b. DnaJB6 is required for p150 distribution along the spindle

The interaction between DnaJB6 and p150, together with the phenotypes observed in microtubule organization in DnaJB6 silenced cells, suggested that the activity of the Dynactin complex could be impaired in these cells. We first analyzed the localization of p150 in mitosis in two different systems. On one hand, we looked at the p150 distribution along the spindle in DnaJB6 silenced cells. On the other, we checked p150 distribution in *Xenopus laevis* cycled EE spindles after the depletion of DnaJB6 and adding back the recombinant MBP-xDnaJB6-L.

To analyze the distribution of p150 in the spindle in HeLa cells, we fixed unsynchronized cells and performed IF to visualize p150 (fig.R.19.a). Changes in the distribution pattern of p150 were observed in DnaJB6 silenced cells. To obtain quantitative data, using FIJI software, we selected images of individual cells in metaphase and draw a rectangle, with a conserved size, from pole to pole (with the metaphase plate centered in the middle of the rectangle) (fig.R.19.b) and obtained the mean of the intensity per pixel for each position over the horizontal-axis (X-

axis) of the rectangle. The intensity values were measured for tubulin and for p150 separately. The values obtained from these mesurements are represented together in a XY graph (fig.R.19.c). The intensity of p150 is higher in DnaJB6 silenced cells, in agreement with the overall visual evaluation. However, there were also differences on the tubulin intensities in control and DnaJB6 silenced cells. In order to determine if the differences in p150 intensity were associated to differences in microtubules number, we normalized the intensity values of p150 with the ones of tubulin (per each specific "X" point) after subtracting the background of both. This normalization showed that p150 accumulates at the spindle poles in absence of DnaJB6. As detailed in the next chapter, we have also normalized the length of the spindles in order to better compare p150 intensity at the poles and confirmed that the observed significant differences were maintained (data not shown). We conclude that the silencing of DnaJB6 induces changes in the distribution of p150 to the spindle in HeLa cells.

The limitation of using cells for silencing DnaJB6 was that both the long and the short isoforms of DnaJB6 were silenced and therefore it was not possible to assign the associated phenotypes to one specific isoform. We therefore decided to move to *Xenopus laevis* EE system to deplete both isoforms and rescue with the long isoform (x-DnaJB6-L). We depleted both isoforms of the endogenous protein from the CSF-extract using Dynabeads coated with anti-xDnaJB6 (fig.R.19.e). As a control, the same extract was incubated with generic IGs coated beads in parallel. Xenopus sperm, rhodamine tubulin and calcium was added to both CSF-extracts (control and depleted) to induce their entry to interphase by incubation at 20ºC. After 90 minutes, CSF-extract (control or depleted) was added to the interphase extracts in order to induce the entry to mitosis. The DnaJB6 depleted extract was then supplemented with MBP (final concentration of 0,017μM as control) or with MBP-xDnaJB6-L (final concentration of 0,017μM). After 60' of incubation at 20ºC, the microtubule structures of the three samples (control, depleted and add back) were centrifuged on a coverslip and fixed. After staining p150 by a classical immunofluorescence, pictures of all the bipolar spindles present in each sample were taken. In this experiment, just bipolar spindles with proper shape were

analyzed (spindle abnormalities due to the protein depletion are described in chapter 4.e.b. of the results section). We measured the intensity of p150 and tubulin following the same strategy as in cells (fig.R.19.b). Again, we subtracted the background and normalized the obtained data from the p150 on the tubulin intensity. As shown in fig.R.19.f, depletion of x-DnaJB6 in cycled EE induces an increase of p150 intensity at the spindle poles. Interestingly, this increase was totally rescued by the addition of MBP-xDnaJB6-L recombinant protein at 0,017uM (fig.R.19.f), suggesting that the observed effect is dependent on the activity of the long isoform of DnaJB6. No differences regarding the total concentration of p150 within the extracts were detected when depleting DnaJB6 (fig.R.19.d).

**Fig.R.19. DnaJB6 affects the distribution of p150 along the spindle:** A, B and C) p150 distribution along the bipolar spindle in HeLa cells. A) Representative IF images of control and DnaJB6 silenced cells. B) Schematic representation of how the measurements were done (see material and methods for a detailed description) C) Graphic representation of the protein intensities average obtained from the measurements along the drawn rectangle, 47 control and 37 silenced cells are represented. Top graph, absolute intensities of p150 and tubulin for control and silenced cells. Bottom, p150 intensity values after normalization with tubulin (tubulin absolute intensity ÷ 100 also shown as reference). D, E and F) p150 distribution along the spindle upon DnaJB6 depletion in EE. In D, WB using 1µl of control or DnaJB6 depleted EE bloated with α-p150 to confirm that p150 abundance on the EE is not affected by the deletion of DnaJB6. In E, WB using 1µl of control, DnaJB6 depleted or "added back" (0,017µM of MBP-xDnaJB6-L) EEs bloated with α-xDnaJB6 to confirm the efficiency of the depletion and the re-addition of xDnaJB6. P150 intensities along the spindle normalized by tubulin intensity are represented in F graphs. Bipolar spindles images were processed as for HeLa cells spindles. Control and depleted EEs are represented in top graph and control and added back EEs in the graph below. (⋆) Indicates significant differences between conditions at the indicated position, ANOVA test.

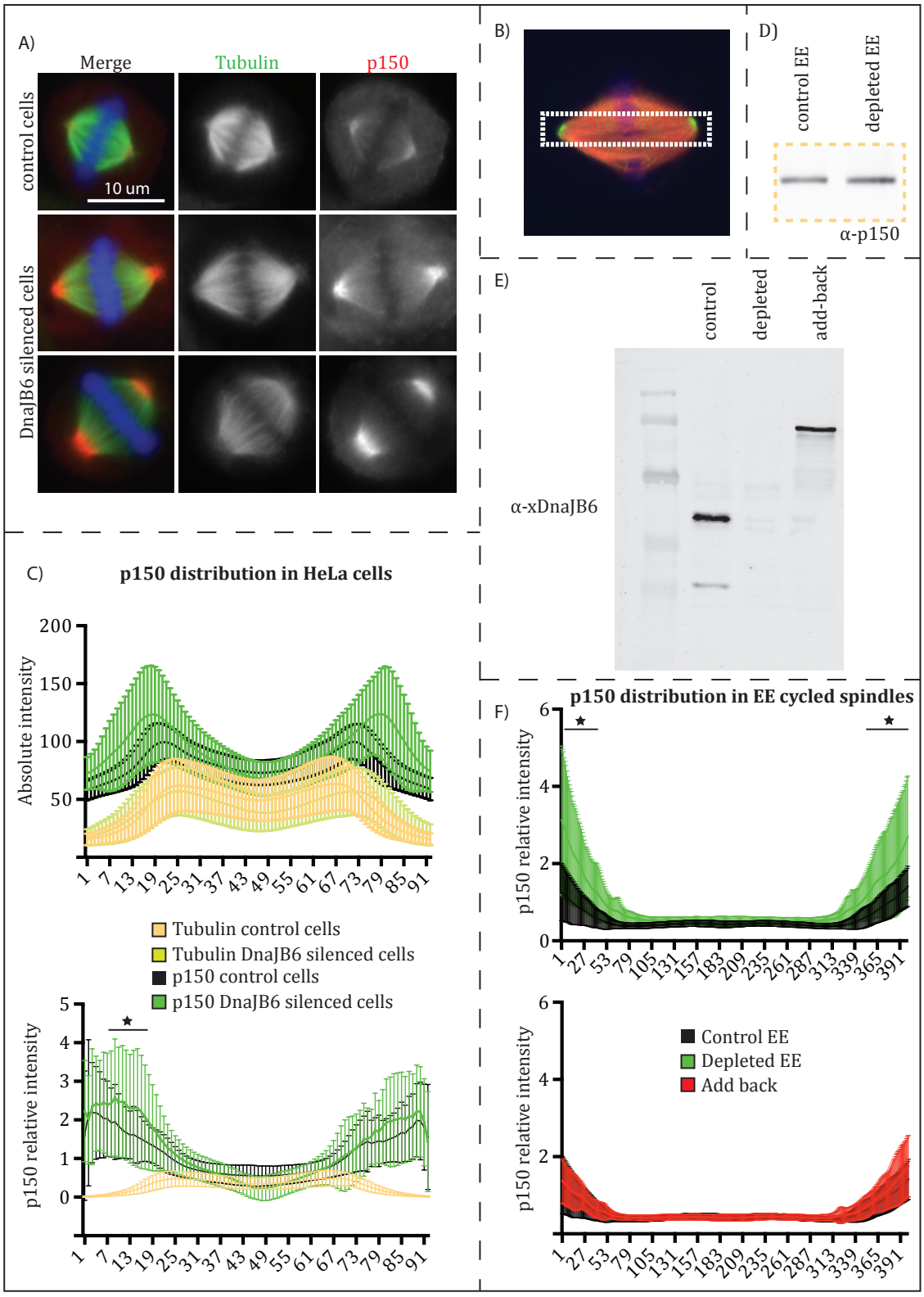
A)
Merge
Tubulin
p150
control cells
DnaJB6 silenced cells
10 um
B)
D)
control EE
depleted EE
α-p150
E)
control
depleted
add-back
α-xDnaJB6
C)
p150 distribution in HeLa cells
Absolute intensity
Tubulin control cells
Tubulin DnaJB6 silenced cells
p150 control cells
p150 DnaJB6 silenced cells
p150 relative intensity
F)
p150 distribution in EE cycled spindles
p150 relative intensity
Control EE
Depleted EE
Add back

## 4.c. DnaJB6 also affects the spindle localization of some other proteins

We wondered whether the distribution patterns of specific proteins along the spindle could be affected by the silencing of DnaJB6, as we observed with p150. We tested the localization of the following proteins: NuMA, HSET, EG5 and TACC3. We used the same approach that we adopted for analyzing p150. We fixed HeLa cells either control or silenced and stained for the proteins of interest and tubulin with specific antibodies (as detailed in material and methods). We then imaged between 30 and 50 metaphase cells per condition, with normal focused spindle poles (fig.R.20.a). Quantification of the respective intensities was conducted by analyzing the images with FIJI. We draw a rectangle (with a fixed size) with the metaphase plate at the center and the poles contained within the figure. We then took the intensity profile of the rectangle (obtaining the pixel average intensity of each line along the horizontal axis). We performed these measurements for each specific protein and tubulin in each cell. Normalization of the protein intensity on the tubulin intensity was applied. Because the length of the spindles was longer in DnaJB6 silenced cells, the spindle poles did not coincide with the control cells when tubulin intensities were plotted together. This means that we could compare the intensities in the center of the spindles with much more certainty than at the spindle poles. Therefore to compare the intensity at the spindle poles, we measured the distance between the two points with highest tubulin intensity (in average) in control and silenced cells. We then subtracted the observed difference of this distance from the center of the silenced spindles. By doing so, we were able to compare the protein intensity at the spindle poles and confirm the results obtained before size normalization (fig.R.20.b).

**NuMA** is a non-motor Dynein-Dynactin interacting protein, with essential role in microtubule focusing at the spindle poles (Merdes et al. 2000; Silk et al. 2009). NuMA directly interacts with the microtubules linking the Dynein-Dynactin complex to them (Merdes et al. 1996). The protein accumulates mainly to the spindle poles in mitosis (Tang et al. 1994), as we could also detect (fig.R.20.c). No differences in NuMA relative intensity were detected along the spindle (from pixel

47 to 151), but a strong increase in intensity was found at the spindle poles, as it was already clear at the microscope (60 cells per condition have been analyzed). After adapting the length as previously described, we compared the NuMA intensity at the extremes of the spindle, and we could detect a significant higher intensity in DnaJB6 silenced cells (from 1 to 46 and from 146 to the end). So, a similar effect on NuMA and p150 localization was observed when silencing DnaJB6.

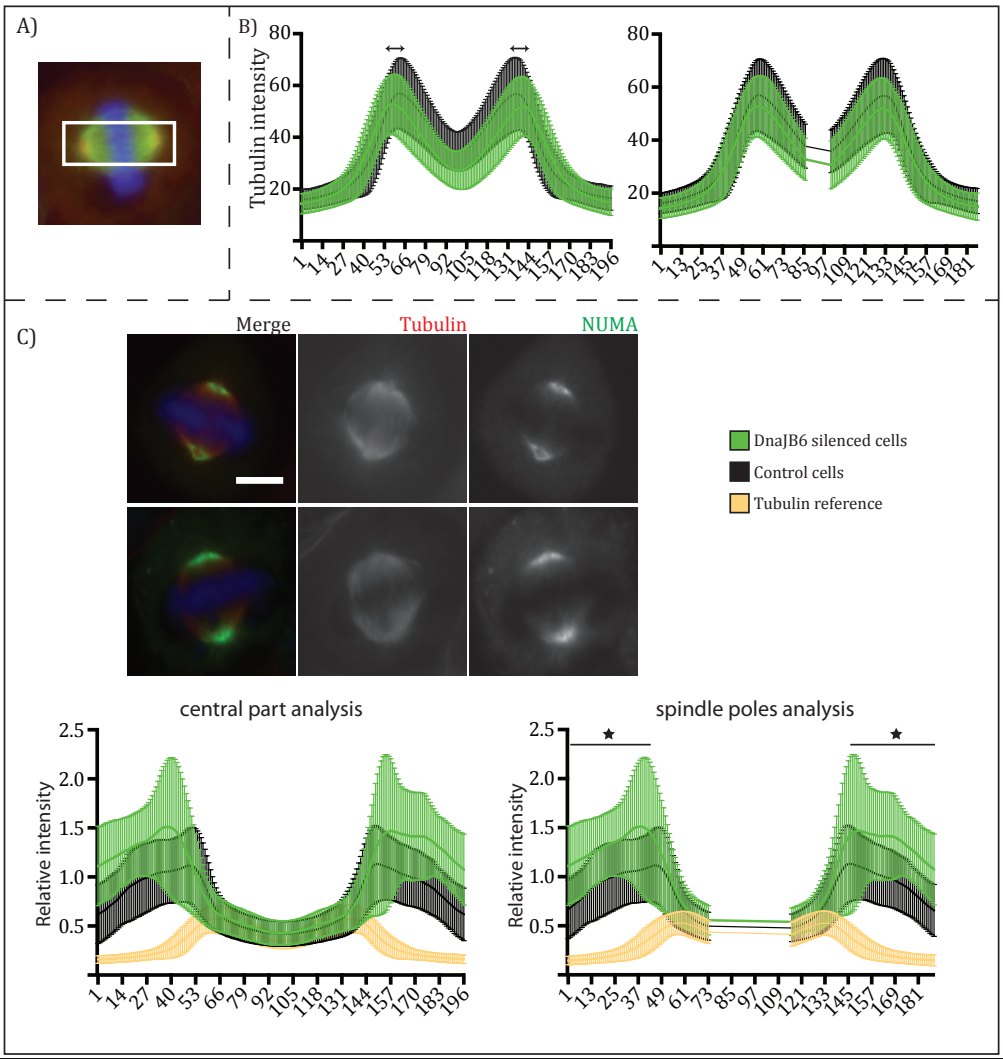


**Fig.R.20. DnaJB6 affects the distribution of NuMA along the spindle:** Analysis of NuMA distribution along the bipolar spindle in HeLa cells. A) Schematic representation of the process of data collection. B) Tubulin intensity graphs as example of the spindle size normalization. C) Top subfigure, Representative IF images of NuMA distribution in control and DnaJB6 silenced cells. Bottom graphs, graphic representation of NuMA relative intensity average obtained from the measurements along the drawn rectangle and normalized for the tubulin intensity (tubulin absolute intensity ÷ 100 also shown as reference). Left graph, results before length adaptation, right graph, results after adapting the spindle sizes. (★) Indicates significant differences between conditions at the indicated position, ANOVA test.

**HSET** is the other main minus-end directed motor protein in human cells. The protein is also involved in the focusing of the microtubules at the spindle poles (Mountain et al. 1999; Gordon et al. 2001; Silk et al. 2009; Kleylein-Sohn et al. 2012). By using specific antibodies we could detect the protein on the microtubules all along the spindle (fig.R.21.a). 33 control and 36 silenced spindles were analyzed. After normalizing, a significant higher intensity of HSET was detected in the central part of the spindle (from the positions 83 to 100 and 107 to 128), whereas no differences were detected at the spindle poles after length normalization (2 way ANOVA tests with multiple comparisons, considering P-Value<0.05 as significant differences).

**TACC3** is a non-motor protein that interacts directly with the microtubules (Gergely et al. 2000) and localizes all along the spindle (at the centrosomes, at the spindle poles, along the spindle MTs, on the k-fibres, and at MT plus tips). TACC3 is important for the organization of the spindle pole (Gergely et al. 2003). The protein plays also an essential role in the stabilization of the K-Fibers by forming inter-microtubule bridges together with ch-TOG and clathrin (Booth et al. 2011) and is also involved in microtubule assembly by the centrosome (Kinoshita et al. 2005) and microtubule plus-end dynamics (Gutiérrez-Caballero et al. 2015). No relation with the Dynein-Dynactin complex has been established until now. We were able to detect the protein all along the spindle in control cells. Silencing of DnaJB6 results instead in an accumulation of TACC3 at the central zone of the spindle (from pixel 116 to 123 and 143-144; 2 way ANOVA tests with multiple comparisons, considering P-Value<0.05 as significant differences), possibly at the plus-ends of the K-Fibres (fig.R.21.b). In contrast, no differences were detected when looking at the protein localization at the spindle poles. Further studies will be necessary to understand the reason of this TACC3 accumulation at the plus-ends of the microtubules in DnaJB6 silenced cells.

**EG5** is a plus-end directed motor protein that localizes to all along the spindle microtubules and slides apart antiparallel microtubules promoting spindle pole separation (Sawin et al. 1992; Sawin & Mitchison 1995; Walczak et al. 1998; Kapitein et al. 2005). The activities of EG5 and Dynein-Dynactin generate opposing

forces within the spindle (Gaglio et al. 1996). The counteracting forces generated by these motor complexes are very well regulated, so an improper balance induces severe defects in spindle assembly such as monopolarity or multipolarity. We analyzed the localization of EG5 to test the possibility that silencing of DnaJB6 could have a general effect on the distribution of the motor proteins, or if a difference could be observed due to the balance of the forces within the spindle. We detected the presence of EG5 all along the spindle, as already described (fig.R.21.c). No differences were detected neither at the central part of the spindle, nor at the spindle poles after length normalization (47 control and 34 silenced spindles have been analyzed).

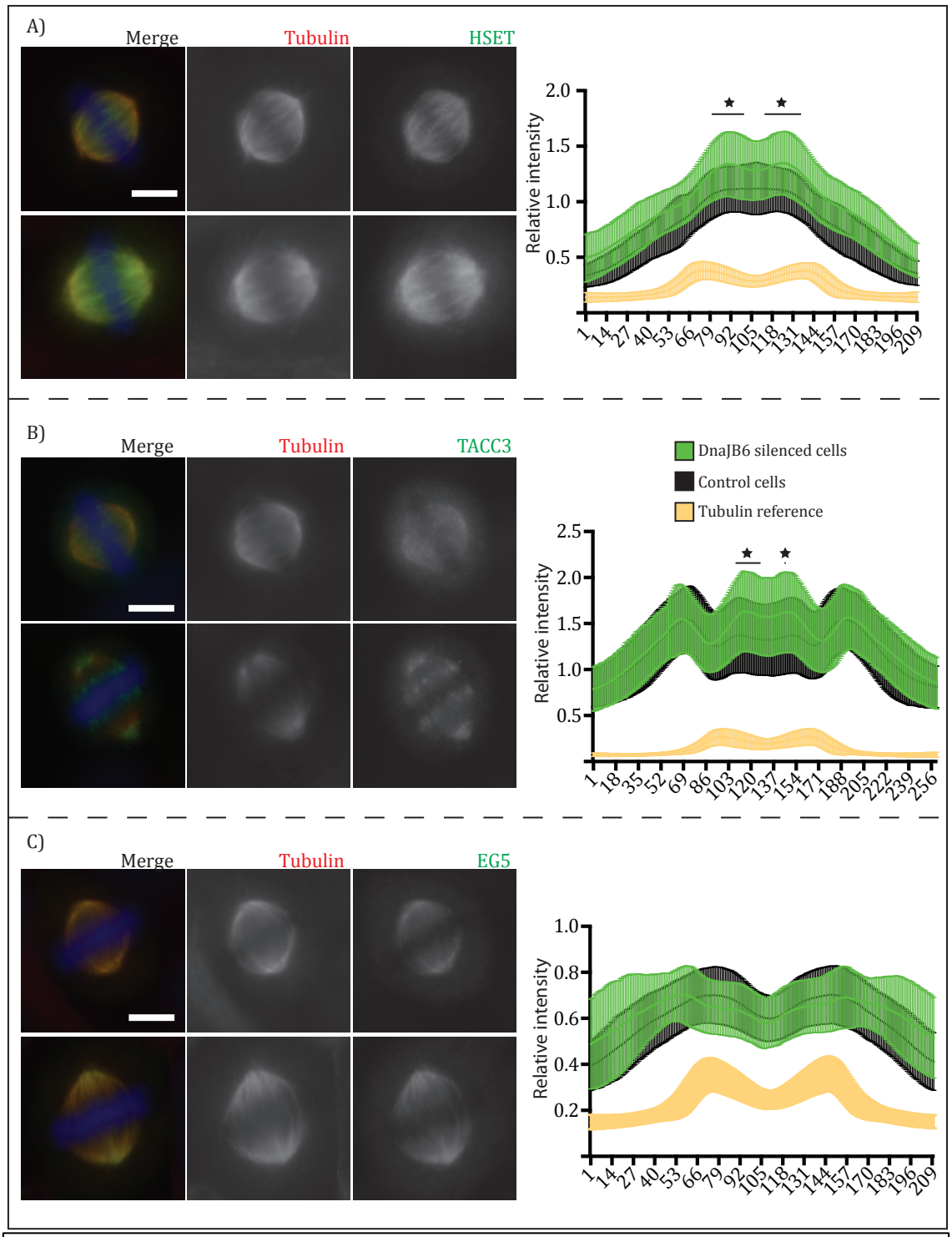


**Fig.R.21. DnaJB6 effect on the distribution of HSET, TACC3 and Eg5 along the spindle:** In all subfigures, representative IF images of specific proteins distribution in control and DnaJB6 silenced cells and graphic representation of the protein relative intensities average obtained from the measurements along the drawn rectangle and normalized for the tubulin intensity (tubulin absolute intensity ÷ 100 also shown as reference). (★) Indicates significant differences between conditions at the indicated position. A) HSET B) TACC3 C) Eg5.

## 4.d. DnaJB6 is required for the stability of the Dynactin motor protein complex, specifically in mitosis

We have shown that xDnaJB6-L interacts with p150, and it is required for the correct distribution of p150 along the spindle (both in human cells and *Xenopus* EEs). We also observed microtubule organization defects within the spindle, compatible with defects of the activity of the Dynein-Dynactin complex. Together, our data suggest that DnaJB6 mitotic function is to regulate the Dynein-Dynactin complex. Since DnaJB6 is a co-chaperon from the HSP40 family, it could help the formation of the Dynactin complex or confer stability to it. In order to test this hypothesis, we have checked the stability of the human Dynactin complex in absence of DnaJB6. The addition of potassium iodide (KI) to the cell lysate has been shown to disrupt the Dynein and Dynactin complexes in a concentration dependent manner (King et al. 2002). We decided to test if the absence of DnaJB6 affects the dissociation rate of the Dynactin complex upon the treatment with KI.

We prepared lysates of HeLa cells either in interphase or in mitosis (synchronized by 15 hours incubation in 2μM nocodazole and releasing them 45 minutes before recovering). We then added KI to the lysates at increasing concentrations of 0, 100 or 150 μM and incubated them for 1 hour on ice. The lysates were then centrifuged on a sucrose density gradient (from 8 to 20%). The gradients were then fractioned in 9 consecutive fractions and analyzed by SDS PAGE and western blotting, to visualize p150. As a consequence of the incubation with KI, a clear shift on the distribution of p150 along the fractions was detected, both in interphase and mitosis. Due to the lack of appropriated tools, the Dynein complex could not be studied.

Silencing of DnaJB6 did not affect the stability of the Dynactin complex in interphase cells lysates (fig.R.22). In absence of KI, p150 was detected from fraction 5 to 9, with a major peak at the $6^{th}$ and $7^{th}$. Incubation with 100 and 150μM of KI induces a shift on the detection of p150, from fraction 2 to 6, with a major peak at fractions 4 and 5 at 100μM and from 3 to 5 at 150μM. In contrast, a clear shift was observed when DnaJB6 silenced mitotic cell lysates where

incubated in 150µM KI (fig.R.22). P150 was clearly detected from the 2nd fraction of DnaJB6 silenced cell lysates with 150µM KI, while a very weak or no signal was detected at this fraction of control lysates. A shift was also observed when comparing the most intense fractions from both lysates. In addition, a shift was also detected in 100µM KI lysates, although it was less clear than at 150µM KI. Finally, p150 was visualized from the 5th to the 9th fractions in absence of KI, with no effect due to the silencing of DnaJB6.

In conclusion, the absence of DnaJB6 affects the stability of the Dynactin complex specifically during mitosis. Interestingly, the stability of the Dynactin complex upon incubation with different concentration of KI was different in interphase and in mitosis cells lysates.

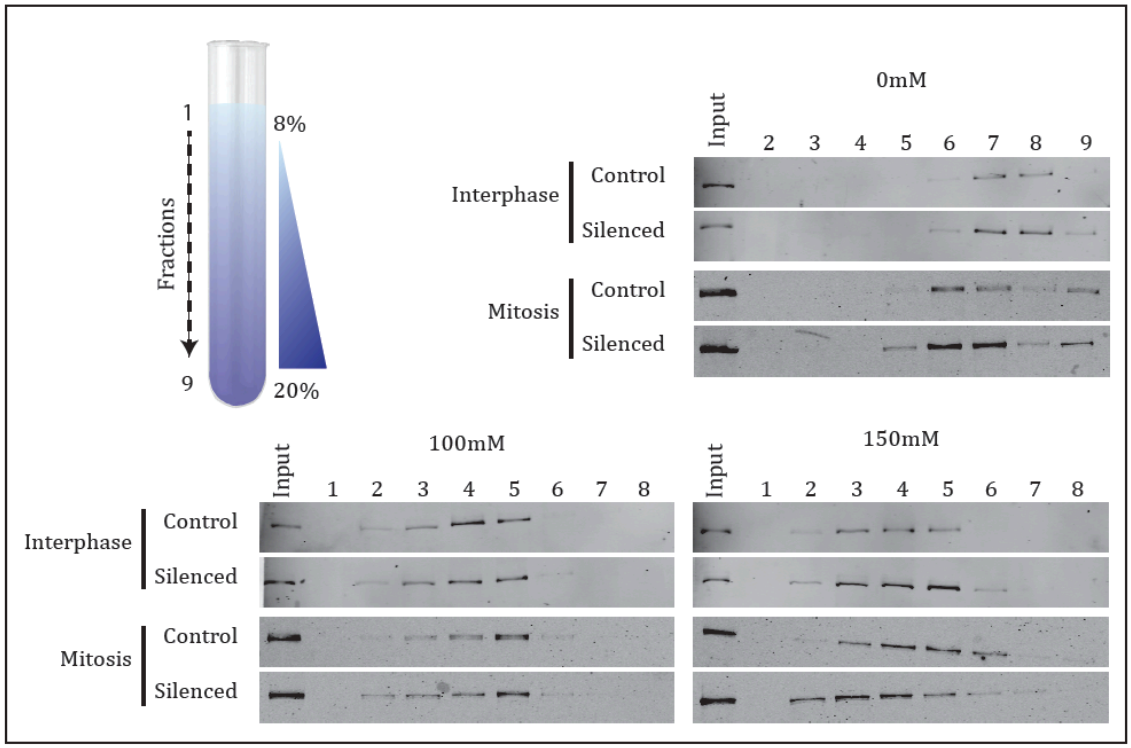


**Fig.R.22. DnaJB6 affects the stability of the Dynactin complex specifically in mitosis:** Sucrose gradient testing the Dynactin complex resistance to disassemble upon incubation with KI. Schematic example of the gradient is shown on top left. Interphase or mitotic HeLa cells lysates were incubated in different concentrations of KI (0, 100 or 150mM), added to the top of the sucrose gradient column and centrifuged. Consecutive fractions of the gradient were collected and loaded to SDS PAGE gels and processed by WB using α -p150 antibodies. Different p150 distribution along the fraction is observed between the different concentrations of KI. A shift is observed between DnaJB6 silenced and control gradients in mitosis, whereas it is not detectable in interphase lysates. Differences are also observed between interphase and mitosis in control lysates.

## 4.e. DnaJB6 is important for the function of the Dynein-Dynactin complex in mitosis

### 4.e.a. The silencing of DnaJB6 rescues bipolar spindle assembly in Eg5 inhibited cells

Mitotic bipolar spindle assembly relies on the presence of opposite forces exerted by different motor proteins complexes with antagonist activities (Walczak et al. 1998). The proper balance of these internal forces within the spindle is essential to avoid the formation of spindles with aberrant number of poles and other abnormalities (Gaglio et al. 1996; Walczak et al. 1998). Together with HSET, the Dynein-Dynactin complex counteracts the activity of the plus-end tetrameric motor Eg5 by exerting antagonistically forces (Tanenbaum et al. 2008; Ferenz et al. 2009; Florian & Mayer 2012). Inhibition of Eg5 with S-trityl-l-cysteine (STLC) promotes the collapse of the spindle and the formation of monopolar spindles (Mayer et al. 1999). Disruption of Dynein activity in STLC treated cells was shown to rescue bipolar spindle formation (Raaijmakers et al. 2013). We used this approach in order to test (in a more direct manner) whether silencing of DnaJB6 affects the activity of the Dynein-Dynactin complex and therefore rescues bipolar spindle assembly. DnaJB6 silenced HeLa cells were incubated with 2μM of STLC for 2 hours at 37ºC and fixed. The percentages of the different microtubule structures in mitotic cells were then quantified by IF analysis (in three independent experiments). In STLC treated control cells, 88.4% (± 2.1 SD) had a monopolar spindle and 10.3% (± 2.3 SD) were bipolar. Instead, the percentage of monopolar spindles was reduced by a 23.1% (65.3% ± 5.6 SD) in DnaJB6 silenced cells (Turkey's multiple comparisons test; p-Value<0.0001), and the percentage of bipolar structures increased by a 17.9% (28.2% ± 8.5 SD) (Turkey's multiple comparisons test; p-Value<0.001) (fig.R.23). No significant differences were detected on the percentages of multipolar spindles (0.3% ± 0.2 SD in control cells and 3.7% ± 3.9 SD in DnaJB6 silenced cells) and non-defined structures (1% ± 0.7 SD in control cells and 2.8% ± 2.8 in DnaJB6 silenced cells). Interestingly, the rescue of spindle bipolarization obtained upon silencing DnaJB6 is very similar to that observed upon silencing of the Dynein light intermediate chain (Jones et al.

2014). Our result suggests that the activity of the Dynein-Dynactin complex to generate inward forces in the spindle is reduced in the absence of DnaJB6.

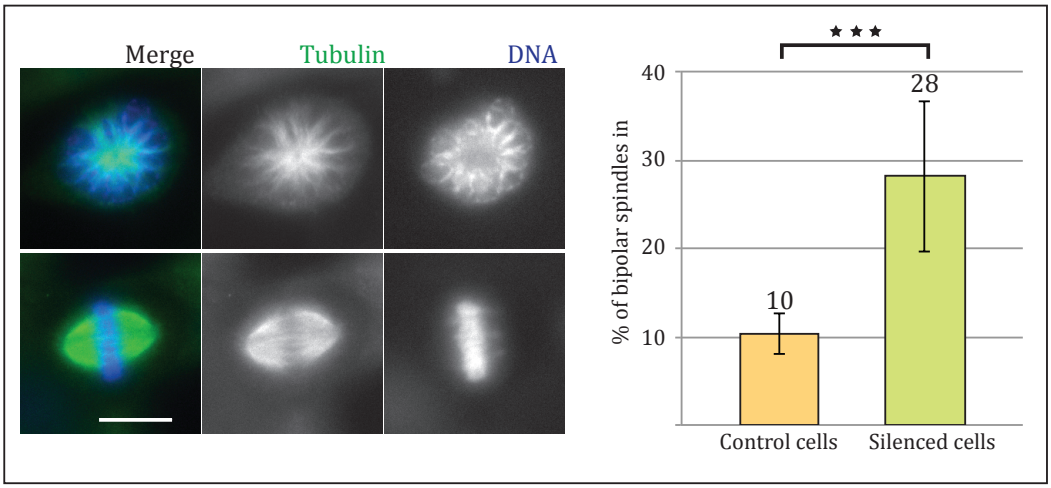


**Fig.R.23. DnaJB6 silencing promotes bipolar spindle rescue in STLC treated cells:** Control and DnaJB6 silenced HeLa cells treated with STLC show different proportion of monopolar and bipolar spindles. On the left side of the figure, examples of both categories. On the right side of the figure, quantifications, average of the percentage of bipolar spindles (from the total of spindles) of three replicas. Standard deviation represented with a line in top of the columns. (★★★) Indicates p-value<0.001 of ANOVA tests.

### 4.e.b. DnaJB6 is required for microtubule focusing at the spindle poles

The Dynein-Dynactin complex plays a major role in microtubule focusing at the spindle poles. We therefore wanted to determine whether DnaJB6 is required as well for this pole focusing activity. In order to test this possibility, we used two different approaches. On one side, we silenced DnaJB6 in HeLa cells and checked the integrity of the metaphase spindle poles. On the other, we looked at the morphology of the poles in spindles assembled in cycled *Xenopus laevis* EE depleted for DnaJB6 and rescued by addition of recombinant xDnaJB6-L.

We first looked at the integrity of the spindle poles in HeLa cells. We classified the poles as closed poles (with all the microtubule ends tightly focused at the spindle pole) or open poles (with the microtubule ends at the pole more spread out or forming more than one focus) (fig.R.24.a). We found that microtubules were tightly focused in 86% of the poles of metaphase control cells. Interestingly, in DnaJB6 silenced cells, only 71 % of the metaphase spindle poles were focused while 29% were not properly focused (fig.R.24.a). Therefore, in silenced cells there is a

decrease of 15% of focused poles compared with the control (fisher's exact test; p-Value<0.001).

To further obtain support to the idea that DnaJB6 is required for spindle pole focusing, we used the *Xenopus* EE system. We performed depletion and add back experiments (as previously described in chapter 4.b of the results section) to test if any phenotype could be reverted by the addition of the recombinant long isoform of the protein. The percentage of bipolar spindles formed under the different conditions was very similar. However, defects in spindle pole focusing were detected in the DnaJB6 depleted EE. In control extracts, 86.8% (± 10.9 SD) of the spindle poles had focused microtubules. Instead, this percentage was reduced to 64% (± 5.7 SD) in depleted extracts, corresponding to a 22.6% reduction (Turkey's multiple comparisons test control-vs-depleted; p-Value<0.0001). This phenotype was rescued by adding MBP-xDnaJB6-L to the depleted EE (81,4% ± 6.8 SD; Turkey's multiple comparisons test of control-vs-rescue; NS). Two different phenotypes were observed at the unfocused poles (fig.R.24.b): unfocused microtubules forming an open pole (similar to the phenotypes observed upon addition of p50/dynamitin to the EE (Wittmann & Hyman 1999)) or pole splitting into two sub-poles. Statistical analysis showed an increase of both types of structures in DnaJB6 depleted extracts (Turkey's multiple comparisons test; p-Value<0.05) and their rescue by the addition of MBP-xDnaJB6-L (fig.R.24.c).

In order to obtain further insights on the role of DnaJB6 in spindle pole focusing we added recombinant MBP-xDnaJB6-L in excess (1μM) to the cycled EE. We classified the spindle poles in two categories depending on their shape: non-tightly focused poles, presenting microtubules focused at the pole with an increasing curvature close to the pole, or tightly focused poles, with microtubules much more clustered in the vicinity of the pole. As shown in fig.R.24.D, the non-tightly focused poles are the most frequent in control extracts. Most of the spindles (68% of 114 analyzed spindles from 3 independent experiments) had two non-tightly focused poles (MBP 1μM) and were classified as non-tightly focused. Addition of MBP-xDnaJB6-L in excess (1μM) resulted in the significant increase of the percentage of spindles with tightly focused poles (fisher's exact test; P-value<0.0001) reaching

69% of the spindles (from 258 analyzed spindles). In addition, a careful analysis of the tightly focused poles in both conditions showed that in EE containing an excess of MBP-xDnaJB6-L, the microtubules seemed to focus more tightly than in control extracts. We measured the thickness of the tightly focused poles of imaged spindles using the FIJI program. By drawing a line, perpendicular to the spindle length, at a fixed distance of the pole end we obtained the thickness of individual poles (fig.R.24.e). The thickness of the tightly focused poles was significantly higher in MBP spindles than in MBP-xDnaJB6-L spindles (man-withney test; P-value<0,0001) (fig.R.24.f).

Altogether, our results indicate that DnaJB6 is involved in spindle pole focusing, both in Xenopus EE and human cells, probably by affecting the activity of the Dynein-Dynactin complex.

**Fig.R.24. DnaJB6 is involved in spindle pole focusing:** A) Open poles presence in DnaJB6 silenced HeLa cells. On the left side, examples of open and closed (DM1A staining). On the right, percentage of open spindle poles (from a total of 200 poles per condition). Fisher's test for statistical analysis. B, C and D) Spindle poles integrity in cycled EE. Representative images of the different categories (DNA in blue and rhodamine-Tubulin in red) and graphs legend shown in B. In C, graph representing average percentages of focused spindle poles in "control", "depleted" and "add back" (0,017μM) EEs, for three replicas. Standard deviation represented with a line in top of the columns. ANOVA test for statistical analysis. In D, columns graph with the percentage of tightly focused poles in cycled EEs with an excess of DnaJB6 (1μM) and controls. Fisher's test for statistical analysis. E and F) Spindle poles thickness measurement in EEs with an excess of DnaJB6 and controls. E shows an image of a bipolar spindle with a white dashed line representing how the thickness was measured. F quartiles graph shows the spindle poles thickness, in μm. T-test for statistical analysis. In all graphs, (★★★) indicates p-value<0.001.

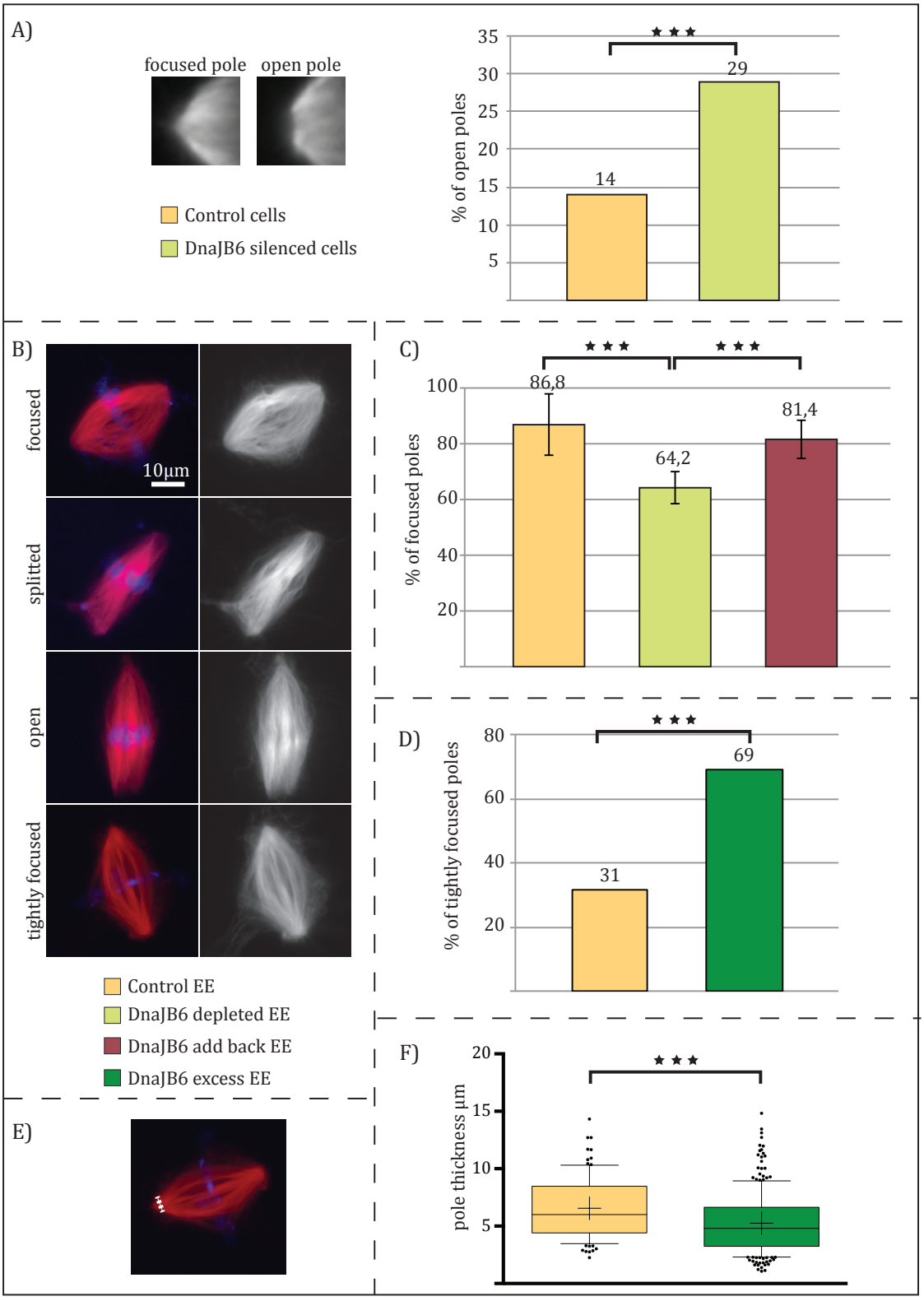
A)
focused pole
open pole
Control cells
DnaJB6 silenced cells
% of open poles
35
30
25
20
15
10
5
14
29
★ ★ ★
B)
focused
splitted
open
tightly focused
10µm
Control EE
DnaJB6 depleted EE
DnaJB6 add back EE
DnaJB6 excess EE
C)
% of focused poles
100
80
60
40
20
86,8
64,2
81,4
★ ★ ★
★ ★ ★
D)
% of tightly focused poles
80
60
40
20
31
69
★ ★ ★
E)
F)
pole thickness µm
20
15
10
5
★ ★ ★

# Annex 1: DnaJB6 localizes inside the cilium. Cilia formation is impaired in DnaJB6 silenced cells.

We used RPE1 cells in order to test whether DnaJB6 is involved in cilia formation. We first confirmed the localization of DnaJB6 within the cilium. We seeded RPE1 cells on coverslip containing dishes in normal growing conditions. The day after (with an 80% of cells confluence) the media was washed out and substituted by starving medium (medium without serum) in order to induce the entry of the cells to G0 and the formation of cilia. After 24 hours of incubation at 37ºC the cells were fixed in MTOH as usual and immunostained with the appropriated antibodies. We visualized the cilia by using anti-acetylated tubulin and DnaJB6 with our homemade antibody. DnaJB6 appears to localize to the cilium in a non-continuous manner, detected as couples of spots within the cilia (fig.R.25.a).

We then tested the effect of silencing DnaJB6 on the cilia formation efficiency. In order to do that, we seeded RPE1 cells in coverslip containing dishes and transfected them with siRNA control or against DnaJB6. 48 hours after transfection the media was substituted by starved medium and incubated for 24 hours at 37ºC. Cells were fixed and the cilia were visualized using anti-acetylated tubulin. Number of cells containing or not containing a cilium was quantified using a fluorescence microscope (Leica wide-field inverted microscope). 84% (± 3.4 SD) of control cells contained a cilium after 24 hours in starved medium (fig.R.25.b), indicating that cilia induction has worked properly. In contrast, just 60% (± 0.7 SD) of DnaJB6 silenced cells contained a properly formed cilium, significantly less than in control cells (Sidak's multiple comparizons test; p-Value<0.05). In order to confirm the G0 state of the silenced cells, we check the expression of KI67 after starvation. We could confirm that DnaJB6 silenced cells have been properly synchronized in G0, so most of the cells were negative for KI67 staining (fig.R.25.c).

Together, we have shown that DnaJB6 localizes to the cilium in a discrete manner and plays an important role in cilia formation, without affecting the cells entry to G0 state.

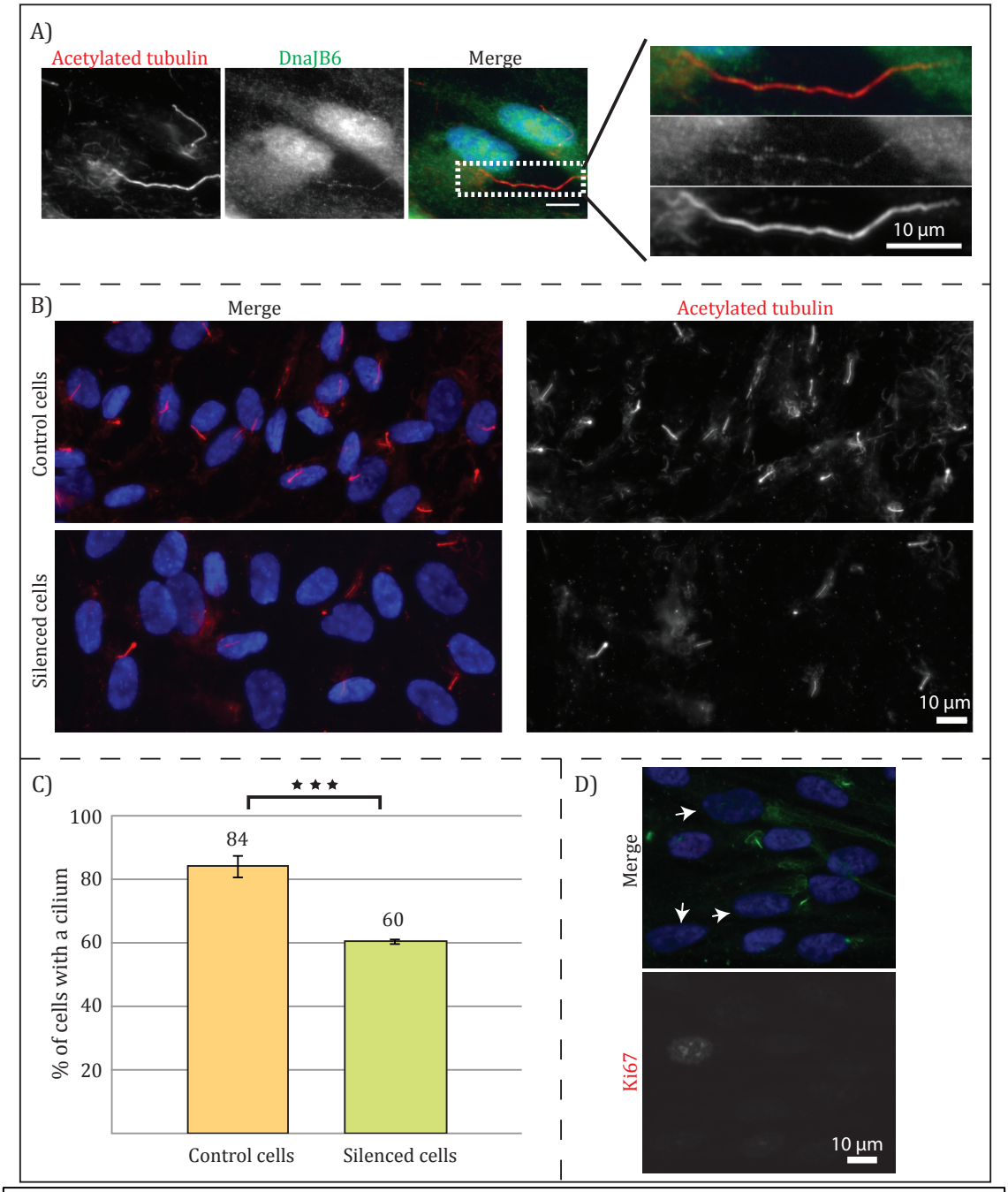


**Fig.R.25. DnaJB6 localizes to the cilium affecting its formation:** A) IF images showing DnaJB6 localization in RPE1 control cells in G0. Cilia are marked using α-acetylated tubulin (red) and α-DnaJB6 (green) and Hoechst (blue) are used. DnaJB6 is detected inside the cilium. B and C) DnaJB6 silencing impairs cilia assembly. In B, representative field of a control and a DnaJB6 silenced sample. In C quantification of the percentage of cells with a cilia 22 hours after G0 induction. Average of three experiments with ST-deviation as a line at the top. (★★★) indicates p-value<0.001 in ANOVA test. D) KI67 IF staining in DnaJB6 silenced RPE1 after G0 induction, confirming that cells without cilium are not cycling cells (arrows). In blue Hoechst and in green d δ2- tubulin marking the cilia.

# DISCUSSION

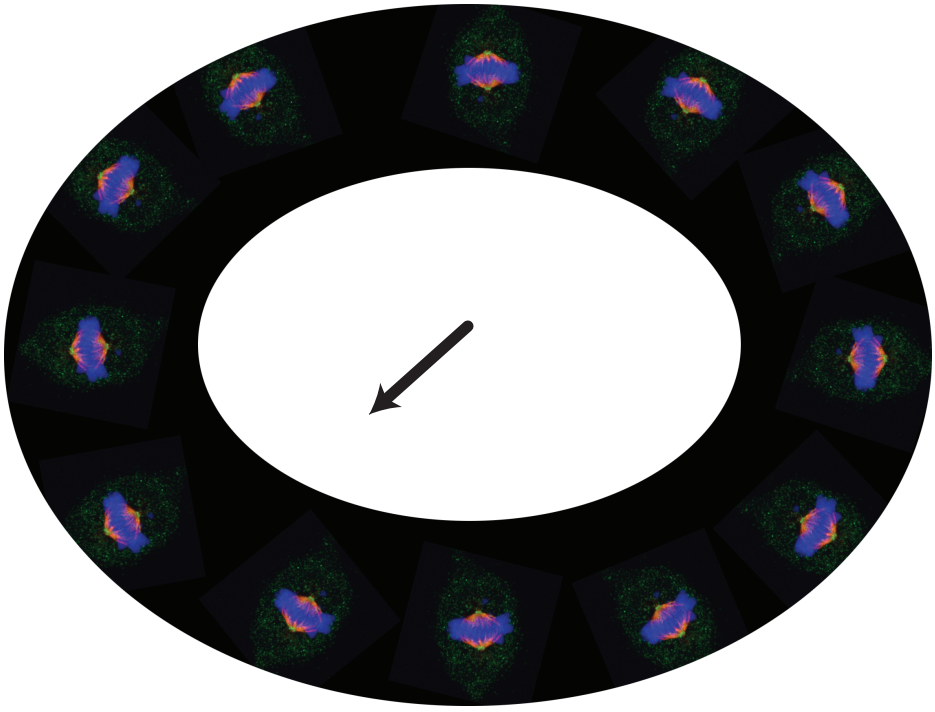

# 1. The RanGTP-MTs proteome

## 1.a. The Xenopus egg extract system as a powerful system for studying MT regulation in M-phase

One of the best features of the Xenopus EE system is that it is an open system and therefore it is easy to manipulate and to test several conditions in parallel in the same extract. Moreover, as mentioned in the introduction, the EE is a concentrated cytoplasmic fraction, naturally blocked in M-phase, that includes all the cytoplasmic and nuclear components required for spindle assembly in excess and that is free of DNA and centrosomes. It is therefore easy to manipulate to study various aspects of spindle assembly or independently the different MT assembly pathways occurring in M-phase.

Spindle assembly can be triggered by addition of *Xenopus laevis* sperm nuclei or DNA-coated beads. The addition of centrosomes allows to study their activity in MT nucleation whereas addition of recombinant RanGTP is used to study the pathway that in the proximity of the chromosomes triggers MT nucleation, stabilization and organization, but in the absence of chromosomes. Also, the function of specific proteins can be addressed at different levels in this system. Their microtubule binding properties and their regulation during M-phase can be studied using MT-stabilizing drugs. Functional assays can be performed upon depletion of the endogenous proteins from the EE using specific antibodies coated to beads and rescue experiments performed by addition of recombinant proteins to the depleted EE.

However, there are a number of difficulties and inconveniences that are intrinsic to the system. First of all, a high variability exists amongst different extracts. This variability can be due to the quality of the starting eggs and/or to their manipulation to obtain the extract, that is not always very well defined. Another difficulty is that, as a fully functional open system, the extract can “dye” during the experiment, even when being carefully manipulated. In summary, although the EE is a very powerful and flexible system, it is essential to obtain good quality EEs in order to get consistent and reliable results.

## 1.b. Proteomics as a useful approach to study the RanGTP MT assembly pathway

Proteomics and system biology approaches are really potent tools to obtain global pictures on cellular processes. However, although it is possible to obtain a lot of information from a proteomic study, it can be difficult to analyze the data to extract the relevant information for a particular study. It is usually difficult to link the long list of identified proteins to specific molecular processes.

We decided to test whether we could use a proteomic approach to study the dynamics of RanGTP MT assemblies over time in EE. It was actually difficult to predict whether the changes in MT dynamics and organization could be reflected in variations of protein composition. These changes in principle could occur at the level of protein composition, variations in the relative amounts of the proteins or changes through post-translational modifications that could change protein activity or complex formation. In addition, a given protein could be present in different complexes each performing different functions and this could also be associated to specific localizations, but also on the specific phase of mitosis. For example, the Dynein complex has different functions and forms different complexes that show different localizations (spindle poles, kinetochores, membrane associated MTs, etc) that can change depending on the cell cycle stage (for example in prophase it is associated to the nuclear envelope and centrosomal MTs and later on to different localizations). The function of the Dynein subunits may not be easy to address using proteomics, because they may be present throughout the different phases of the process, but this does not necessarily mean that they are stable or that they do not induce changes in the system (which they do). In any case to obtain the dynamics of the proteomes, quantitative information is needed at least at the level of the relative amounts of the proteins at the different time points.

We validated and compared our results to previously published proteomes obtained by different groups, approaches and instruments. The comparison of different proteomes from similar processes is a good way to validate the data and

to identify proteins involved in these processes. However, some experimental factors can promote differences between the proteomes that are not functionally relevant.

The first key point is the method used to obtain the sample and how it is processed before mass spectrometry analysis. Sometimes, liquid protein solutions are used, but often proteins are separated by SDS PAGE and selected bands are cut and processed. This may be useful when some proteins are particularly abundant (in our sample it is the case for the tubulins) since having these proteins altogether with less abundant ones could prevent the identification of some of them. To improve the detection of low abundance proteins, we decided to first separate the proteins by SDS PAGE and cut the bands containing the tubulins to process them separately from the other ones in order to increase the chances of identification of low abundance proteins.

The mass spectrometry results can also be analyzed using different parameters and filters. There is not strict consensus for example to define the FDR (False Discovery Rate). Using a lower FDR reduces the number of putative false positives but it can also eliminate real positives. Here we considered only proteins with an FDR of 1% or lower, but this is not an established parameter, some studies do filter the results using different FDR values (for example 5% FDR). In fact, several proteins detected with a 5% FDR were filtered out when the 1% FDR filter was applied. Few known mitotic MTs related proteins were also filtered out (like TACC3, that was filtered out at 15 and 30 minutes), but we prioritized the reduction of false positives, although with the risk of losing a small number of interesting proteins.

It is sometimes difficult to have a good negative control. Our negative control was EE not supplemented with RanGTP and processed in parallel with the other samples. However, we finally did not use the data from the analysis of this sample because we know from previous work in the lab that some protein complexes tend to pellet easily and this does not preclude that they may actually bind specifically to MTs. This would make our RanGTP-MTs proteome incomplete.

After considering all these aspects of the proteomics analysis we obtained a final

extensive list of proteins that defines the RanGTP-MTs proteome. The significant overlapping of our list of proteins with previously published spindle and Taxol stabilized MT proteomes indicates that, even considering the technical variability, we have obtained good and reliable data. This proteome will provide a powerful source for the identification of novel RanGTP regulated and non-regulated factors involved in spindle assembly.

## 1.c. The RanGTP-MTs proteome as a dynamic proteome

The proteomic analysis of the RanGTP dependent MT asters assembled after the different incubation time points identified 1263 proteins. Very little differences were detected along these time points, with 150 proteins recruited at 20 minutes and 11 at 30 minutes. Overall, there were no differences concerning proteins with a known function in spindle assembly. The absence of major changes at the level of the proteome composition suggests that if there are changes in the proteome of the MT assemblies formed at the different time points they may occur at the level of the relative abundance of the proteins involving a much finer regulation. We are working on determining the relative changes in abundance for each identified protein over the time of incubation to determine whether their profiles are different from that of tubulin.

However, this is only an approximation because the MT structures formed at any given time point are not homogeneous. Therefore, a protein that would specifically associate with a given structure (for example a small asters), would probably be detected at all the time-points (since there is always a certain proportion of asters in the samples) although maybe in a different amount.

To obtain some insights into the mechanism that could regulate the activity of proteins and participate in the process of MT self-organization, we have looked for enzymes involved in post-translational modifications. Several kinases were identified. Some of them, such as Aurora-A and –B, have known roles in mitosis, whereas others do not. The identification of these kinases as associated with the RanGTP dependent MT asters suggest that at least some of them may have a role in spindle formation. Further analysis will be needed to explore these possibilities.

## 1.d. The RanGTP-MTs proteome as a tool for identification of new mitotic players

The proteome that we described is richer than the previously published Taxol-stabilized MTs and spindle (HeLa and CHO) proteomes. The difference with the Taxol-stabilized MTs proteome is particularly interesting. This proteome was also obtained using Xenopus EEs, but inducing MT assembly through a different method. The large difference in the number of identified proteins suggests that RanGTP triggers a whole pathway that is much more complex and involves many more factors than those associating to Taxol stabilized MTs. The higher level or organization of the MTs in mini-spindles, compared with the Taxol-MT asters indicates, indeed, that an extra level of protein regulation exists upon addition of RanGTP. Interestingly, in contrast to their absence in the Taxol MT proteome, we identified all the components of the augmin complex, which is proposed to act predominantly on RanGTP dependent microtubules.

The analysis of our proteome using functional protein groups showed that we have recovered many proteins involved in various aspects of MT nucleation, dynamics and organization. By looking for the interactomes of selected proteins in each of these groups we could obtain a more global analysis of our proteome. We indeed found a large network of interconnected proteins in each functional group. Some of these proteins have known functions, but many others have unknown functions in mitosis, and are therefore interesting putative new players for the regulation of the MTs in mitosis.

The comparison of the RanGTP-MTs proteome with previous published proteomes, the nuclear GOs and the functional groups has provided a powerful method for the identification of new RanGTP regulated factors in mitosis. The specific study of some preselected candidates validated this idea. In my thesis, I focused on one of them, DnaJB6. My results suggest that the RanGTP proteome provides an interesting source of novel RanGTP regulated factors with a function in MT and spindle assembly.

# 2. DnaJB6

## 2.a. DnaJB6 is a RanGTP regulated protein

DnaJB6 is one of the proteins identified in our mass spec analysis that we decided to further characterize. As explained in the introduction, DnaJB6 is a HSP40 co-chaperon with two isoforms, generated by alternative splicing. The short isoform is known to localize to the cytoplasm during interphase, whereas the long one that has a putative NLS localizes to the nucleus. We confirmed that, indeed, at least a fraction of DnaJB6 accumulates in the nucleus during interphase. By showing that xDnaJB6-L interacts with importin-β in *Xenopus laevis* EE a RanGTP dependent manner, we demonstrated that its NLS functions also in mitosis. We also showed that DnaJB6 localizes to the spindle microtubules during mitosis and that it is involved in the assembly and organization of the chromosome dependent microtubule asters in HeLa cells.

We have shown that the silencing of DnaJB6 leads to an increase of the number of microtubule asters after nocodazole release, and these asters seem to be smaller than in control cells. The interpretation of this result individually is not an easy task, although it can give us valuable information. The presence of a higher number of MT asters with smaller sizes in DnaJB6 silenced cells could indicate a role for DnaJB6 at three possible levels: in MT nucleation, stabilization or organization. Previous studies have shown a decrease of the number of asters and their size upon silencing or depletion of proteins involved in MT nucleation such as TPX2 (Tulu et al. 2006; Meunier and Vernos 2011). The effect of silencing DnaJB6 does not fit with this phenotype, neither with the opposite, suggesting that it does not have a role in MT nucleation (neither promoting nor inhibiting). The silencing of MCRS1, which has a MT stabilizing activity, has been shown to induce a decrease in the number of MT asters in MT regrowth experiments after nocodazole washout (Meunier and Vernos 2011). This phenotype is the opposite of what we observed when silencing DnaJB6, as we observe an increase in the number of MT asters under similar experimental conditions. This suggests that DnaJB6 is not involved in MT stabilization, although I will discuss better this possibility in the next section.

Our results do not suggest either that DnaJB6 is involved in MT destabilization, because we did not observe any increase on the size of the MT-asters. The last possibility is that DnaJB6 could be involved in the organization of the microtubules, as I will discuss later. Defects in the organization or clustering of the MT asters could, indeed, promote a higher number of asters with a lower size than in the control, as it is the case in our experiment. In summary, we have shown that DnaJB6-L interacts with the importin machinery in M-phase and seems to be involved in the organization of the chromosomal MT asters.

## 2.b. DnaJB6 is not directly involved in MT dynamics regulation

As I will discuss in this section, although some individual results could suggest that DnaJB6 is involved in microtubule stabilization, they are in contradiction with other results that suggest that it is not the case. When considering and interpreting all our results, we concluded that DnaJB6 is not directly involved in microtubule dynamics regulations and it is, instead, involved in MT organization and bipolar spindle assembly.

Two main results suggest that DnaJB6 plays a role in K-Fiber stability: the localization of DnaJB6 to the K-Fibers (with some more accumulation at their minus-ends) and the decrease of the K-Fibers resistance to cold-induced depolymerization in DnaJB6 silenced HeLa cells (after 30 minutes incubation on ice). However, this hypothesis does not fit with our results on the number and size of MT asters during MT regrowth experiments after nocodazole washout. If DnaJB6 has a MT stabilization activity, the number of asters after nocodazole washout should be reduced, as well as their size. Instead, we observed an increase of the number of asters per cell with a smaller size in DnaJB6 silenced cells. It is however possible to consider an unlikely possibility that could relate this phenotype with an effect on MT dynamics. If the size of the MT asters would be highly reduced in absence of DnaJB6, this could reduce the frequency of contact events with surrounding asters, impairing the clustering of these asters. In this case, the size of the asters would decrease in silenced cells and (if the microtubules would not be shortened enough to disassemble the aster) the number of small MT-asters could increase. In contrast with the putative role of DnaJB6 in MT-

stabilization, the length of the K-Fibers in STLC treated cells is not affected by the silencing of DnaJB6. Moreover, the length of bipolar spindles assembled in DnaJB6 silenced cells is longer than in control cells, the opposite of what would be expected for a MT-stabilizer protein. Indeed, our experiments suggest that the increase in spindle length in absence of DnaJB6 is due to an unbalance of forces within the spindle (generated by the motor proteins) instead of changes in MT dynamics, as I will discuss later.

Altogether, our results suggest that, although DnaJB6 is localized to the K-fibers minus-ends affecting their resistance to depolymerization induced by cold, a direct or major implication of the protein on the protection of these MTs from depolymerization does not seem to exist. Instead, the rest of our results indicate that DnaJB6 could play an important role in the organization of the microtubules during mitosis, as I am discussing in the following sections.

## 2.c. DnaJB6 is involved in microtubule organization in mitosis through the interaction with p150

Our results strongly suggest that DnaJB6 is involved in spindle organization. This role in spindle organization seems to be related with an interaction with p150. The absence of DnaJB6 is associated to several microtubule organization defects. In non-synchronized cycling cells, the silencing of DnaJB6 leads to the formation of multipolar spindles that are not associated with the presence of extra centrosomes, as well as the presence of ectopic MT clusters away from the bipolar spindle. The extra poles seem to be centrosome-independent (as detected through the absence of centrin staining), suggesting that they may be formed either by de novo formation or by disruption of a preexisting pole.

We showed that MT aster organization and bipolar spindle assembly are impaired in DnaJB6 silenced cells after nocodazole washout. The clustering of the MT asters is indeed significantly slower in DnaJB6 silenced cells after nocodazole washout, impairing the assembly of the bipolar spindle even after 60 minutes, in 40% of the cells. These results suggest that DnaJB6 affects the activity of MT minus-end motor proteins. MT minus-end directed motor proteins provide the main activity for the

organization of MTs and for the focusing of their minus-ends. Specifically, it has been shown that the Dynein-Dynactin complex plays a major role in the organization of Taxol stabilized and RanGTP induced MTs in *Xenopus* EE. Indeed, we have demonstrated that xDnaJB6-L interacts with p150, an essential subunit of the Dynactin complex. Interestingly, we have shown that this interaction is dependent of the presence of RanGTP. Altogether our results suggest that DnaJB6 is involved in microtubule organization during mitosis, both in the assembly of the mitotic spindle and the organization of the microtubule asters after nocodazole washout. This role seems to be related to a RanGTP regulated interaction of DnaJB6 and p150, which could affect the activity of the Dynein-Dynactin complex in these processes.

Our results suggest that specific activities of the Dynein-Dynactin complex are, indeed, affected by the absence of DnaJB6. As detailed in the introduction (chapter 3.c), Dynein is involved in MT minus-end focusing at the spindle poles and spindle poles integrity maintenance. We have shown that the absence of DnaJB6 induces defects in MT minus-end focusing at the spindle poles, promoting the formation of open poles in EE and HeLa cells. In EE, this phenotype is rescued by the addition of recombinant MBP-xDnaJB6-L, indicating that the phenotype is not due to the co-depletion of other proteins or other putative roles of DnaJB6 in interphase. Interestingly, the addition of an excess of the protein leads to the opposite effect, with more tightly focused spindle poles.

Altogether, our results suggest that DnaJB6 is involved in microtubule organization and MT minus-end focusing at the spindle poles, probably by affecting the activity of Dynein-Dynactin through an interaction with p150.

## 2.d. DnaJB6 regulates the activity of Dynactin by affecting the stability of the complex

DnaJB6 is a member of the HSP40 family of co-chaperons. As detailed in the introduction, many members of this family are known to mediate protein complexes assembly and stabilization. Because Dynactin is a huge complex with many subunits, we wondered whether DnaJB6 could be needed to form the

complex or maintain its stability. We analyzed the integrity of the Dynactin complex using sucrose gradient protein separation techniques in interphase and mitotic cell extracts separately. We treated the lysates with different concentrations of KI that were previously shown to disrupt the integrity of the Dynein-Dynactin complex (Jones et al. 2014). We found that the absence of DnaJB6 affects the integrity of the Dynactin complex specifically in mitotic extracts. This suggests that DnaJB6 promotes the stabilization of this complex, an activity that could be consistent with a co-chaperon. By controlling the stability of the Dynein-Dynactin complex, DnaJB6 could play a role in Dynein activity. Interestingly we also found that DnaJB6 plays a role in p150 spindle localization, with p150 accumulating at the spindle poles in the absence of DnaJB6.

We also obtained further evidence for a functional interaction between DnaJB6 and the Dynein-Dynactin complex. As mentioned in the introduction, a balance of forces drives and maintains spindle bipolarity. The kinesin Eg5, together with hKLP2, exert pushing forces that separate the two spindle poles. Pulling forces exerted by Dynein and kinesin-14 counteracts these pushing forces. The disruption of the balance of forces impairs spindle formation. Inhibition of Eg5 induces the formation of monopolar spindles (with the MT minus-ends at the center of the structure). But impairing the activity of Dynein and therefore the pulling forces rescues the formation of bipolar spindles. We therefore hypothesized that, if DnaJB6 affects the activity of the Dynein-Dynactin complex, DnaJB6 silencing could also rescue spindle bipolarity in Eg5 inhibited cells. Indeed, we found that the formation of bipolar spindles in STLC treated cells is rescued upon DnaJB6 silencing, suggesting that the force generation activity of the Dynein-Dynactin complex is altered. Accordingly, the length of the bipolar spindles is increased upon DnaJB6 silencing, suggesting defective pulling forces. Altogether, our results suggest that DnaJB6 regulates the stability of the Dynein-Dynactin complex in mitosis and thereby plays an important role for its activity in spindle assembly, MT minus-ends focusing at the spindle poles and force generation.

## 2.e. Dynein and Dynactin specific activities

As mentioned in the introduction, the specific role of the Dynactin complex in the

variety of functions of Dynein is still under debate. Defects in pole focusing and force generation have been extensively described upon the disruption of the Dynactin complex (with addition of p50) or impairing its interaction with Dynein (by using specific antibodies that recognize Dynein IC), suggesting that Dynactin could be involved in these two processes in cooperation with Dynein. However the individual silencing of several Dynactin subunits did not induce these phenotypes (Raaijmakers, Tanenbaum, and Medema 2013). This may suggest that the release of p150 subunits within the cell in the presence of an excess of p50 could compete out the interaction of Dynein IC with NudE. NudE interacts with Dynein IC forming a complex with NudEL and LIS1, which is involved in spindle pole focusing and pole generation. We have shown that DnaJB6 interacts with p150 in a RanGTP regulated manner, and absence of DnaJB6 affects spindle pole formation and force generation by Dynein. In the context of a putative binding competition, the decrease of Dynactin stability induced by the absence of DnaJB6 could lead to an increase of free p150 molecules or a certain conformation of Dynactin that could compete with Ndel1 for the binding with Dynein IC. In this context, DnaJB6 activity would induce a certain conformation of the Dynactin complex that would impair its interaction with Dynein at the spindle poles. This action of DnaJB6 would protect the Dynein complex from its partial inhibition by the Dynactin complex, ensuring the proper functioning of Dynein in the processes of spindle pole focusing and force generation. This model could explain the described accumulation of p150 at the spindle poles in absence of DnaJB6.

Altogether, our results suggest that DnaJB6 interacts with the Dynactin complex (probably trough p150) in a RanGTP regulated manner. This interaction affects the stability or formation of the Dynactin complex. DnaJB6 would regulate the activity of the Dynactin complex during mitosis, potentially by enhancing the generation of forces by the Dynein complex that would counteract the spindle pole separation forces exerted by Eg5 within the spindle, but also enhancing Dynein activity in MT minus-ends focusing at the spindle poles.

## 2.f. DnaJB6 short and long, different isoforms with different activities?

Different functions have been described for the two isoforms of DnaJB6 in humans (as described in the introduction). In this work, we have used specific antibodies for the detection of the human and the Xenopus protein, and siRNAs and antibodies for the silencing or depletion in human or Xenopus EE. In both cases, we could not knockdown each isoform individually with the tools that we had, but we have tested the rescue capability of the long isoform specifically in EE. In order to generate the recombinant xDnaJB6-L we have first determined the sequence of the protein, because it was not previously annotated. Although we have amplified successfully the mRNA of xDnaJB6-L, we never managed to detect or amplify the mRNA of the short isoform of DnaJB6 using several EE preparations, suggesting that this short isoform may not be expressed in *Xenopus* oocytes. However, we could detect a band that could correspond to xDnaJB6-S by western blot using our homemade antibody, although only in a few EE. A very low abundance of this form in EE or alternatively an unspecific reaction of the antibody could explain this. The rescue of the DnaJB6 depletion phenotypes by addition of xDnaJB6-L suggests anyway that this isoform carries all the functional information for spindle assembly. Whether the short isoform could also contribute to this process, when it is present, is not clear. In any case, it would probably not be regulated by RanGTP. Further rescue experiments in EE using recombinant x-DnaJB6-S will be needed to elucidate whether DnaJB6 activity in spindle assembly is restricted to the long and/or short isoform.

## 2.g. DnaJB6 is involved in cilia assembly

DnaJB6 interacts with some proteins of the IFT-B complex in interphase. We found that DnaJB6 localizes to the cilia, and its silencing impairs cilia formation, suggesting that it is involved in cilia assembly. DnaJB6-L is translocated to the nucleus in interphase depending on an NLS and we have shown that DnaJB6-L is a RanGTP regulated protein in mitosis. But how is DnaJB6 transported to the cilium? Since it has been proposed that a RanGTP regulated protein transport system

exists between the cilia and the cytoplasm, it would be interesting to test whether DnaJB6-L could be transported to the nucleus and the cilium in a RanGTP regulated manner. If this is the case it would also be important to determine how a protein, and the importin machinery is regulated to know where to go. A possible answer could be that posttranslational modifications of the NLSs/CLSs could define their affinity for specific importins that would drive their transport to the specific destination. In this direction, recent experiments (not included in this thesis) suggest that the affinity of importin-β for an NLS containing protein is severely decreased upon the phosphorylation of some NLS residues, impairing the transport of the protein to the nucleus in interphase.

# CONCLUSIONS

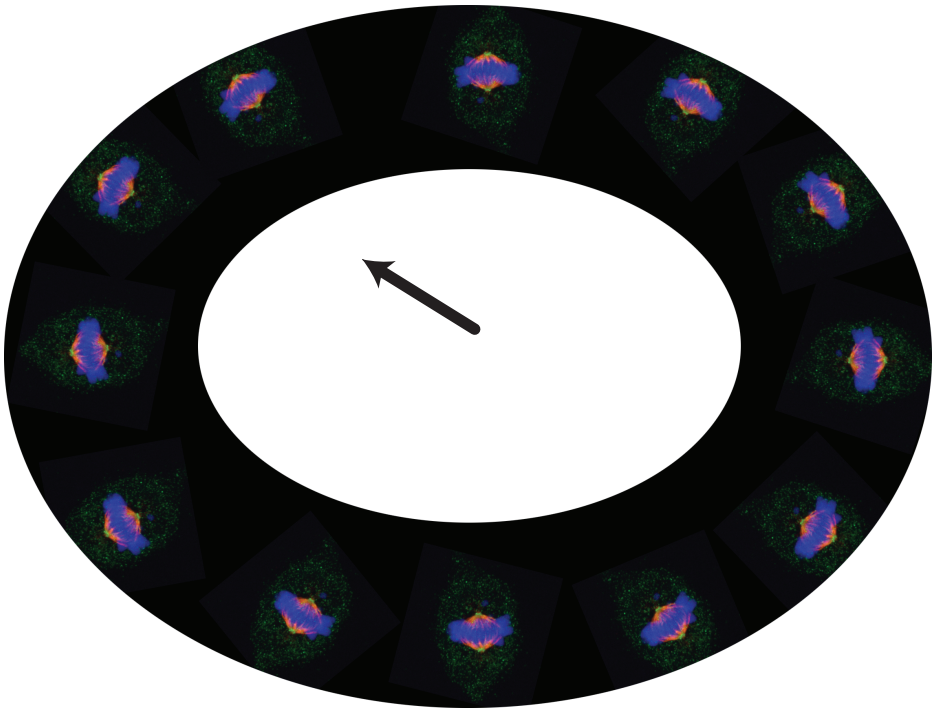

- We have identified 1263 human proteins that associate with RanGTP induced MTs in M-phase.

- This proteome is enriched in spindle assembly factors and includes several proteins with known functions in MT nucleation, stabilization, destabilization and organization.

- The dynamic composition of the proteome in terms of relative abundance of the proteins over time may correlate with the specific type of MT structures that are formed at these times.

- We have identified DnaJB6 as a novel RanGTP regulated protein with a function in bipolar spindle assembly and pole focusing.

- DnaJB6 interacts with p150 in a RanGTP dependent manner.

- DnaJB6 favors Dynactin complex stability specifically during mitosis and thereby its role in bipolar spindle assembly and microtubules minus-ends focusing at the spindle poles.

- Our results suggest a mechanism by which RanGTP promotes MT organization and bipolar spindle formation.

- DnaJB6 localizes to the cilium and is involved in cilia assembly.

# FUTURE DIRECTIONS

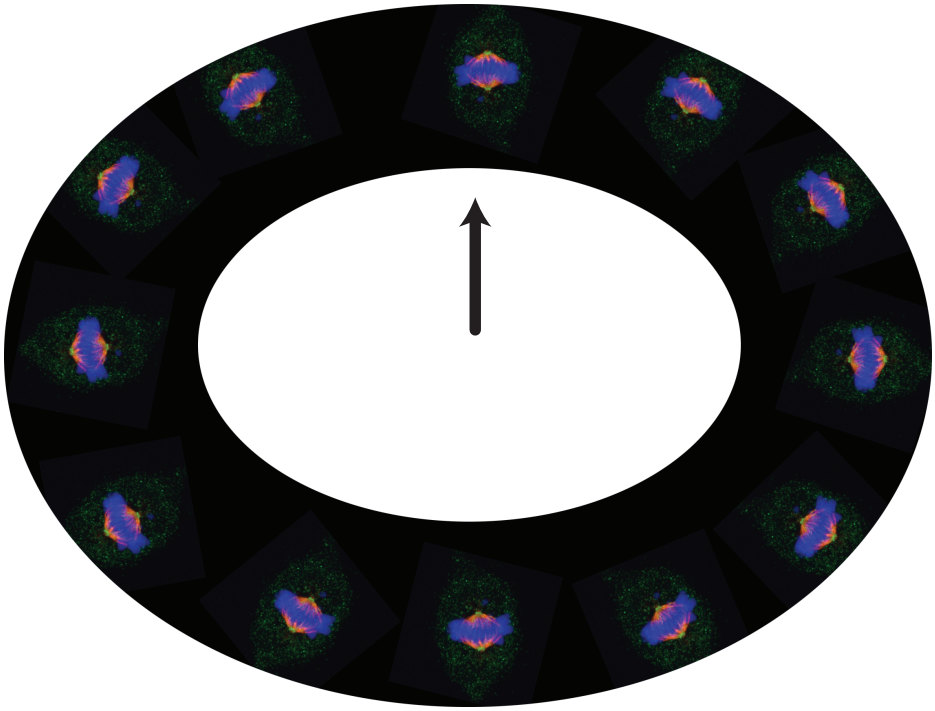

- To analyze the relative abundance variation of the proteins identified at the RanGTP-MTs proteome. Elucidate whether these variations could correlate to the dynamicity of the self-organization process.
- To determine whether DnaJB6 directly interacts with the Dynactin complex and how this interaction affects Dynein-Dynactin proprieties, as their interaction *in vitro* or the processivity of the complex.
- To study whether the role of DnaJB6 described in this thesis is related to the regulation of a putative activity of Hsp70. Preliminary experiments using a specific Hsp70 inhibitor have been conducted. The effect of the inhibition of Hsp70 on the distribution of the mitotic phases and the organization of the MT-asters after nocodazole release is not similar to the silencing of DnaJB6. These results suggest that the activity of DnaJB6 in regulating the Dynein-Dynactin complex activity could be independent of Hsp70; however further experiments will be needed to confirm this hypothesis.
- To determine what is the specific role of DnaJB6 in cilia formation and whether RanGTP regulates this activity.
- To determine whether RanGTP regulates a similar set of components involved in spindle and cilia. To test the cilia assembly phenotypes associated with the silencing of different mitotic RanGTP regulated proteins. I have tested the effect of the silencing of few mitotic RanGTP regulated MAPs in cilia assembly and found that silencing of one of them impairs cilia assembly (data not shown). To study whether modifications of the NLS/CLS (mutations or post-translation modifications) within the "positive" proteins affect their import efficiency to the cilia.

# REFERENCES

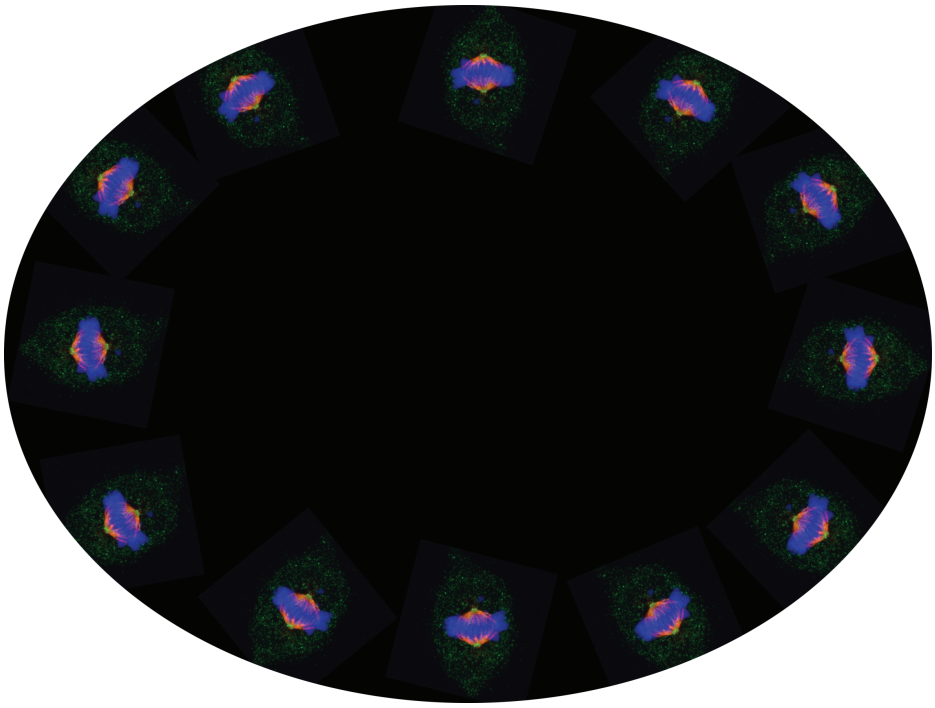

- Akhmanova, A. et al., 2001. CLASPs are CLIP-115 and -170 associating proteins involved in the regional regulation of microtubule dynamics in motile fibroblasts. Cell, 104(6), pp.923–935.
- Akhmanova, A. & Hoogenraad, C.C., 2015. Microtubule Minus-End-Targeting Proteins. Current Biology, 25(4), pp.R162–R171. Available at: http://linkinghub.elsevier.com/retrieve/pii/S0960982214016303.
- Akhmanova, A. & Steinmetz, M.O., 2015. Control of microtubule organization and dynamics: two ends in the limelight. Nature Reviews Molecular Cell Biology, (November). Available at: http://www.nature.com/doifinder/10.1038/nrm4084.
- Akhmanova, A. & Steinmetz, M.O., 2008. Tracking the ends: a dynamic protein network controls the fate of microtubule tips. Nature Reviews Molecular Cell Biology, 9(4), pp.309–322. Available at: http://www.nature.com/doifinder/10.1038/nrm2369.
- Al-Bassam, J. et al., 2010. CLASP promotes microtubule rescue by recruiting tubulin dimers to the microtubule. Developmental Cell, 19(2), pp.245–258. Available at: http://dx.doi.org/10.1016/j.devcel.2010.07.016.
- Allan, V.J., 2011. Cytoplasmic dynein. Biochemical Society transactions, 39(5), pp.1169–78. Available at: http://www.biochemsoctrans.org/content/39/5/1169.abstract.
- Alushin, G.M. et al., 2014. High-Resolution microtubule structures reveal the structural transitions in αβ-tubulin upon GTP hydrolysis. Cell, 157(5), pp.1117–1129. Available at: http://dx.doi.org/10.1016/j.cell.2014.03.053.
- Andrews, J.F. et al., 2012. Cellular stress stimulates nuclear localization signal (NLS) independent nuclear transport of MRJ. Experimental Cell Research, 318(10), pp.1086–1093. Available at: http://dx.doi.org/10.1016/j.yexcr.2012.03.024.
- Asenjo, A.B. et al., 2013. Structural model for tubulin recognition and deformation by kinesin-13 microtubule depolymerases. Cell Reports, 3(3), pp.759–768. Available at: http://dx.doi.org/10.1016/j.celrep.2013.01.030.
- Bakhoum, S.F. et al., 2009. Genome stability is ensured by temporal control of kinetochore-microtubule dynamics. Nature cell biology, 11(1), pp.27–35.
- Barisic, M. et al., 2010. Spindly/CCDC99 Is Required for Efficient Chromosome Congression and Mitotic Checkpoint Regulation. Molecular biology of the cell, 21(22), pp.4042–4056.
- Basto, R. et al., 2006. Flies without Centrioles. Cell, 125(7), pp.1375–1386.
- Becker, J. et al., 1995. RNA1 encodes a GTPase-activating protein specific for Gsp1p, the Ran/TC4 homologue of Saccharomyces cerevisiae. Journal of Biological Chemistry, 270(20), pp.11860–11865.
- Bettencourt-Dias, M. & Glover, D.M., 2007. Centrosome biogenesis and function: centrosomics brings new understanding. Nature reviews. Molecular cell biology, 8(June), pp.451–463.
- Bhabha, G. et al., 2016. How Dynein Moves Along Microtubules. Trends in Biochemical Sciences, 41(1), pp.94–105.

- Bhogaraju, S., Engel, B.D. & Lorentzen, E., 2013. Intraflagellar transport complex structure and cargo interactions. Cilia, 2, p.10. Available at: http://www.pubmedcentral.nih.gov/articlerender.fcgi?artid=3751104&tool=pmcentrez&rendertype=abstract.
- Bhowmick, R. et al., 2009. Photoreceptor IFT complexes containing chaperones, guanylyl cyclase 1 and rhodopsin. Traffic (Copenhagen, Denmark).
- Bischoff, F.R. et al., 1995. Co-activation of RanGTPase and inhibition of GTP dissociation by Ran-GTP binding protein RanBP1. The EMBO journal, 14(4), pp.705–715.
- Bischoff, F.R. et al., 1994. RanGAP1 induces GTPase activity of nuclear Ras-related Ran. Proceedings of the National Academy of Sciences of the United States of America, 91(7), pp.2587–91. Available at: http://www.pubmedcentral.nih.gov/articlerender.fcgi?artid=43414&tool=pmcentrez&rendertype=abstract.
- Bischoff, F.R. & Görlich, D., 1997. RanBP1 is crucial for the release of RanGTP from importin β-related nuclear transport factors. FEBS Letters, 419(2–3), pp.249–254. Available at: http://dx.doi.org/10.1016/S0014-5793(97)01467-1.
- Bischoff, F.R. & Ponstingl, H., 1991. Catalysis of guanine nucleotide exchange on Ran by the mitotic regulator RCC1. Letters To Nature, 353, pp.737–740.
- Bischoff, F.R. & Ponstingl, H., 1991. Mitotic regulator protein RCC1 is complexed with a nuclear ras-related polypeptide. Proceedings of the National Academy of Sciences of the United States of America, 88(23), pp.10830–4. Available at: http://www.pubmedcentral.nih.gov/articlerender.fcgi?artid=53025&tool=pmcentrez&rendertype=abstract.
- Bonner, M.K. et al., 2011. Mitotic spindle proteomics in Chinese hamster ovary cells. PLoS ONE, 6(5).
- Booth, D.G. et al., 2011. A TACC3/ch-TOG/clathrin complex stabilises kinetochore fibres by inter-microtubule bridging. The EMBO journal, 30(5), pp.906–19. Available at: http://www.pubmedcentral.nih.gov/articlerender.fcgi?artid=3049211&tool=pmcentrez&rendertype=abstract.
- Brouhard, G.J. et al., 2008. XMAP215 Is a Processive Microtubule Polymerase. Cell, 132(1), pp.79–88.
- Brown, K.R. & Jurisica, I., 2005. Online Predicted Human Interaction Database. *Bioinformatics*, 21(9), pp.2076–2082. Available at: http://dx.doi.org/10.1093/bioinformatics/bti273.
- Brown, K.R. & Jurisica, I., 2007. Unequal evolutionary conservation of human protein interactions in interologous networks. *Genome Biology*, 8(5), pp.R95–R95. Available at: http://www.ncbi.nlm.nih.gov/pmc/articles/PMC1929159/.

- Bukau, B., Weissman, J. & Horwich, A., 2006. Molecular Chaperones and Protein Quality Control. Cell, 125(3), pp.443–451. Available at: http://dx.doi.org/10.1016/j.cell.2006.04.014.
- Burns, K.M. et al., 2014. Nucleotide exchange in dimeric MCAK induces longitudinal and lateral stress at microtubule ends to support depolymerization. Structure, 22(8), pp.1173–1183. Available at: http://dx.doi.org/10.1016/j.str.2014.06.010.
- Cai, S., O'Connell, C.B., et al., 2009. Chromosome congression in the absence of kinetochore fibres. Nature cell biology, 11(7), pp.832–838. Available at: http://dx.doi.org/10.1038/ncb1890.
- Cai, S., Weaver, L.N., et al., 2009. Kinesin-14 Family Proteins HSET/XCTK2 Control Spindle Length by Cross-Linking and Sliding Microtubules. Molecular biology of the cell, 20(4), pp.327–331.
- Calarco-Gillam, P.D. et al., 1983. Centrosome development in early mouse embryos as defined by an autoantibody against pericentriolar material. Cell, 35(3 PART 2), pp.621–629.
- Cameron, L.A. et al., 2006. Kinesin 5-independent poleward flux of kinetochore microtubules in PtK1 cells. Journal of Cell Biology, 173(2), pp.173–179.
- Carazo-Salas, R.E. et al., 1999. Generation of GTP-bound Ran by RCC1 is required for chromatin-induced mitotic spindle formation. Nature, 400(6740), pp.178–81. Available at: http://www.ncbi.nlm.nih.gov/pubmed/10408446.
- De Cárcer, G. et al., 2001. Requirement of Hsp90 for centrosomal function reflects its regulation of Polo kinase stability. EMBO Journal, 20(11), pp.2878–2884.
- Carter, A.P. et al., 2011. Crystal structure of the dynein motor domain. Science (New York, N.Y.), 331(6021), pp.1159–65. Available at: http://www.pubmedcentral.nih.gov/articlerender.fcgi?artid=3169322&tool=pmcentrez&rendertype=abstract.
- Carter, A.P. et al., 2008. Structure and Functional Role of Dynein's Microtubule-Binding Domain. Science (New York, N.Y.), 321(August 2008), pp.960–965.
- Carvalho-Santos, Z. et al., 2011. Tracing the origins of centrioles, cilia, and flagella. Journal of Cell Biology, 194(2), pp.165–175.
- Caudron, M., 2005. Spatial Coordination of Spindle Assembly by Chromosome-Mediated Signaling Gradients. Science, 309(5739), pp.1373–1376. Available at: http://www.sciencemag.org/cgi/doi/10.1126/science.1115964.
- Cavazza, T. & Vernos, I., 2016. The RanGTP Pathway : From Nucleo-Cytoplasmic Transport to Spindle Assembly and Beyond. , 3(January).
- Chatr-aryamontri, A. et al., 2015. The BioGRID interaction database: 2015 update. *Nucleic Acids Research*, 43(Database issue), pp.D470–D478. Available at: http://www.ncbi.nlm.nih.gov/pmc/articles/PMC4383984/.

- Chavali, P.L. et al., 2016. A CEP215-HSET complex links centrosomes with spindle poles and drives centrosome clustering in cancer. Nature communications, 7, p.11005. Available at: http://www.pubmedcentral.nih.gov/articlerender.fcgi?artid=4802056&tool=pmcentrez&rendertype=abstract.
- Cheeseman, I.M. et al., 2006. The Conserved KMN Network Constitutes the Core Microtubule-Binding Site of the Kinetochore. Cell, 127(5), pp.983–997.
- Cheeseman, I.M., 2016. The Kinetochore. Cold Spring Harbor Perspectives in Biology, 6(7), pp.1–19.
- Cheeseman, I.M. & Desai, A., 2008. Molecular architecture of the kinetochore–microtubule interface. Nature Reviews Molecular Cell Biology, 9(1), pp.33–46. Available at: http://www.nature.com/doifinder/10.1038/nrm2310.
- Chen, Y.J. et al., 2014. HSP70 colocalizes with PLK1 at the centrosome and disturbs spindle dynamics in cells arrested in mitosis by arsenic trioxide. Archives of Toxicology, 88(9), pp.1711–1723.
- Cheng, X., Belshan, M. & Ratner, L., 2008. Hsp40 Facilitates Nuclear Import of the Human Immunodeficiency Virus Type 2 Vpx-Mediated Preintegration Complex. Journal of Virology, 82(3), pp.1229–1237. Available at: http://jvi.asm.org/cgi/doi/10.1128/JVI.00540-07.
- Chuang, J.Z. et al., 2002. Characterization of a brain-enriched chaperone, MRJ, that inhibits huntingtin aggregation and toxicity independently. Journal of Biological Chemistry, 277, pp.19831–19838.
- Cianfrocco, M.A. et al., 2015. Mechanism and Regulation of Cytoplasmic Dynein.
- Clarke, P.R. & Zhang, C., 2008. Spatial and temporal coordination of mitosis by Ran GTPase. Nature reviews. Molecular cell biology, 9(june), pp.464–477.
- Clift, D. & Schuh, M., 2013. Restarting life: fertilization and the transition from meiosis to mitosis. Nature Reviews Molecular Cell Biology, 14(9), pp.549–562. Available at: http://www.nature.com/doifinder/10.1038/nrm3643.
- Coutavas, E. et al., 1993. characterization of proteins that interact with the cell-cycle regulatory protein Ran/TC4. Nature Letters, 363.
- Cox, J. & Mann, M., 2008. MaxQuant enables high peptide identification rates, individualized p.p.b.-range mass accuracies and proteome-wide protein quantification. Nature Biotechnology, 26(12), pp.1367–1372. Available at: http://www.nature.com/doifinder/10.1038/nbt.1511.
- Croft, D. et al., 2014. The Reactome pathway knowledgebase. *Nucleic Acids Research*, 42(Database issue), pp.D472–D477. Available at: http://www.ncbi.nlm.nih.gov/pmc/articles/PMC3965010/.
- Cross, R. a. & McAinsh, A., 2014. Prime movers: the mechanochemistry of mitotic kinesins. Nature Reviews Molecular Cell Biology, 15(4), pp.257–271. Available at:

http://www.nature.com/nrm/journal/v15/n4/abs/nrm3768.html?lang=en?WT.ec_id=NRM-201404\nhttp://www.nature.com/nrm/journal/v15/n4/pdf/nrm3768.pdf

- Culver-Hanlon, T.L. et al., 2006. A microtubule-binding domain in dynactin increases dynein processivity by skating along microtubules. Nature cell biology, 8(3), pp.264–70. Available at: http://www.ncbi.nlm.nih.gov/pubmed/16474384.
- Delaval, B. et al., 2011. The cilia protein IFT88 is required for spindle orientation in mitosis. Nature cell biology, 13(4), pp.461–468. Available at: http://dx.doi.org/10.1038/ncb2202.
- Desai, A. et al., 1998. Chapter 20 The Use of Xenopus Egg Extracts to Study Mitotic Spindle Assembly and Function in Vitro. Methods in cell biology, 61, pp.385–412. Available at: http://www.ncbi.nlm.nih.gov/pubmed/9891325\nhttp://linkinghub.elsevier.com/retrieve/pii/S0091679X08619913.
- Desai, A. et al., 1999. Kin I kinesins are microtubule-destabilizing enzymes. Cell, 96(1), pp.69–78.
- Desai, a & Mitchison, T.J., 1997. Microtubule polymerization dynamics. Annual review of cell and developmental biology, 13, pp.83–117.
- DeWitt, M.A. et al., 2012. Cytoplasmic dynein moves through uncoordinated stepping of the AAA+ ring domains. Science (New York, N.Y.), 335(6065), pp.221–5. Available at: http://www.ncbi.nlm.nih.gov/pubmed/22157083\nhttp://www.pubmedcentral.nih.gov/articlerender.fcgi?artid=PMC4033606.
- Dey, S., Banerjee, P. & Saha, P., 2009. Cell cycle specific expression and nucleolar localization of human J-domain containing co-chaperon Mrj. Molecular and Cellular Biochemistry, 322, pp.137–142.
- Diamant, S. & Goloubinoff, P., 1998. Temperature-controlled activity of DnaK-DnaJ-GrpE chaperones: Protein- folding arrest and recovery during and after heat shock depends on the substrate protein and the GrpE concentration. Biochemistry, 37(27), pp.9688–9694.
- Dishinger, J.F. et al., 2010. Ciliary entry of the kinesin-2 motor KIF17 is regulated by importin-beta2 and RanGTP. Nature cell biology, 12(7), pp.703–710. Available at: http://dx.doi.org/10.1038/ncb2073.
- Drivas, G.T. et al., 1990. Characterization of four novel ras-like genes expressed in a human teratocarcinoma cell line. Molecular and cellular biology, 10(4), pp.1793–8. Available at: http://www.pubmedcentral.nih.gov/articlerender.fcgi?artid=362288&tool=pmcentrez&rendertype=abstract.
- Dumont, J., Oegema, K. & Desai, A., 2010. A kinetochore-independent mechanism drives anaphase chromosome separation during acentrosomal meiosis. Nature cell biology, 12(9), pp.894–901. Available at: http://dx.doi.org/10.1038/ncb2093.

- Echeverri, C.J. et al., 1996. Molecular characterization of the 50-kD subunit of dynactin reveals function for the complex in chromosome alignment and spindle organization during mitosis. Journal of Cell Biology, 132(4), pp.617–633.
- Evans, L., Mitchison, T. & Kirschner, M., 1985. Influence of Nucleated of the Centrosome Microtubules the Structure. The Journal of cell biology, 100(4), pp.1185–1191. Available at: http://www.jcb.org/cgi/doi/10.1083/jcb.100.4.1185\npapers2://publication/doi/10.1083/jcb.100.4.1185.
- Fabregat, A. et al., 2016. The Reactome pathway Knowledgebase. *Nucleic Acids Research*, 44(Database issue), pp.D481–D487. Available at: http://www.ncbi.nlm.nih.gov/pmc/articles/PMC4702931/.
- Fan, C.-Y., Lee, S. & Cyr, D.M., 2003. Mechanisms for regulation of Hsp70 function by Hsp40. Cell stress & chaperones, 8(4), pp.309–316.
- Fan, S. et al., 2007. A novel Crumbs3 isoform regulates cell division and ciliogenesis via importin β interactions. Journal of Cell Biology, 178(3), pp.387–398.
- Fan, S. et al., 2011. Induction of Ran GTP drives ciliogenesis. Molecular Biology of the Cell, 22, pp.4539–4548.
- Fang, C.T. et al., 2016. HSP70 regulates the function of mitotic centrosomes. Cellular and Molecular Life Sciences, 73(20), pp.3949–3960. Available at: "http://dx.doi.org/10.1007/s00018-016-2236-8.
- Faulkner, N.E. et al., 2000. A role for the lissencephaly gene LIS1 in mitosis and cytoplasmic dynein function. Nature cell biology, 2(11), pp.784–791. Available at: http://www.nature.com/ncb/journal/v2/n11/abs/ncb1100_784.html.
- Ferenz, N.P. et al., 2009. Dynein Antagonizes Eg5 by Crosslinking and Sliding Antiparallel Microtubules. Current Biology, 19(21), pp.1833–1838. Available at: http://dx.doi.org/10.1016/j.cub.2009.09.025.
- Florian, S. & Mayer, T.U., 2012. The Functional Antagonism between Eg5 and Dynein in Spindle Bipolarization Is Not Compatible with a Simple Push-Pull Model. Cell Reports, 1(5), pp.408–416. Available at: http://dx.doi.org/10.1016/j.celrep.2012.03.006.
- Friel, C.T. & Howard, J., 2012. Coupling of kinesin ATP turnover to translocation and microtubule regulation: One engine, many machines. Journal of Muscle Research and Cell Motility, 33(6), pp.377–383.
- Gache, V. et al., 2010. Xenopus meiotic microtubule-associated interactome. PLoS ONE, 5(2).
- Gadde, S. & Heald, R., 2004. Mechanisms and molecules of the mitotic spindle. Current Biology, 14, pp.797–805.
- Gaglio, T. et al., 1996. Opposing motor activities are required for the organization of the mammalian mitotic spindle pole. Journal of Cell Biology, 135(2), pp.399–414.

- Gaglio, T., Dionne, M.A. & Compton, D.A., 1997. Mitotic spindle poles are organized by structural and motor proteins in addition to centrosomes. Journal of Cell Biology, 138(5), pp.1055–1066.
- Gardner, M.K. et al., 2011. Depolymerizing kinesins Kip3 and MCAK shape cellular microtubule architecture by differential control of catastrophe. Cell, 147(5), pp.1092–1103. Available at: http://dx.doi.org/10.1016/j.cell.2011.10.037.
- Gässler, C.S. et al., 2001. Bag-1M Accelerates Nucleotide Release for Human Hsc70 and Hsp70 and Can Act Concentration-dependent as Positive and Negative Cofactor. Journal of Biological Chemistry, 276(35), pp.32538–32544.
- Gassmann, R. et al., 2010. Removal of Spindly from microtubule- attached kinetochores controls spindle checkpoint silencing in human cells. Genes & development, 24, pp.957–971.
- Gee, M. a, Heuser, J.E. & Vallee, R.B., 1997. An extended microtubule-binding structure within the dynein motor domain. Nature, 390(6660), pp.636–639.
- Gergely, F. et al., 2000. The TACC domain identifies a family of centrosomal proteins that can interact with microtubules. Proceedings of the National Academy of Sciences of the United States of America, 97(26), pp.14352–14357.
- Gergely, F., Draviam, V.M. & Raff, J.W., 2003. The ch-TOG/XMAP215 Protein is Essential for Spindle Pole Organization in Human Somatic Cells. Genes & Development, 17, pp.336–341.
- Gill, S.R. et al., 1991. Dynactin, a conserved, ubiquitously expressed component of an activator of vesicle motility mediated by cytoplasmic dynein. Journal of Cell Biology, 115(6), pp.1639–1650.
- Gillis, J. et al., 2013. The DNAJB6 and DNAJB8 protein chaperones prevent intracellular aggregation of polyglutamine peptides. Journal of Biological Chemistry, 288(24), pp.17225–17237.
- Goodenough, U. & Heuser, J., 1984. Structural comparison of purified dynein proteins with in situ dynein arms. Journal of Molecular Biology, 180(4), pp.1083–1118.
- Gordon, M.B., Howard, L. & Compton, D.A., 2001. Chromosome movement in mitosis requires microtubule anchorage at spindle poles. Journal of Cell Biology, 153(3), pp.425–434.
- Görlich, D. et al., 1996. Identification of different roles for RanGDP and RanGTP in nuclear protein import. The EMBO journal, 15(20), pp.5584–94. Available at: http://www.pubmedcentral.nih.gov/articlerender.fcgi?artid=452303&tool=pmcentrez&rendertype=abstract.
- Görlich, D. et al., 1995. Two different subunits of importin cooperate to recognize nuclear localization signals and bind them to the nuclear envelope. Current Biology, 5(4), pp.383–392.

- Goshima, G., Nédélec, F. & Vale, R.D., 2005. Mechanisms for focusing mitotic spindle poles by minus end-directed motor proteins. Journal of Cell Biology, 171(2), pp.229–240.
- Goshima, G. & Vale, R.D., 2003. The roles of microtubule-based motor proteins in mitosis: Comprehensive RNAi analysis in the Drosophila S2 cell line. Journal of Cell Biology, 162(6), pp.1003–1016.
- Greene, M.K., Maskos, K. & Landry, S.J., 1998. Role of the J-domain in the cooperation of Hsp40 with Hsp70. Proceedings of the National Academy of Sciences of the United States of America, 95(11), pp.6108–13. Available at: http://www.pubmedcentral.nih.gov/articlerender.fcgi?artid=27593&tool=pmcentrez&rendertype=abstract.
- Griffis, E.R., Stuurman, N. & Vale, R.D., 2007. Spindly, a novel protein essential for silencing the spindle assembly checkpoint, recruits dynein to the kinetochore. Journal of Cell Biology, 177(6), pp.1005–1015.
- Gutiérrez-Caballero, C. et al., 2015. TACC3-ch-TOG track the growing tips of microtubules independently of clathrin and Aurora-A phosphorylation. Biology open, 4(2), pp.170–9. Available at: http://www.pubmedcentral.nih.gov/articlerender.fcgi?artid=4365485&tool=pmcentrez&rendertype=abstract.
- Hageman, J. et al., 2010. A DNAJB Chaperone Subfamily with HDAC-Dependent Activities Suppresses Toxic Protein Aggregation. Molecular Cell, 37(3), pp.355–369. Available at: http://linkinghub.elsevier.com/retrieve/pii/S1097276510000262.
- Heald, R. et al., 1996. Self-organization of microtubules into bipolar spindles around artificial chromosomes in Xenopus egg extracts. Nature, 382(6590), pp.420–5. Available at: http://www.ncbi.nlm.nih.gov/pubmed/8684481.
- Heald, R. et al., 1997. Spindle Assembly in Xenopus Egg Extracts: Respective Roles of Centrosomes and Mircotubule Self-Organization. Journal of Cell Biology, 138(3), pp.615–628. Available at: papers://ccfe1747-fd17-4ac8-b851-d909290feba4/Paper/p675.
- Heck, M.M.S. et al., 1993. The kinesin-like protein KLP61F is essential for mitosis in Drosophila. Journal of Cell Biology, 123(3), pp.665–679.
- Hentrich, C. & Surrey, T., 2010. Microtubule organization by the antagonistic mitotic motors kinesin-5 and kinesin-14. , 189(3).
- Holt, C.E. & Bullock, S.L., 2010. Subcellular mRNA Localization in Animal Cells and Why It Matters. Science, 1212(November), pp.1212–6. Available at: http://www.sciencemag.org/cgi/doi/10.1126/science.1176488.
- Hoogenraad, C.C. et al., 2001. Mammalian golgi-associated Bicaudal-D2 functions in the dynein-dynactin pathway by interacting with these complexes. EMBO Journal, 20(15), pp.4041–4054.
- Hsia, K.-C. et al., 2014. Reconstitution of the augmin complex provides insights into its architecture and function. Nature cell biology, 16(9), pp.852–63. Available at: http://www.ncbi.nlm.nih.gov/pubmed/25173975.

- Hunter, A.W. et al., 2003. The kinesin-related protein MCAK is a microtubule depolymerase that forms an ATP-hydrolyzing complex at microtubule ends. Molecular Cell, 11(2), pp.445–457.
- Hunter, P.J. et al., 1999. Mrj encodes a DnaJ-related co-chaperone that is essential for murine placental development. Development (Cambridge, England), 126, pp.1247–1258.
- Hurd, T.W., Fan, S. & Margolis, B.L., 2011. Localization of retinitis pigmentosa 2 to cilia is regulated by Importin beta2. Journal of cell science, 124, pp.718–726.
- Hyman, A.A. et al., 1995. Structural Changes Accompanying GTP Hydrolysis in Microtubules: Information from a Slowly Hydrolyzable Analogue Guanylyl-(c ,/3)-Methylene-Diphosphonate. Journal of Cell Biology, 128(January), pp.117–125.
- Izawa, I. et al., 2000. Identification of Mrj, a DnaJ/Hsp40 family protein, as a keratin 8/18 filament regulatory protein. Journal of Biological Chemistry, 275(44), pp.34521–34527.
- Jacquot, G., Maidou-Peindara, P. & Benichou, S., 2010. Molecular and functional basis for the scaffolding role of the p50/dynamitin subunit of the microtubule-associated dynactin complex. Journal of Biological Chemistry, 285(30), pp.23019–23031.
- Janson, M.E., De Dood, M.E. & Dogterom, M., 2003. Dynamic instability of microtubules is regulated by force. Journal of Cell Biology, 161(6), pp.1029–1034.
- Jha, R. & Surrey, T., 2015. Regulation of processive motion and microtubule localization of cytoplasmic dynein. Biochemical Society Transactions, 43(1), pp.48–57. Available at: http://www.biochemsoctrans.org/bst/043/bst0430048.htm.
- Jiang, J. et al., 2007. Structural Basis of J Cochaperone Binding and Regulation of Hsp70. Molecular Cell, 28(3), pp.422–433.
- Johmura, Y. et al., 2011. Regulation of microtubule-based microtubule nucleation by mammalian polo-like kinase 1. Proceedings of the National Academy of Sciences of the United States of America, 108(28), pp.11446–11451.
- Jonassen, J.A. et al., 2008. Deletion of IFT20 in the mouse kidney causes misorientation of the mitotic spindle and cystic kidney disease. The Journal of Cell Biology, 183(3), pp.377–384. Available at: http://www.jcb.org/cgi/doi/10.1083/jcb.200808137.
- Jonassen, J. a. et al., 2012. Disruption of IFT Complex A Causes Cystic Kidneys without Mitotic Spindle Misorientation. Journal of the American Society of Nephrology, 23, pp.641–651.
- Jones, L.A. et al., 2014. Dynein light intermediate chains maintain spindle bipolarity by functioning in centriole cohesion. Journal of Cell Biology, 207(4), pp.499–516.

- Kalab, P.P. et al., 2006. Analysis of a RanGTP-regulated gradient in mitotic somatic cells. Nature, 440(7084), pp.697–701. Available at: http://eutils.ncbi.nlm.nih.gov/entrez/eutils/elink.fcgi?dbfrom=pubmed&id=16572176&retmode=ref&cmd=prlinks\npapers2://publication/doi/10.1038/nature04589.
- Kalantzaki, M. et al., 2015. Kinetochore-microtubule error correction is driven by differentially regulated interaction modes. Nat Cell Biol, 17(4), pp.421–433. Available at: http://www.ncbi.nlm.nih.gov/pmc/articles/PMC4380510/pdf/emss-62030.pdf.
- Kampinga, H.H. & Craig, E. a, 2010. The HSP70 chaperone machinery: J proteins as drivers of functional specificity. Nature reviews. Molecular cell biology, 11(8), pp.579–592. Available at: http://dx.doi.org/10.1038/nrm2941.
- Kanehisa, M. et al., 2014. Data, information, knowledge and principle: back to metabolism in KEGG. *Nucleic Acids Research*, 42(Database issue), pp.D199–D205. Available at: http://www.ncbi.nlm.nih.gov/pmc/articles/PMC3965122/.
- Kapitein, L.C. et al., 2005. The bipolar mitotic kinesin Eg5 moves on both microtubules that it crosslinks. Nature, 435(May), pp.114–418.
- Kapoor, T.M. et al., 2000. Probing spindle assembly mechanisms with monastrol, a small molecule inhibitor of the mitotic kinesin, Eg5. Journal of Cell Biology, 150(5), pp.975–988.
- Karabay, A. & Walker, R.A., 1999. Identification of microtubule binding sites in the Ncd tail domain. Biochemistry, 38(6), pp.1838–1849.
- Kardon, J.R., Reck-Peterson, S.L. & Vale, R.D., 2009. Regulation of the processivity and intracellular localization of Saccharomyces cerevisiae dynein by dynactin. Proceedings of the National Academy of Sciences of the United States of America, 106(14), pp.5669–74. Available at: http://www.pubmedcentral.nih.gov/articlerender.fcgi?artid=2657088&tool=pmcentrez&rendertype=abstract.
- Kardon, J.R. & Vale, R.D., 2009. Regulators of the cytoplasmic dynein motor. Nature reviews. Molecular cell biology, 10(12), pp.854–865. Available at: http://dx.doi.org/10.1038/nrm2804.
- Kashina, A.S. et al., 1996. A bipolar kinesin. Nature, 379(6562), pp.270–272. Available at: http://eutils.ncbi.nlm.nih.gov/entrez/eutils/elink.fcgi?dbfrom=pubmed&id=8538794&retmode=ref&cmd=prlinks\npapers3://publication/doi/10.1038/379270a0.
- Kashina, A.S., Rogers, G.C. & Scholey, J.M., 1997. The bimC family of kinesins: Essential bipolar mitotic motors driving centrosome separation. Biochimica et Biophysica Acta - Molecular Cell Research, 1357(3), pp.257–271.
- Kee, H.L. et al., 2012. A size-exclusion permeability barrier and nucleoporins characterize a ciliary pore complex that regulates transport

into cilia. Nature Cell Biology, 14(4), pp.431–437. Available at: http://dx.doi.org/10.1038/ncb2450.

- Kerrien, S. et al., 2012. The IntAct molecular interaction database in 2012. *Nucleic Acids Research*, 40(Database issue), pp.D841–D846. Available at: http://www.ncbi.nlm.nih.gov/pmc/articles/PMC3245075/.
- Keshava Prasad, T.S. et al., 2009. Human Protein Reference Database—2009 update. *Nucleic Acids Research*, 37(Database issue), pp.D767–D772. Available at: http://www.ncbi.nlm.nih.gov/pmc/articles/PMC2686490/.
- Khodjakov, A. et al., 2003. Minus-end capture of preformed kinetochore fibers contributes to spindle morphogenesis. Journal of Cell Biology, 160(5), pp.671–683.
- Khodjakov, a et al., 2000. Centrosome-independent mitotic spindle formation in vertebrates. Current biology : CB, 10, pp.59–67.
- Kim, H., Fernandes, G. & Lee, C. Protein Phosphatases Involved in Regulating Mitosis: Facts and Hypotheses. *Mol. Cells* **39,** 654–62 (2016).
- King, S.J. et al., 2002. Subunit organization in cytoplasmic dynein subcomplexes. Protein science : a publication of the Protein Society, 11(5), pp.1239–1250.
- King, S.J. & Schroer, T. a, 2000. Dynactin increases the processivity of the cytoplasmic dynein motor. Nature cell biology, 2(1), pp.20–24.
- Kinoshita, K. et al., 2005. Aurora A phosphorylation of TACC3/maskin is required for centrosome-dependent microtubule assembly in mitosis. Journal of Cell Biology, 170(7), pp.1047–1055.
- Klein, S.L. et al., 2002. A PEER REVIEWED FORUM Genetic and Genomic Tools for Xenopus Research : The NIH Xenopus Initiative. , 391(August), pp.384–391.
- Kleylein-Sohn, J. et al., 2012. Acentrosomal spindle organization renders cancer cells dependent on the kinesin HSET. Journal of Cell Science.
- Knoblich, J. a, 2010. Asymmetric cell division: recent developments and their implications for tumour biology. Nature Reviews Molecular Cell Biology, 11(12), pp.849–860. Available at: http://dx.doi.org/10.1038/nrm3010\nhttp://www.nature.com/doifinder/10.1038/nrm3010.
- Kollman, J.M. et al., 2011. Microtubule nucleation by γ-tubulin complexes. Nature Reviews Molecular Cell Biology, 12(11), pp.709–21. Available at: http://www.ncbi.nlm.nih.gov/pubmed/21993292.
- Kollu, S., Bakhoum, S.F. & Compton, D.A., 2009. Interplay of Microtubule Dynamics and Sliding during Bipolar Spindle Formation in Mammalian Cells. Current Biology, 19(24), pp.2108–2113. Available at: http://dx.doi.org/10.1016/j.cub.2009.10.056.
- Komarova, Y.A. et al., 2002. Cytoplasmic linker proteins promote microtubule rescue in vivo. Journal of Cell Biology, 159(4), pp.589–599.

- Kon, T., Sutoh, K. & Kurisu, G., 2011. X-ray structure of a functional full-length dynein motor domain. Nature structural & molecular biology, 18(6), pp.638–642. Available at: http://dx.doi.org/10.1038/nsmb.2074.
- Kumar, P. et al., 2009. GSK33 phosphorylation modulates CLASP-microtubule association and lamella microtubule attachment. Journal of Cell Biology, 184(6), pp.895–908.
- Kumar, P. & Wittmann, T., 2012. +TIPs: SxIPping along microtubule ends. Trends in Cell Biology, 22(8), pp.418–428. Available at: http://dx.doi.org/10.1016/j.tcb.2012.05.005.
- Kwon, M. et al., 2008. Mechanisms to suppress multipolar divisions in cancer cells with extra centrosomes. Genes and Development, 22(16), pp.2189–2203.
- Lampson, M. a. & Cheeseman, I.M., 2011. Sensing centromere tension: Aurora B and the regulation of kinetochore function. Trends in Cell Biology, 21(3), pp.133–140. Available at: http://dx.doi.org/10.1016/j.tcb.2010.10.007.
- Lang, I., Scholz, M. & Peters, R., 1986. Molecular mobility and nucleocytoplasmic flux in hepatoma cells. Journal of Cell Biology, 102(4), pp.1183–1190.
- Lange, B.M. et al., 2000. Hsp90 is a core centrosomal component and is required at different stages of the centrosome cycle in Drosophila and vertebrates. The EMBO journal, 19(6), pp.1252–1262.
- Launay, G. et al., 2015. MatrixDB, the extracellular matrix interaction database: updated content, a new navigator and expanded functionalities. *Nucleic Acids Research*, 43(Database issue), pp.D321–D327. Available at: http://www.ncbi.nlm.nih.gov/pmc/articles/PMC4383919/.
- Lawo, S. et al., 2009. HAUS, the 8-Subunit Human Augmin Complex, Regulates Centrosome and Spindle Integrity. Current Biology, 19(10), pp.816–826.
- Lawo, S. et al., 2012. Subdiffraction imaging of centrosomes reveals higher-order organizational features of pericentriolar material. Nature Cell Biology, 12(1), pp.308–317. Available at: http://linkinghub.elsevier.com/retrieve/pii/S1097276505016011\nhttp://linkinghub.elsevier.com/retrieve/pii/S0092867415008491\nhttp://ac.els-cdn.com/S0092867415008491/1-s2.0-S0092867415008491-main.pdf?_tid=c001743e-375e-11e5-8a78-00000aab0f26&acdnat=143833.
- Lawrence, C.J. et al., 2004. A standardized kinesin nomenclature. Journal of Cell Biology, 167(1), pp.19–22.
- Lee, J.C., Field, D.J. & Lee, L.L., 1980. Effects of nocodazole on structures of calf brain tubulin. Biochemistry, 19(26), pp.6209–15. Available at: http://www.ncbi.nlm.nih.gov/pubmed/7470461.
- Liang, Y. et al., 2007. Nudel Modulates Kinetochore Association and Function of Cytoplasmic Dynein in M Phase. Molecular biology of the cell, 6(6), pp.569–583.

- Licata, L. et al., 2012. MINT, the molecular interaction database: 2012 update. *Nucleic Acids Research*, 40(Database issue), pp.D857–D861. Available at: http://www.ncbi.nlm.nih.gov/pmc/articles/PMC3244991/.
- Loschi, M. et al., 2009. Dynein and kinesin regulate stress-granule and P-body dynamics. Journal of cell science, 122(Pt 21), pp.3973–82. Available at: http://www.pubmedcentral.nih.gov/articlerender.fcgi?artid=2773196&tool=pmcentrez&rendertype=abstract.
- Lüders, J., Patel, U.K. & Stearns, T., 2006. GCP-WD is a gamma-tubulin targeting factor required for centrosomal and chromatin-mediated microtubule nucleation. Nature cell biology, 8(2), pp.137–147.
- Lydersen, B.K. & Pettijohn, D.E., 1980. Human-specific nuclear protein that associates with the polar region of the mitotic apparatus: Distribution in a human/hamster hybrid cell. Cell, 22(2), pp.489–499.
- Ma, H. T. & Poon, R. Y. C. How protein kinases co-ordinate mitosis in animal cells. *Biochem. J.* **435,** 17–31 (2011).
- Magidson, V. et al., 2011. The spatial arrangement of chromosomes during prometaphase facilitates spindle assembly. Cell, 146, pp.555–567.
- Mahoney, N.M. et al., 2006. Making microtubules and mitotic spindles in cells without functional centrosomes. Current Biology, 16(6), pp.564–569.
- Maiato, H. & Logarinho, E., 2014. Mitotic spindle multipolarity without centrosome amplification. Nature cell biology, 16(5), pp.386–94. Available at: http://www.ncbi.nlm.nih.gov/pubmed/24784849.
- Maiato, H., Rieder, C.L. & Khodjakov, A., 2004. Kinetochore-driven formation of kinetochore fibers contributes to spindle assembly during animal mitosis. Journal of Cell Biology, 167(5), pp.831–840.
- Makhnevych, T. & Houry, W.A., 2013. The control of spindle length by Hsp70 and Hsp110 molecular chaperones. FEBS Letters, 587(8), pp.1067–1072. Available at: http://dx.doi.org/10.1016/j.febslet.2013.02.018.
- Mallik, R. et al., 2004. Cytoplasmic dynein functions as a gear in response to load. Nature, 427(6975), pp.649–52. Available at: http://www.ncbi.nlm.nih.gov/pubmed/14961123.
- Manning, G., 2002. The Protein Kinase Complement of the Human Genome. Science, 298(5600), pp.1912–1934. Available at: http://www.sciencemag.org/cgi/doi/10.1126/science.1075762.
- Maresca, T.J. & Salmon, E.D., 2010. Welcome to a new kind of tension: translating kinetochore mechanics into a wait-anaphase signal. J Cell Sci, 123(Pt 6), pp.825–835. Available at: http://jcs.biologists.org/content/joces/123/6/825.full.pdf.
- Martins, T. et al., 2009. Sgt1, a co-chaperone of Hsp90 stabilizes Polo and is required for centrosome organization. The EMBO journal, 28(3), pp.234–47. Available at: http://www.pubmedcentral.nih.gov/articlerender.fcgi?artid=2637337&tool=pmcentrez&rendertype=abstract.

- Mayer, T.U. et al., 1999. Small Molecule Inhibitor of Mitotic Spindle Bipolarity Identified in a Phenotype-Based Screen Published by : American Association for the Advancement of Science Stable URL : http://www.jstor.org/stable/2899503 Linked references are available on JSTOR for. Science, 286(5441), pp.971–974.
- McAinsh, A. et al., 2006. The human kinetochore proteins Nnf1R and Mcm21R are required for accurate chromosome segregation. The EMBO Journal, 25(17), pp.4033–4049. Available at: http://www.ncbi.nlm.nih.gov/entrez/query.fcgi?cmd=Retrieve&db=PubMed&dopt=Citation&list_uids=16932742\npapers2://publication/uuid/9D7DA4DB-89AB-43A2-BDD7-1BFEF241D314.
- McAinsh, A.D. & Meraldi, P., 2011. The CCAN complex: Linking centromere specification to control of kinetochore-microtubule dynamics. Seminars in Cell and Developmental Biology, 22(9), pp.946–952. Available at: http://dx.doi.org/10.1016/j.semcdb.2011.09.016.
- McEwen, B.F. et al., 1997. Kinetochore fiber maturation in PtK1 cells and its implications for the mechanisms of chromosome congression and anaphase onset. Journal of Cell Biology, 137(7), pp.1567–1580.
- McKenney, R.J. et al., 2014. Activation of cytoplasmic dynein motility by dynactin-cargo adapter complexes. Science (New York, N.Y.), 345(6194), pp.337–41. Available at: http://www.ncbi.nlm.nih.gov/pubmed/25035494\nhttp://www.pubmedcentral.nih.gov/articlerender.fcgi?artid=PMC4224444.
- McKenney, R.J. et al., 2010. LIS1 and NudE induce a persistent dynein force-producing state. Cell, 141(2), pp.304–314. Available at: http://dx.doi.org/10.1016/j.cell.2010.02.035.
- McKenney, R.J. et al., 2011. Mutually exclusive cytoplasmic dynein regulation by NudE-Lis1 and dynactin. Journal of Biological Chemistry, 286(45), pp.39615–39622.
- Megraw, T.L., Kao, L.-R. & Kaufman, T.C., 2001. Zygotic development without functional mitotic centrosomes. Current Biology, 11(2), pp.116–120. Available at: http://www.sciencedirect.com/science/article/pii/S0960982201000173.
- Melchior, F. et al., 1993. Inhibition of nuclear protein import by nonhydrolyzable analogues of GTP and identification of the small GTPase Ran/TC4 as an essential transport factor. Journal of Cell Biology, 123(6 II), pp.1649–1659.
- Melkonian, K.A. et al., 2007. Mechanism of dynamitin-mediated disruption of dynactin. Journal of Biological Chemistry, 282(27), pp.19355–19364.
- Meng, E., Shevde, L.A. & Samant, R.S., 2016. Emerging roles and underlying molecular mechanisms of DNAJB6 in cancer. Oncotarget. Available at: http://www.ncbi.nlm.nih.gov/pubmed/27276715.
- Mennella, V. et al., 2012. Subdiffraction-resolution fluorescence microscopy reveals a domain of the centrosome critical for pericentriolar material

organization. Nature cell biology, 14(11), pp.1159–68. Available at: http://dx.doi.org/10.1038/ncb2597.

- Merdes, A. et al., 1996. A complex of NuMA and cytoplasmic dynein is essential for mitotic spindle assembly. Cell, 87(3), pp.447–458.
- Merdes, A. et al., 2000. Formation of spindle poles by dynein/dynactin-dependent transport of NuMA. Journal of Cell Biology, 149(4), pp.851–861.
- Meunier, S. & Vernos, I., 2011. K-fibre minus ends are stabilized by a RanGTP-dependent mechanism essential for functional spindle assembly. Nature Cell Biology, 13(12), pp.1406–1414. Available at: http://www.nature.com/doifinder/10.1038/ncb2372.
- Mitchison, T. & Kirschner, M., 1984. Dynamic instability of microtubule growth. Nature, 312, pp.237–242.
- Mitchison, T.J. et al., 2004. Bipolarization and Poleward Flux Correlate during Xenopus Extract Spindle Assembly. Molecular biology of the cell, 16(1), pp.1–13.
- Mitchison, T.J., Maddox, P., Gaetz, J., Groen, A., Shirasu, M., Desai, A., Salmon, E.D. & Kapoor, T.M., 2005. Roles of Polymerization Dynamics, Opposed Motors, and a Tensile Element in Governing the Length of Xenopus Extract Meiotic Spindles. Genetics, 125(2), pp.351–369.
- Mitchison, T.J., Maddox, P., Gaetz, J., Groen, A., Shirasu, M., Desai, A., Salmon, E.D. & Kapoor, M.T., 2005. Roles of polymerization dynamics, opposed motors, and a tensile element in governing the length of Xenopus extract meiotic spindles. Molecular biology of the cell, 16(2), pp.3064–3076.
- Mitra, A. et al., 2008. Large isoform of MRJ (DNAJB6) reduces malignant activity of breast cancer. Breast cancer research : BCR, 10(2), p.R22.
- Miyamoto, D.T. et al., 2004. The kinesin Eg5 drives poleward microtubule flux in Xenopus laevis egg extract spindles. Journal of Cell Biology, 167(5), pp.813–818.
- Mohr, D. et al., 2009. Characterisation of the passive permeability barrier of nuclear pore complexes. The EMBO Journal, 28(17), pp.2541–2553. Available at: http://emboj.embopress.org/cgi/doi/10.1038/emboj.2009.200.
- Monen, J. et al., 2005. Differential role of CENP-A in the segregation of holocentric C. elegans chromosomes during meiosis and mitosis. Nature cell biology, 7(12), pp.1248–1255.
- Moore, M.S. & Blobel, G., 1993. The GTP-binding protein Ran/TC4 is required for protein import into the nucleus. Nature Letters, 363.
- Moore, W., Zhang, C. & Clarke, P., 2002. Targeting of RCC1 to chromosomes is required for proper mitotic spindle assembly in human cells. , 12(2), pp.1442–1447.
- Moores, C.A. et al., 2002. A mechanism for microtubule depolymerization by KinI kinesins. Molecular Cell, 9(4), pp.903–909.

- Morales-Mulia, S. & Scholey, J.M., 2005. Spindle Pole Organization in Drosophila S2 Cells by Dynein, Abnormal Spindle Protein (Asp), and KLP10A□. Molecular biology of the cell, 16(1), pp.1–13.
- Moritz, M. et al., 1995. Microtubule nucleation by gamma-tubulin-containing rings in the centrosome. Nature, 378(C), p.592.
- Mountain, V. et al., 1999. The Kinesin-related Protein, HSET, Opposes the Activity of Eg5 and Cross-links microtubules in mamalian mitotic spindle. Jcb, 147(2), pp.351–365.
- Murphy, S.M., Urbani, L. & Stearns, T., 1998. The mammalian ϒ-tubulin complex contains homologues of the yeast spindle pole body components Spc97p and Spc98p. Journal of Cell Biology, 141(3), pp.663–674.
- Murray, A.W., 1991. Chapter 30 Cell Cycle Extracts. In B. K. Kay & H. B. B. T.-M. in C. B. Peng, eds. Xenopus laevis: Practical Uses in Cell and Molecular Biology. Academic Press, pp. 581–605. Available at: http://www.sciencedirect.com/science/article/pii/S0091679X08602988.
- Muscat, C.C. et al., 2015. Kinetochore-independent chromosome segregation driven by lateral microtubule bundles. eLife, 4, pp.1–24. Available at: http://elifesciences.org/lookup/doi/10.7554/eLife.06462.
- Najafi, M., Maza, N. a. & Calvert, P.D., 2012. Steric volume exclusion sets soluble protein concentrations in photoreceptor sensory cilia. Proceedings of the National Academy of Sciences, 109(1), pp.203–208.
- Nédélec, F., 2002. Computer simulations reveal motor properties generating stable antiparallel microtubule interactions. Journal of Cell Biology, 158(6), pp.1005–1015.
- Nédélec, F.J. et al., 1997. Self-organization of microtubules and motors. , 389(September), pp.305–308.
- Neumann, B. et al., 2010. Phenotypic profiling of the human genome by time-lapse microscopy reveals cell division genes. Nature, 464(7289), pp.721–7. Available at: http://dx.doi.org/10.1038/nature08869\nhttp://www.nature.com/doifinder/10.1038/nature08869\nhttp://www.ncbi.nlm.nih.gov/pubmed/20360735\nhttp://www.pubmedcentral.nih.gov/articlerender.fcgi?artid=PMC3108885.
- Neuwald, A.F. et al., 1999. AAA+: A class of chaperone-like ATPases associated with the assembly, operation, and disassembly of protein complexes. Genome Research, 9(1), pp.27–43.
- Nollen, E.A.A. et al., 2000. Bag1 Functions In Vivo as a Negative Regulator of Hsp70 Chaperone Activity Bag1 Functions In Vivo as a Negative Regulator of Hsp70 Chaperone Activity. Molecular and Cellular Biology, 20(3), pp.1083–1088.
- Nyarko, A., Song, Y. & Barbar, E., 2012. Intrinsic disorder in dynein intermediate chain modulates its interactions with NudE and dynactin. Journal of Biological Chemistry, 287(30), pp.24884–24893.

- O'Connell, C. B. & Khodjakov, A. L. Cooperative mechanisms of mitotic spindle formation. *J. Cell Sci.* **120,** 1717–1722 (2007).
- O'Connell, M.J. et al., 1993. Suppression of the bimC4 Mitotic Spindle Defect by Deletion of klpA, a Gene Encoding a KAR3-related Kinesin-like Protein in AspergiUus nidulans. Cell, 120(1), pp.153–162.
- O'Regan, L. et al., 2015. Hsp72 is targeted to the mitotic spindle by Nek6 to promote K-fiber assembly and mitotic progression. The Journal of Cell Biology, 209(3). Available at: http://www.jcb.org/cgi/doi/10.1083/jcb.201409151.
- Oakley, C.E. & Oakley, B.R., 1989. Identification of gamma-tubulin, a new member of the tubulin superfamily encoded by mipA gene of Aspergillus nidulans. Nature, 338(6217), pp.662–664.
- Ohtsubo, M. et al., 1987. Isolation and characterization of the active cDNA of the human cell cycle gene(RCC1) involved in the regulation of onset of chromosome condensation. Gene & Development., 1, p.585–593.
- Ohtsubo, M., Okazaki, H. & Nishimoto, T., 1989. The RCC1 protein, a regulator for the onset of chromosome condensation locates in the nucleus and binds to DNA. Journal of Cell Biology, 109(4 I), pp.1389–1397.
- Orchard, S. et al., 2014. The MIntAct project—IntAct as a common curation platform for 11 molecular interaction databases. *Nucleic Acids Research*, 42(Database issue), pp.D358–D363. Available at: http://www.ncbi.nlm.nih.gov/pmc/articles/PMC3965093/.
- Ounjai, P. et al., 2013. Architectural insights into a ciliary partition. Current Biology, 23(4), pp.339–344. Available at: http://dx.doi.org/10.1016/j.cub.2013.01.029.
- Pagel, P. et al., 2005. The MIPS mammalian protein–protein interaction database. *Bioinformatics*, 21(6), pp.832–834. Available at: http://dx.doi.org/10.1093/bioinformatics/bti115.
- Pante, N. & Kann, M., 2002. Nuclear Pore Complex Is Able to Transport Macromolecules with Diameters of 39 nm. Molecular biology of the cell, 13(2), pp.425–434. Available at: http://www.molbiolcell.org/cgi/doi/10.1091/mbc.01-06-0308.
- Paschal, B.M., 1987. MAP 1C Is a Microtubule-activated ATPase Which Translocates Microtubules In Vitro and Has Dynein-l e Properties. Journal of Cell Biology, 105(September), pp.1273–1282.
- Paschal, B.M. & Vallee, R.B., 1987. Retrograde transport by the microtubule-associated protein MAP 1C. Nature, 330(6144), pp.181–183. Available at: http://www.ncbi.nlm.nih.gov/pubmed/3670402\nhttp://www.nature.com/nature/journal/v330/n6144/pdf/330181a0.pdf.
- Pearring, J.N. et al., 2015. Guanylate cyclase 1 relies on rhodopsin for intracellular stability and ciliary trafficking. , 1, pp.1–13.
- Petosa, C. et al., 2004. Architecture of CRM1/Exportin1 suggests how cooperativity is achieved during formation of a nuclear export complex. Molecular Cell, 16(5), pp.761–775.

- Petry, S. et al., 2013. Branching microtubule nucleation in xenopus egg extracts mediated by augmin and TPX2. Cell, 152(4), pp.768–777. Available at: http://dx.doi.org/10.1016/j.cell.2012.12.044.
- Piehl, M. et al., 2004. Centrosome maturation: measurement of microtubule nucleation throughout the cell cycle by using GFP-tagged EB1. Proceedings of the National Academy of Sciences of the United States of America, 101(6), pp.1584–1588.
- Pinyol, R., Scrofani, J. & Vernos, I., 2013. The role of NEDD1 phosphorylation by aurora a in chromosomal microtubule nucleation and spindle function. Current Biology, 23(2), pp.143–149. Available at: http://dx.doi.org/10.1016/j.cub.2012.11.046.
- Qiu, W. et al., 2012. Dynein achieves processive motion using both stochastic and coordinated stepping. Nature structural & molecular biology, 19(2), pp.193–200. Available at: http://www.pubmedcentral.nih.gov/articlerender.fcgi?artid=3272163&tool=pmcentrez&rendertype=abstract.
- Raaijmakers, J.A., Tanenbaum, M.E. & Medema, R.H., 2013. Systematic dissection of dynein regulators in mitosis. Journal of Cell Biology, 201(2), pp.201–215.
- Rappsilber, J., Mann, M. & Ishihama, Y., 2007. Protocol for micro-purification, enrichment, pre-fractionation and storage of peptides for proteomics using StageTips. Nature Protocols, 2(8), pp.1896–1906. Available at: http://www.nature.com/doifinder/10.1038/nprot.2007.261.
- Reck-Peterson, S.L. et al., 2006. Single-Molecule Analysis of Dynein Processivity and Stepping Behavior. Cell, 126(2), pp.335–348.
- Redwine, W.B. et al., 2012. Structural Basis for Microtubule Binding and Release by Dynein. Science, 1532(September).
- Renault, L. et al., 2001. Structural basis for guanine nucleotide exchange on Ran by the regulator of chromosome condensation (RCC1). Cell, 105(2), pp.245–255.
- Rieder, C.L., 1981. The structure of the cold-stable kinetochore fiber in metaphase PtK1 cells. Chromosoma, 84(1), pp.145–158.
- Rosenblatt, J., 2005. Spindle assembly: asters part their separate ways. Nature cell biology, 7(3), pp.219–222.
- Ross, J.L. et al., 2006. Processive bidirectional motion of dynein-dynactin complexes in vitro. Nature cell biology, 8(6), pp.562–570.
- Ruggieri, A. et al., 2016. DNAJB6 Myopathies: Focused Review on an Emerging and Expanding Group of Myopathies. Frontiers in Molecular Biosciences, 3(September). Available at: http://journal.frontiersin.org/Article/10.3389/fmolb.2016.00063/abstract.
- Sahi, C. & Craig, E.A., 2007. Network of general and specialty J protein chaperones of the yeast cytosol. Proceedings of the National Academy of Sciences of the United States of America, 104(17), pp.7163–7168.

- Saibil, H., 2013. Chaperone machines for protein folding, unfolding and disaggregation. Nature reviews. Molecular cell biology, 14(10), pp.630–42. Available at: http://www.ncbi.nlm.nih.gov/pubmed/24026055.
- Sarparanta, J. et al., 2012. Mutations affecting the cytoplasmic functions of the co-chaperone DNAJB6 cause limb-girdle muscular dystrophy. Nature Genetics, 44(4), pp.450–455. Available at: http://dx.doi.org/10.1038/ng.1103.
- Sauer, G. et al., 2005. Proteome analysis of the human mitotic spindle. Mol Cell Proteomics, 4(1), pp.35–43. Available at: http://www.ncbi.nlm.nih.gov/entrez/query.fcgi?cmd=Retrieve&db=PubMed&dopt=Citation&list_uids=15561729.
- Saunders, W.S. & Hoyt, M.A., 1992. Kinesin-related proteins required for Assembly of the Mitotic Spindle. Cell, 118(1), pp.95–108. Available at: http://www.ncbi.nlm.nih.gov/pubmed/1643659.
- Sawin, K.E. et al., 1992. Mitotic spindle organization by a plus-end-directed microtubule motor. Nature, 359, pp.540–543.
- Sawin, K.E. & Mitchison, T.J., 1995. Mutations in the kinesin-like protein Eg5 disrupting localization to the mitotic spindle. Proceedings of the National Academy of Sciences of the United States of America, 92(10), pp.4289–93. Available at: http://www.ncbi.nlm.nih.gov/pubmed/7753799.
- Sawin, K.E. & Mitchison, T.J., 1991. Poleward microtubule flux in mitotic spindles assembled in vitro. Journal of Cell Biology, 112(5), pp.941–954.
- Scheffzek, K. et al., 1995. Crystal structure of the nuclear Ras-related protein Ran in its GDP-bound form.
- Schlager, M. a et al., 2014. In vitro reconstitution of a highly processive recombinant human dynein complex. The EMBO journal, 33(17), pp.1–14. Available at: http://www.ncbi.nlm.nih.gov/pubmed/24986880.
- Scholey, J.M., 2003. Intraflagellar transport. Annual review of cell and developmental biology, 19, pp.423–443.
- Schroer, T.A., 2004. Dynactin. Annual Review of Cell and Developmental Biology, 20(1), pp.759–779. Available at: http://www.annualreviews.org/doi/10.1146/annurev.cellbio.20.012103.094623.
- Schroer, T.A. & Sheetz, M.P., 1991. Two activators of microtubule-based vesicle transport. Journal of Cell Biology, 115(5), pp.1309–1318.
- Sdelci, S. et al., 2012. Nek9 phosphorylation of NEDD1/GCP-WD contributes to Plk1 control of γ-tubulin recruitment to the mitotic centrosome. Current Biology, 22(16), pp.1516–1523.
- Seewald, M.J. et al., 2002. RanGAP mediates GTP hydrolysis without an arginine finger. Nature, 415(6872), pp.662–666.
- Seki, N. et al., 1999. Cloning, tissue expression, and chromosomal assignment of human MRJ gene for a member of the DNAJ protein family. Journal of human genetics, 44, pp.185–189.

- Sharp, D.J. & Ross, J.L., 2012. Microtubule-severing enzymes at the cutting edge. Journal of Cell Science, 125(11), pp.2561–2569.
- Silk, A.D., Holland, A.J. & Cleveland, D.W., 2009. Requirements for NuMA in maintenance and establishment of mammalian spindle poles. Journal of Cell Biology, 184(5), pp.677–690.
- Siller, K.H. et al., 2005. Live Imaging of Drosophila Brain Neuroblasts Reveals a Role for Lis1/Dynactin in Spindle Assembly and Mitotic Checkpoint Control. Molecular Biology of the Cell, 125(2), pp.351–369.
- Slangy, A. et al., 1995. Phosphorylation by p34cdc2 regulates spindle association of human Eg5, a kinesin-related motor essential for bipolar spindle formation in vivo. Cell, 83(7), pp.1159–1169.
- Splinter, D. et al., 2010. Bicaudal D2, dynein, and kinesin-1 associate with nuclear pore complexes and regulate centrosome and nuclear positioning during mitotic entry. PLoS Biology, 8(4).
- Splinter, D. et al., 2012. BICD2, dynactin, and LIS1 cooperate in regulating dynein recruitment to cellular structures. Molecular Biology of the Cell, 23(21), pp.4226–4241. Available at: http://www.molbiolcell.org/cgi/doi/10.1091/mbc.E12-03-0210.
- Stark, C. et al., 2006. BioGRID: a general repository for interaction datasets. *Nucleic Acids Research*, 34(Database issue), pp.D535–D539. Available at: http://www.ncbi.nlm.nih.gov/pmc/articles/PMC1347471/.
- Stehman, S.A. et al., 2007. NudE and NudEL are required for mitotic progression and are involved in dynein recruitment to kinetochores. Journal of Cell Biology, 178(4), pp.583–594.
- Surrey, T. et al., 2001. Physical properties determining self-organization of motors and microtubules. Science (New York, N.Y.), 292(5519), pp.1167–71. Available at: http://www.ncbi.nlm.nih.gov/pubmed/11349149.
- Tanenbaum, M.E. et al., 2008. Dynein, Lis1 and CLIP-170 counteract Eg5-dependent centrosome separation during bipolar spindle assembly. The EMBO journal, 27(24), pp.3235–3245.
- Tanenbaum, M.E. et al., 2009. Kif15 Cooperates with Eg5 to Promote Bipolar Spindle Assembly. Current Biology, 19, pp.1703–1711.
- Tanenbaum, M.E. & Medema, R.H., 2010. Mechanisms of Centrosome Separation and Bipolar Spindle Assembly. Developmental Cell, 19(6), pp.797–806.
- Tang, T.K. et al., 1994. Nuclear mitotic apparatus protein (NuMA): spindle association, nuclear targeting and differential subcellular localization of various NuMA isoforms. Journal of cell science, 107 ( Pt 6, pp.1389–1402.
- Teixidó-Travesa, N. et al., 2010. The gammaTuRC revisited: a comparative analysis of interphase and mitotic human gammaTuRC redefines the set of core components and identifies the novel subunit GCP8. Molecular biology of the cell, 116(2), pp.295–306.
- Teixidó-Travesa, N., Roig, J. & Lüders, J., 2012. The where, when and how of microtubule nucleation - one ring to rule them all. Journal of cell science,

125(Pt 19), pp.4445–56. Available at: http://www.ncbi.nlm.nih.gov/pubmed/23132930.

- Tran, P.T., Walker, R.A. & Salmon, E.D., 1997. A metastable intermediate state of microtubule dynamic instability that differs significantly between plus and minus ends. Journal of Cell Biology, 138(1), pp.105–117.
- Tripathy, S.K. et al., 2014. Autoregulatory mechanism for dynactin control of processive and diffusive dynein transport. Nature Cell Biology, 16(12), pp.1192–1201. Available at: http://www.nature.com/doifinder/10.1038/ncb3063.
- Tsai, J. & Douglas, M.G., 1996. A conserved HPD sequence of the J-domain is necessary for YDJ1 stimulation of Hsp70 ATPase activity at a site distinct from substrate binding. Journal of Biological Chemistry, 271(16), pp.9347–9354.
- Tulu, U.S. et al., 2006. Molecular requirements for kinetochore-associated microtubule formation in mammalian cells. Current Biology, 16, pp.536–541.
- Uchida, K.S.K. et al., 2009. Kinetochore stretching inactivates the spindle assembly checkpoint. Journal of Cell Biology, 184(3), pp.383–390.
- Uehara, R. et al., 2009. The augmin complex plays a critical role in spindle microtubule generation for mitotic progression and cytokinesis in human cells. Proceedings of the National Academy of Sciences of the United States of America, 106(17), pp.6998–7003. Available at: http://www.pubmedcentral.nih.gov/articlerender.fcgi?artid=2668966&tool=pmcentrez&rendertype=abstract.
- Urnavicius, L. et al., 2015. The structure of the dynactin complex and its interaction with dynein. Science, 347(6229), pp.1441–1446. Available at: http://www.ncbi.nlm.nih.gov/pubmed/25814576.
- Urrutia, R. et al., 1991. Purified kinesin promotes vesicle motility and induces active sliding between microtubules in vitro. Proceedings of the National Academy of Sciences of the United States of America, 88(15), pp.6701–5.
- Vale, R.D., Reese, T.S. & Sheetz, M.P., 1985. Identification of a novel force-generating protein, kinesin, involved in microtubule-based motility. Cell, 42(1), pp.39–50.
- Vanneste, D. et al., 2009. The Role of Hklp2 in the Stabilization and Maintenance of Spindle Bipolarity. Current Biology, 19(20), pp.1712–1717. Available at: http://dx.doi.org/10.1016/j.cub.2009.09.019.
- Vanneste, D., Ferreira, V. & Vernos, I., 2011a. Chromokinesins: localization-dependent functions and regulation during cell division. Biochemical Society Transactions, 39, pp.1154–1160.
- Vanneste, D., Ferreira, V. & Vernos, I., 2011b. Chromokinesins: localization-dependent functions and regulation during cell division. Biochemical Society Transactions, 39(5), pp.1154–1160. Available at: http://biochemsoctrans.org/lookup/doi/10.1042/BST0391154.

- Varga, V. et al., 2009. Kinesin-8 Motors Act Cooperatively to Mediate Length-Dependent Microtubule Depolymerization. Cell, 138(6), pp.1174–1183. Available at: http://dx.doi.org/10.1016/j.cell.2009.07.032.
- Vaughan, K.T. & Vallee, R.B., 1995. Cytoplasmic dynein binds dynactin through a direct interaction between the intermediate chains and p150Glued. Journal of Cell Biology, 131(6 I), pp.1507–1516.
- Vergnolle, M.A.S. & Taylor, S.S., 2007. Cenp-F Links Kinetochores to Ndel1/Nde1/Lis1/Dynein Microtubule Motor Complexes. Current Biology, 17(13), pp.1173–1179.
- Vetter, I.R. et al., 1999. Structure of a Ran-binding domain complexed with Ran bound to a GTP analogue: implications for nuclear transport. Nature, 398(6722), pp.39–46. Available at: http://www.ncbi.nlm.nih.gov/pubmed/10078529.
- Vicente, J.J. & Wordeman, L., 2015. Mitosis, microtubule dynamics and the evolution of kinesins. Experimental Cell Research, 334(1), pp.61–69. Available at: http://dx.doi.org/10.1016/j.yexcr.2015.02.010.
- Walczak, C.E. et al., 1998. A model for the proposed roles of different microtubule-based motor proteins in establishing spindle bipolarity. Current biology : CB, 8(16), pp.903–13. Available at: http://www.ncbi.nlm.nih.gov/pubmed/9707401.
- Walker, R.A., Inoue, S. & Salmon, E.D., 1989. Asymmetric behavior of severed microtubule ends after ultraviolet-microbeam irradiation of individual microtubules in vitro. Journal of Cell Biology, 108(3), pp.931–937.
- Wang, S. et al., 2013. Nudel/NudE and Lis1 promote dynein and dynactin interaction in the context of spindle morphogenesis. Molecular biology of the cell, 24(22), pp.3522–33. Available at: http://www.pubmedcentral.nih.gov/articlerender.fcgi?artid=3826990&tool=pmcentrez&rendertype=abstract.
- Wang, S.A. et al., 2009. Heat Shock Protein 90 Is Important for Sp1 Stability during Mitosis. Journal of Molecular Biology, 387(5), pp.1106–1119. Available at: http://dx.doi.org/10.1016/j.jmb.2009.02.040.
- Watson, E.D. et al., 2011. Cell-cell adhesion defects in Mrj mutant trophoblast cells are associated with failure to pattern the chorion during early placental development. Developmental Dynamics, 240(October), pp.2505–2519.
- Watson, E.D. et al., 2007. The Mrj co-chaperone mediates keratin turnover and prevents the formation of toxic inclusion bodies in trophoblast cells of the placenta. Development (Cambridge, England), 134, pp.1809–1817.
- Welburn, J.P.I., 2013. The molecular basis for kinesin functional specificity during mitosis. Cytoskeleton, 70(9), pp.476–493.
- Wendt, T. et al., 2003. A structural analysis of the interaction between ncd tail and tubulin protofilaments. Journal of Molecular Biology, 333(3), pp.541–552.

- Whitehead, C.M. & Rattner, J.B., 1998. Expanding the role of HsEg5 within the mitotic and post-mitotic phases of the cell cycle. Journal of cell science, 111 ( Pt 1, pp.2551–2561.
- Wignall, S.M. & Villeneuve, A.M., 2009. Lateral microtubule bundles promote chromosome alignment during acentrosomal oocyte meiosis. Nature cell biology, 11(7), pp.839–844. Available at: http://dx.doi.org/10.1038/ncb1891.
- Winey, M. & O'Toole, E., 2014. Centriole structure. Philosophical transactions of the Royal Society of London. Series B, Biological sciences, 369(1650), p.20130457-. Available at: http://rstb.royalsocietypublishing.org/content/369/1650/20130457.abstract\nhttp://rstb.royalsocietypublishing.org/content/369/1650/20130457\nhttp://www.ncbi.nlm.nih.gov/pubmed/25047611\nhttp://www.pubmedcentral.nih.gov/articlerender.fcgi?artid=PMC41.
- Wittmann, T. & Hyman, T., 1999. Recombinant p50/dynamitin as a tool to examine the role of dynactin in intracellular processes. Methods in cell biology, 61, pp.137–43. Available at: http://www.ncbi.nlm.nih.gov/pubmed/9891312.
- Wühr, M. et al., 2014. Deep proteomics of the xenopus laevis egg using an mRNA-derived reference database. Current Biology, 24(13), pp.1467–1475.
- Yagi, T., 2009. Bioinformatic approaches to dynein heavy chain classification. First edit., Elsevier. Available at: http://dx.doi.org/10.1016/S0091-679X(08)92001-X.
- Ying, W.C. et al., 2009. Mitotic control of kinetochore-associated dynein and spindle orientation by human Spindly. Journal of Cell Biology, 185(5), pp.859–874.
- Yokoyama, H. et al., 2008. Cdk11 is a RanGTP-dependent microtubule stabilization factor that regulates spindle assembly rate. Journal of Cell Biology, 180(5), pp.867–875.
- Yokoyama, N. et al., 1995. A giant nucleopore protein that binds Ran/TC4. Nature, 376(6536), pp.184–188.
- Zhai, Y., Kronebusch, P.J. & Borisy, G.G., 1995. Kinetochore microtubule dynamics and the metaphase-anaphase transition. Journal of Cell Biology, 131(3), pp.721–734.
- Zhang, R. et al., 2015. Mechanistic origin of microtubule dynamic instability and its modulation by EB proteins. Cell, 162(4), pp.849–859. Available at: http://dx.doi.org/10.1016/j.cell.2015.07.012.
- Zw, Z. et al., 2008. A new mechanism controlling kinetochore – microtubule interactions revealed by comparison of two dynein-targeting components : SPDL-1 and the Rod / Zwilch / Zw10 complex. Genes & Development, pp.2385–2399.